Optimal Crop Planning in A Canal Command Area with Due Emphasis on Nutrient Balance and Climate Change

Thesis submitted

for the partial fulfillment of the requirements

for the award of the degree of

DOCTOR OF PHILOSOPHY

by

Mridusmita Debnath

(146104018)

DEPARTMENT OF CIVIL ENGINEERING

INDIAN INSTITUTE OF TECHNOLOGY GUWAHATI

Guwahati-781039, Assam

April 2023

Optimal Crop Planning in A Canal Command Area with Due Emphasis on Nutrient Balance and Climate Change

Thesis submitted

for the partial fulfillment of the requirements

for the award of the degree of

DOCTOR OF PHILOSOPHY

by

Mridusmita Debnath

(146104018)

DEPARTMENT OF CIVIL ENGINEERING

INDIAN INSTITUTE OF TECHNOLOGY GUWAHATI

Guwahati-781039, Assam

April 2023

Department of Civil Engineering
Indian Institute of Technology Guwahati
Guwahati-781039, Assam, India

Prof. Arup Kumar Sarma
Professor
aks@iitg.ac.in

Prof. Chandan Mahanta
Professor
chandan@iitg.ac.in

Certificate

It is certified that the work included in this thesis entitled "**Optimal crop planning in a canal command area with due emphasis on nutrient balance and climate change**" by **Mridusmita Debnath**, Roll Number 146104018, a Research Scholar in the Department of Civil Engineering, Indian Institute of Technology Guwahati for the award of Doctor of Philosophy has been carried out under our supervision and that the outcomes of the thesis work have not been submitted to any institution or research organization for the award of degree.

Date:

Place: Guwahati

(Prof. Arup Kumar Sarma)

(Prof. Chandan Mahanta)

Declaration of Authorship

I, Mridusmita Debnath, declare that this thesis titled "**Optimal crop planning in a canal command area with due emphasis on nutrient balance and climate change**" and the works delivered in it has been carried out by me under the supervision of Prof. Arup Kr. Sarma, and Prof. Chandan Mahanta, Civil Engineering Department, Indian Institute of Technology Guwahati. The writing of the work was generated from my own words and expression of thoughts. Furthermore, wherever ideas from others' works were included, I have faithfully made citations to the sources of literature. Also, this work has not been submitted elsewhere for the award of any other degree.

Date:

(**MRIDUSMITA DEBNATH**)
Department of Civil Engineering
Indian Institute of Technology Guwahati
Guwahati-781039, Assam, India

Acknowledgment

Every progressive attempt is led by the contributions of many people. Acknowledging for a few might be an inconsiderable task dotted on a piece of paper. Nevertheless, here I get a great opportunity to express my token of thanks to people who in a way, helped and supported me during this investigation. It would have not been possible to complete this work without many people to whom I owe immense gratitude and appreciation.

First and foremost, I am deeply indebted to my supervisors, Prof. Arup Kr. Sarma and Prof. Chandan Mahanta, Indian Institute of Technology (IIT) Guwahati. Their continuous support, inspiring guidance, wholehearted involvement, worthy conversation, meticulous council, gracious encouragement and help throughout the research work was indispensable. Prof. Arup Kr. Sarma especially was a teacher-cum-mentor and academic father who has been the backbone in influencing my academic career since 2014.

No words of thanks can sum up the gratitude that I owe to the Chairman of my Doctoral Committee Prof. Subashisa Dutta, Professor, Department of Civil Engineering, Indian Institute of Technology (IIT) Guwahati, for his constant encouragement, talented advice and treasured inspiration provided during the study.

I would like to express my deepest gratitude to the members of my Doctoral Committee Prof. Bimlesh Kumar, Professor and Dr. P. Sreeja, Associate Professor, Department of Civil Engineering, Indian Institute of Technology (IIT) Guwahati, for their valued suggestions, and timely help at various stages of the investigation and finally compilation of research in the form of thesis.

Sincere thanks are due to Prof. Kanduru V. Krishna, Dean, Academic Affairs, Prof. Sharad Gokhale, Head of Civil Engineering, Indian Institute of Technology (IIT) Guwahati, for providing necessary opportunities and academic support for the successful completion of this PhD.

I express my sincere thanks to Dr. Ujjwal Kumar, former Incharge Director, Indian Council of Agricultural Research-Research Complex for Eastern Region Patna (ICAR-RCER, Patna), Dr. Anup Das, Director, ICAR-RCER, Patna, Dr. Ashutosh Upadhyay, Head of Division of Land and Water Management (DLWM), ICAR-RCER, Patna for their constant motivation, guidance and support throughout my research career so far. My abstruse regard goes to the administration, of my current institute of employment, ICAR-RCER, Patna for allowing me to complete this research

Thanks are due to all my colleagues; without whose support this work could not have been completed. Furthermore, I hereby acknowledge all the project staffs and the students of Department of Civil Engineering, Indian Institute of Technology (IIT) Guwahati, for their sincere help and assistance provided during the field experiments and data collection. Special appreciation is also due to Ms. Jonali Saikia, Technical Officer, Mr. Chitta Ranjan Medhi, Mr. Payodhar Pathak, Technical Superintendent for their immense help during the lab analysis of samples in my research work.

I would also like to acknowledge Mr. Dilip Deka, Mr. Gautam Kakati, Irrigation Department Office, Assam, for urgently helping me get the command area related data, I needed during my Ph.D. work. I am also grateful to Mr. Tapan Debnath, a native of Jamuna command area, who helped me during the questionnaire survey to the farmers of research study area. Dr. Sant Kumar Singh, Dr. A. K. Singh, Kamlesh Soni, colleagues from ICAR, with whom I discussed and improved my research results. I am incredibly thankful to Deepsikha, Bhaswati, Gaurav, Aparamita, Shaivi, Indraneel, research scholars for their friendly affection and help during the compilation of the thesis and many others for their co-operation during the project.

It is impossible to express in words that my parents' inspiration has brought me to this position. Finally, I express my heartfelt reverence to my family, especially my husband and son, for their noble sacrifice and invaluable love and support throughout the period. My hearty thanks to all those who have contributed in one way or another to successfully completing this research work.

This list is incomplete, but let me submit that the omissions are unintentional. Again, I sincerely thank all those who have cooperated with me directly or indirectly in this endeavor.

Place : IIT Guwahati

Date : 6/4/2023 **(Mridusmita Debnath)**

Dedicated to my Parents

and Family

Abstract

Rainfed agriculture plays a vital role in providing food and livelihoods globally. However, its production is adversely affected due to uncertainty in rainfall patterns which is increasing under the impact of climate change. Supplemental irrigation helps minimization of risk thus stabilizes the crop yield. Given that rice is a primarily grown crop in rainfed conditions and is the staple food of half the global population, it is under the pressure of increasing production due to the burgeoning population globally. Therefore, proper farming management such as balanced fertilization practices, irrigation etc are required. On the other hand, monocropping of cereal is a growing phenomenon among the farmers, due to known yield, reduced investment, prior knowledge of the activity calendar, insufficient irrigation and lower market risk resulting in a rice-fallow cultivation system. However, the introduction of pulses, oilseeds and vegetable crops during the fallow season is the key to providing better nutrition and improving household food security. Thus, irrigation water management is required for maximizing yield of these crops during the fallow season.

Climate change impact on global water resources varies spatially and temporally. Besides, many basins encounter difficulties in hydrological modeling due to limited information of hydro-climatological variables and their location specific unique hydrological pattern. Understanding the nutrient balance process and climate change impact in a rice-fallow cropping system is paramount for sustainable crop intensification in fallow lands of rain-shadowed areas. This study proposes a chance-constrained optimization model for optimal crop area planning of rabi crops for maximizing benefit considering the constraints of irrigation water availability, environmental flow requirement (EFR), farmers' choice, local food demand and the availability of residual soil nutrient after rice harvesting. The model is named as Irrigation-Food-Environment-EFR-Chance Constraint Programming (IFEC) model. Further, various modeling concepts and Artificial Neural Network (ANN) are devised for understanding climate change response to hydrological regime and crop water demand in such areas with potential socio-economic, demographic, and geographical factors. Performance of three temperature-based ET_0 (TET) models, namely FAO Penman Monteith, Blaney Criddle, Thornthwaite and Modified Penman was evaluated by comparing the result with the available Pan evaporation data of the study area and the model performing best was identified for estimating future seasonal irrigation demand under climate change. A Multilinear Regression (MLR) model was developed for future temperature projections using predictors from 3 GCM

models. The model was calibrated using historical data and applied to forecast water demand for RCP Scenarios. Downscaling of precipitation by similar model was found to perform poorly in the study basin, as the basin is in a rain-shadowed area with complex topography. Therefore, a hybrid ANN model was established to identify and quantify the impacts of climate change on streamflow. For that, we identified two sets of potential predictors using Iterative Input Selection (IIS) by regression for ANN-Back Propagating model. The method directly regresses observed streamflow value based on the GCM variables without downscaling precipitation and temperature.

These modeling concepts were then applied to the rain-shadowed river basin Jamuna and its associated canal command area. Jamuna is a sub-tributary of Brahmaputra River, which is experiencing severe land degradation due to fallow agricultural lands. Thirteen villages were selected for soil and plant sample collection along with interviewing the farmers of corresponding villages about the farming practices. Rice-fallow and minimal irrigation water availability are the two major agricultural related concerns affecting crop diversification in the command area. Crop diversification not only leads to enhanced food security but also reduces crop water use as compared to single cropping of water-intensive cereal crops such as rice and wheat. Also, farmers' choice of summer rice cultivation indicated that area under this crop can be set to a specific percentage rather than cultivating the whole area to optimize water consumption. Simultaneously, crop area under vegetable crops can be increased to maximize farmer's profit. Further, to assess the stability of planned crop diversification, study was conducted for climate change impact analysis on the watershed hydrology and crop water demand for future period (2025-2100) as compared to the base period (2000-2012) along with demographic growth in the area. Findings suggested that, the demand of irrigation water in the command area increased up to 1% by the end of 21st century. Annual average flow rate has been found to vary with time and scenarios. Maximum increase of as high as 33% is observed towards end of 21st century. On the other hand, for some other scenarios, the flow rate decreases by 4% in mid future. Therefore, irrigation infrastructures and cropping plan need to be planned dynamically and in a more flexible manner to address such possible variation in future. The percentage change in winter flow rate is projected to increase as compared to the base period. This is a positive indication towards scope of enhancing winter crop. This, emphasizes the need for change in infrastructure along with irrigated area expansion associated with crop diversification under growing population. This type of future scenarios of crop water demand and hydrological changes projected by using future climate change scenarios and, demographic

conditions derived from the master plan of an irrigation project provide an opportunity to re-evaluate the irrigation project plan. Several adaptive strategies has also been suggested for increasing the efficiency of agricultural water use inside the command area. In addition, there is also a need for increasing yield per unit area of fallow lands by introducing higher crop yield variety. Also, rice planting period should be advanced by one month (June to September) to avail the maximum water availability in the river. The present situation of food production in eastern India is not sufficient, as they cannot fulfil the required food demand for people residing and depends on exported food. The continued use of amount of water from the current water utilization systems and cultivation practices, argues for an urgent need to shift towards scientific solutions that would then be seen as a rational approach to decision-making on a pragmatic evaluation of alternatives available. Finally, to obtain a sustainable irrigation planning, prevent phosphorus depletion and to limit nitrogen pollution within a permissible limit, the optimal crop area is planned considering the nutrient residues in soil after rice harvest.

The study has revealed that, optimal utilization of land, water and fertilizer in agricultural field not only help enhancing food production, but also help in sustainable use of water and land resources. In the context of climate change, sustainable use of water resources is extremely important. Faster rate of population growth in general demands crop intensification and this study has shown how proper crop area planning can enhance food security. Therefore, concerned authority should take steps to popularize such approaches of optimal crop planning through field implementation to realize real benefit of such study. Stakeholder engagement is crucial for bringing technically and socioeconomically feasible policies and regulations in the firm to achieve balanced water consumption per available water resources.

Table of Contents

List of Tables

List of Figures

List of Notations

IN_{total}	Input in soil
OUT_{total}	Output from soil
ΔS	Change in soil nutrient pool
MF	Mineral fertilisers
NF	Nitrogen fixation
MN	Manure
CH	Harvested crops
LE	Leaching
GL	Gaseous losses
orgN	Internal N
orgP	Internal P
FN	Fertilizer N
FP	Fertilizer P
Δc_{FN}	Concentration gradient for Fertilizer N
Δc_{FP}	Concentration gradient for Fertilizer P
Δc_{orgN}	Concentration gradient for Internal N
Δc_{orgP}	Concentration gradient for Internal P
NEB	Net Economic Benefit
R_{st}	Revenues generated
CC_{st}	Cultivation costs
Y_i	Yield of crop i
P_{it}	Price received by the farmer in the market for crop i in year t
A_{is}	Area allocated to each crop in season s.
FC_{it}	Fertilizers cost
SC_{it}	Seed cost
LC_{it}	Labour cost
PC_{it}	Pesticides cost
OC_{it}	Other costs

RF_{s-1}	Residual fertilizer from previous cultivation
$F_{total,i}$	Total fertilizer required
P_{sub}	Subsidized price of fertilizer
P_r	Probability distribution of random variable
b_j	Random variable of river inflow
$b_{jm}^{P_{jm}}$	Surface water supply for the month m and risk constraint j
$CWR_{i,m,s}$	Crop water requirement for the month m and season s
R_{jm}	R is the EFR for a particular month m and risk constraint j
γ	Irrigation efficiency
$\emptyset$	Percentage release of EFR
CU_p	Gross water use of preference crop
$CWR_{p,m,s}$	Crop water requirement for the month m and season s and crop p
FD_{it}	Annual food demand for the local population
A_{pop}	Area's population
A_{total}	Total agricultural area
A_r	Remaining area after preference crop cultivation
ω	Percentage of area for preference crop cultivation
A_p	Area for preference crop cultivation
A_{inmt}	crops with no government support price
A_{ipt}	the higher priced vegetable crop
T_{SDCorr}	Bias corrected climatic variables
T_{obs}	Observed predictand of climate variables
T_{gcm}	Simulated climate variable from GCM
1-W	Weight of aerodynamic term
W	Weight for radiation term
f(u)	Wind related function
p	Monthly daylight hours

VPD	Vapour pressure deficit
DT	Delta term
PT	Psi term
TT	Temperature term
R_n	Net radiation at the crop surface
I	Annual heat index
ΔSW	Soil moisture storage contribution
ΔGW	Groundwater contribution during the growth of the crop
ER	Effective rainfall
IR	Irrigation requirement
WR	Net water demand of different crops
ET_0	Reference evapotranspiration
hfls	Surface upward latent heat flux
hfss	Surface upward sensible heat flux
ps	Surface air pressure
huss	Specific humidity
pr	Precipitation
sfc	Wind speed
tasmax	Maximum air temperature
tasmin	Minimum air temperature

List of Abbreviations

TKN	Total Kjeldahl Nitrogen
P_{av}	Available Phosphorus
Exc K	Exchangeable Potassium
N	Nitrogen
P	Phosphorus
K	Potassium
DAP	Di-ammonium Phosphate
MOP	Muriate of Potash
JCA	Jamuna Command Area
ANOVA	Analysis of variance
CCLP	Chance-Constrained Linear Programming
EFR	Environmental flow release
IFEC	Irrigation-Food-Environment Chance-Constrained Programming Model
GCM	General Circulation Model
RCP	Representative Concentration Pathways
CMIP5	Coupled Model Intercomparison Project Phase 5
IDW	Inverse distance weighting
SISO	Single Input Single Output
MISO	Multiple Input Single Output
CANESM2	The Second Generation CANadian Earth System Model
GISS-E2-H	NASA Goddard Institute for space studies-ModelEversion2, HYCOM Ocean model
NorESM1- M	The Norwegian Earth System Model
CSIRO- Mk3-6-0	The Commonwealth Scientific and Industrial Research Organisation
CNRM-CM5	Centre National de Recherches Météorologiques
MLR	Multilinear Regression

NSC	Nash-Sutcliffe coefficient
CC	Correlation coefficient
TET	Temperature-based ET_0 model
PMT	FAO 56 Penman-Monteith
MP	Modified Penman
TH	Thornthwaite
BC	Blaney-Criddle
CRMSD	Centralized root mean squared deviation
CWD	Crop water demand
ANN	Artificial Neural Network
FDC	Flow Duration Curve

Chapter 1

Introduction

1.1 Background

In today's world, major challenge faced by agriculture is achieving the desired increase in production in the face of changing climate and food security without hampering the environment. In addition to this, shrinking of land and water resources aggravates the agricultural scenario. The total global water demand is projected to rise by about 50% by 2050 thus increasing pressure on river basins in general and in particular agriculture. Moreover, rising food insecurity triggers intensive cultivation in order to increase food production to meet the projected demand of 50% in 2050. The ambition for good change is named as 'Sustainable Development Goal 2' or SDG 2, which ensures food access to all with the available resources (UN 2016). Globally, rice is the staple food for half of the world's population and Asia is the prime contributor, as over 90% of world's rice is grown in Asia. Further, the Intergovernmental Panel on Climate Change (IPCC) in its Fifth Assessment Report found that the climate has been changing drastically in South Asia (IPCC, 2014), which is a matter of concern. Rise in temperatures and changes in rainfall patterns owing to climate change, will possibly impact freshwater availability, thereby affecting agriculture. Therefore, appropriate management practices of these resources are mandatory for the realization of increased productivity, which can bring positive impact along with sustainable solutions to agriculture.

Rice is cultivated mostly during monsoon due to insufficient irrigation water (Oue and Laban 2020, Sulaiman et al. 2019). Hence rice fallows prevail mostly in rice cultivated areas in South Asia and 79% of it is in India. However, the cultivation of crops in an area sequentially is a requisite, to optimally utilize the natural resources and various inputs such as fertilizer, for production keeping in mind the potentiality and economic advantages of the region. As soil is the primary source of the nutrients to grow good and healthy crops balanced application of fertilizers is also necessary. Much of the chemical fertilizers applied in excess to agricultural fields are lost to the environment (Bennett et al. 2001; Galloway et al. 2008; Seitzinger et al. 2010). Nutrient N, and P accumulated in the soil after crop harvest is prone to hydrologic loss in fallow lands (Bechmann 2014, Smith and Chalk 2018). Therefore, a balanced application of fertilizers is needed. On the other hand, changing environment has implications for food systems' production and stability with increased competition among various water-demanding

sectors (Dawson et al. 2016). Variations in rainfall amount and temperature within the cropping season, due to climate change, may result in an increase in the water supply-demand gap and thus may lead to yield loss, as the crop growth phenomenon directly or indirectly depends on these climatic parameters (Gul et al. 2020).

Water is a vital part of agriculture that helps sustain life and transport nutrients from the soil to plants through transpiration. Both groundwater and surface water are used for the human benefit. However, surface water resources are important in designing, operating, and controlling many vital projects in water-demanding sectors. Thus, estimating the adequacy of freshwater resources in the future is gaining attention, on account of the alteration in water supply and demand dimensions. A local level water supply, depends on the hydrologic cycle, which is altered due to global warming caused by climate change. The impact of climate change on river flow regime forms an important reason for the balanced release of water for irrigation during the whole year, due to the erratic behaviour of rainfall as well as temperature both inter seasonally and intra seasonally for crop cultivation period. Several studies have developed mitigation options for efficient water management practices for increasing agricultural production (Mo 2017, Tang 2021a, Li 2021a). Therefore, inflow prediction of reservoirs and management measures related to downstream water release planning and flood protection are considered for alleviating the adverse impact of climate change on agriculture with the help of various climate models and crop models (Chen et al. 2020).

South Asia is endowed with several mountains and rivers. These mountain barriers create the rain-shadow effect on the river and associated basins, where precipitation is relatively low. People of these basins use freshwater resources for various purposes, such as drinking, and industrial needs including agriculture, and agricultural water demand occupies the lion's share. South Asian River basin plays a vital role in providing livelihood to 700 million people in plain and mountainous areas (Sreshtha et al., 2015). It feeds almost 25% of the world's population with the large Indus-Ganga-Brahmaputra irrigation scheme (FAO 2016). There is tremendous pressure to produce 50% more food than the present availability to feed the projected world population through proper irrigation management for the intensification of rice-fallows. Rice-fallow is a popular cropping system of South Asia and covers around 22.3 Mha (Gumma et al., 2016). However, as increasing production by adding new areas is unlikely due to increasing pressure on croplands for alternative uses (Rahman et al. 2016), agronomists consider improving cropland use planning while using the same land resources as a possible solution.

Additionally, several studies have shown that integrating water and fertilizer management is a viable way to balance water and fertilizer requirements in maximizing crop production as well as promote their efficiencies (Wang et al. 2021; Xiao et al. 2019).

1.2 Purpose of the Study

A river basin and command area are linked ecologically for both hydrological and agricultural analysis and thus form the base for agrarian water resources management governance. Interestingly, each river basin acquires its unique features due to its location. The streamflow model serves as a tool for understanding hydrologic pattern as such they can represent the pattern in the best possible ways and hence provides idea about the agricultural water supply. However, the versatile complexities in gate operation, river inflows, and outflows pose a severe challenge to policymakers, engineers, scientists and environmentalists. Further, without any indigenous soil health records, it becomes difficult to establish a suitable cropping pattern for increasing land and water productivity. India is an agricultural country and with a pretty good amount of rainfall. However, covering more than 50% of the total cultivated area in India, rainfed agriculture contributes only 44% to the national food basket (Sharma 2011). Moreover, rice is the principal food crop cultivated in kharif season and mainly grown under rainfed conditions. Due to various constraints such as irrigation and poor socio-economic conditions, rice-fallows are practiced extensively covering more than 70% of total area in South Asia. If this lasts, the imbalance of agroecosystem is endorsed in the future. It emphasizes the need for a proper management plan to confront the future that involves shrinking land and water resources. Better agricultural management requires the future projection of water demand and supply. Despite this, it is challenging and uncertain since it depends on future policy implementation and the changing of the human attitude towards food choice. Therefore, the management planning is done based on the assumption that the same ‘as usual’ cropping plan will prevail in future. Many studies have been performed focusing on optimal crop area planning depending on available water resources (Brahmanand et al. 2021, Hao et al.,2018). However, catchment-scale studies that can increase both crop productivity and water resource efficiency, are required. These efficient management practices are likely to perform more efficiently if they are applied considering soil nutrients and climate change impact. Such needs have motivated this research work to visualize the climate-induced future cropping scenarios of the rice-fallow areas of South Asia in a more detailed way.

1.3 Objective and Scope of the Proposed Research Work

The specific objectives of the study are as follows:

1. To assess the effect of fertilizer application on nutrient balance and paddy yield in rainfed under unsubmerged conditions in rice-fallow cropping system using farmer participatory approach
2. Optimization of cropping pattern and suggesting the best cropping plan in the fallow period for intensive cultivation incorporating residual nutrient
3. Development of hybrid Artificial Neural Network (ANN) based hydrological model in a rain-shadow river basin using iterative input variable selection approach from GCM outputs for the projection of agricultural water supply.
4. Development of a statistical downscaling model for temperature projection and develop a crop water demand model using temperature–based ET model for future projection of agricultural water demand.
5. To assess the combined impact of demographic growth and outcomes of optimization, hydrology, and crop water demand model on supply-demand gap

1.4 Organization of the Thesis

The complete work is divided into several stages and is presented in different chapters as shown below:

Chapter-2 presents a brief description of the literature survey reported in the past by several researchers worldwide, relating to the topics selected for the present study. All kinds of literature related to the nutrient balance of rice cropping system were initially reviewed to identify the potentiality of subsequent crop production through irrigation. Previous studies pertaining to irrigation planning for crop diversification are included in this chapter. Literatures including methods for development of hydrological model and modelling of ET for irrigation water requirement are briefly described. Later climate change impact studies were reviewed. Finally, a critical appraisal of the reviewed literature was done to identify the goal of the present study.

Chapter-3 details the canal command area as a case study, its associated river and various databases used for the present research work.

Chapter-4 features the nutrient balance sustainability indicator in a rice cropping system. The subsequent impacts at the arable area due to farming activities through a participatory approach and scientific investigation are detailed in this chapter.

Chapter-5 brings forth the pathway for the model development process for crop area planning in fallow areas in the winter season after rice harvest. The model was then applied in the study area for illustrating its effectiveness.

Chapter-6 delivers the general methodology for temperature and precipitation downscaling. Here, the detailed technique for interpolation of gridded GCM data, bias correction is mentioned. Further, results of the downscaled model are utilized for temperature-based ET model development for the study area, which is then finally used for water supply-demand projections.

Chapter-7 presents the methodology for developing, calibrating, and validating the hydrologic ANN model. Further, river inflow for future time period is assessed under changing climate to quantify the amount of irrigation water available upstream of weir in the study area. Analysis of uncertainty pertaining to the GCM and RCPs are also presented in this chapter.

Chapter-8 involves the methodology for modelling of ET for assessing future water demand in the canal command area under changing climate.

Chapter-9 features the complete research work summary and its conclusion. Finally, the thesis is concluded with a brief overview of the limitations and possible future scopes of research.

Chapter 2

Literature Review

2.1 Introduction

During the past few decades, several researchers have contributed to understanding agricultural sustainability in various parts of the world. Further, the significance of climate change impact studies on river basin and how it is affecting the agricultural water demand-supply are highlighted for its application to agriculture areas while emphasizing rice-fallows of India. This chapter begins with an overall view of various sections and literature available on these sections. The various sections including rice nutrient uptake due to fertilization practices, and alternate wetting and drying of rice cultivation are reviewed to realize their practicality in the field of sustainable agriculture. In the subsequent sections optimal area planning for crop intensification and the implementation of climate change impact analysis through various downscaling techniques, are also reviewed in brief. A critical appraisal of the above pieces of literature has been introduced based on which the purpose of the research study was finalized.

2.2 Dynamics of nutrient uptake

The root uptake mechanism of various macro and micronutrients varies according to the soil moisture conditions. Some literature available on nutrient uptake dynamics are discussed below:

Zhang et al. (2012) observed two cultivation methods: dry and moist conditions for both upland (Zhonghan 3) and paddy variety of rice (Yangfujing 8). Results showed an increase in grain yield with an increase in phosphorus level. It also increased the nutritional quality of paddy rice and the head-milled rice rate and appearance quality of both upland and paddy rice. The overall comparison showed that upland rice had better processing and palatability properties.

Nishiyama et al. (2016) observed the uptake of Cs, K, and Rb (total, exchangeable, and water-soluble fractions) in rice soil-plant systems in two different land use conditions (Paddy and upland) for 13 different rice cultivars. Results showed that the soil concentrations and nutrient concentrations Cs, K, and Rb were higher under upland conditions than paddy conditions, except K in upland cultivated in brown rice, which was absorbed by the roots through ion diffusion.

Tisminia et al. (2014) investigated the N uptake in two rice-based cropping system with residues removed and remained at soil test-based fertilizer application and farmers practice. Linear relationship was established between annual N application and total system productivity and Annual N uptake and total system productivity. With no losses considered N fertilizer showed positive balance of 24-190 kg ha-1 whereas no N fertilizer showed negative balance of 40-49 kg ha-1.

Saenchai et al. (2016) investigated the Fe and Zn distribution of 15 genotypes of rice grown both under aerobic and wetland soil. The grain concentration was 3-4% and 54-74% in Fe and Zn for all the varieties grown under different conditions. Nutrient concentration in endosperm increased with an increase in grain allocation of nutrients to the endosperm and decreased with increased allocation to rice bran.

2.3 Alternate wetting and drying in rice cultivation

With erratic rainfall and climate change impact, cultivation of rice in kharif season undergoes unsubmerged conditions such as alternate wetting and drying. Most of them, however, come at the cost of decreased yield. Better yield with minimal water can only be executed by integration of water management with proper crop variety selection and best farm management practices used for cultivation. Therefore, a rice productivity scenario assessment in a relatively dry period is required.

Moya et al. (2004) investigated the farm profitability at two sites with different water management practices within the Zhange Irrigation system for 2 years 1999 and 2000. However, farmers do not practice AWD or continuous flooding in a complete manner. Thus, an AWD score depending on the frequency of soil drying helped in the comparison. No significant correlation was found between AWD score and yield or input use. However, AWD saved water without hampering produce or the farm benefit-to-cost ratio.

Won et al. (2005) compared the effects of various water treatments like very shallow intermittent irrigation (VSII, 2cm), shallow intermittent irrigation (SII, 4cm), and traditional deep-water irrigation (DWI, 10cm) on rice growth and yield in the field for two years. Rice growth and grain yield were not significantly influenced by the treatments besides increasing water productivity in low water use technique. However, with a shallower depth of irrigation enhanced, the lodging resistance is due to the development of deeper roots in the paddy soil.

Feng et al. (2007) developed the ORYZA2000 model for the year 2001-2004 for Kaifeng, Henan Province, China in both lowland and upland varieties of rice. Results showed that During field AWD conditions saved up to 40-70% water in the lowland area while providing a similar yield of 8t/ha as in flooded conditions with 900 mm of water input. Whereas, aerobic rice in the upland area yielded up to only 3.6t/ha, using up to 1100 mm total water input. The model performed well and the model outputs were measured such as biomass, leaf area, and N uptake along with soil water variables like ponded water depth, and soil water tension.

Dong et al. (2012) compared N cycle processes as well as agronomic parameters of AWD and CF water management schemes in Mekong delta alluvial soil. It was found that volatilization losses were more in the case of AWD than in CF. However, no difference was observed in the recovery of fertilizer 15N labelled urea in the surface and deeper layer of soil. Nitrification-denitrification process was 6 times more in AWD than in CF. However, it removed the insignificant amount of fertilizer N which is 2.5%. There were no significant differences among the water treatments for agronomic parameters like plant N uptake, aboveground biomass, or grain yield. Further, the contribution of Fertilizer N is only 20% in plant uptake. It may be due to the initial deposition of N during the flooding season.

Cesari de Maria et al. (2017) compared the water use efficiencies of three water management techniques: Water seeding-continuous FLooding(WFL), Dry seeding-delayed FLooding (DFL) and Dryseeding-intermittent IRrigation (DIR) for 2 years. Results showed that DFL and DIR reduced water use by 20% and 60% of WFL. The yield was decreased by 3% and 28% for DFL and DIR respectively compared to WFL. Results suggested that yield was affected by groundwater level along with environmental factors. Results also showed that first flooding decreased the soil porosity and hydraulic conductivity.

Tan et al. (2013) examined and compared the effects of Alternate Wetting and drying (AWD) and Continuously Flood Irrigation (CFI) water and nitrogen productivity. Results confirmed that AWD declined the irrigation water amount and percolation losses. However, percolation losses were more during the initial days just after the application of irrigation water. Also, nitrogen fertilization gave better yield but at the cost of nitrogen productivity. The volatilization losses were the same for both the water treatments except NO_3-N which was higher for AWD. AWD increased the NO_3-N loading to groundwater and are potential to groundwater pollution.

2.4 Nutrient balance as a sustainability indicator

High fertilizer inputs have serious threats to the environment. Monitoring and investigation of cultivation system are required that aims at designing, examining, and delivering more sustainable practices. Nutrient-budget and nutrient-balance models must rely on a series of assumptions in order to deal with complex nutrient systems. Many nutrient-budgeting exercises treat soil-dynamics processes as a black-box. The basic data for nutrient inputs and outputs are usually selected from literature and production statistics (FAO, 2003). A flow chart diagram of various inputs and outputs are as shown in Fig. 2.1

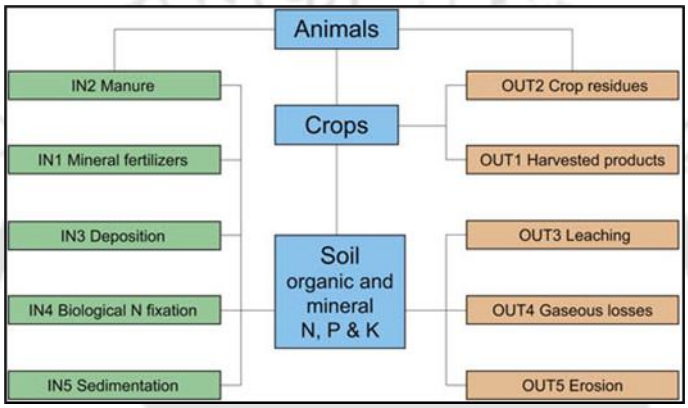

Fig. 2.1 Nutrient flows in the soil (FAO 2003)

De Jager et al. (1998) performed nutrient balance in farm level to monitor nutrient depletion in Kenya using NUTrient MONitoring (NUTMON) model. The average N and K balance was negative and P balance was slightly positive. Net farm income shows no correlation with nutrient balance. The nutrient replenishment cost accounts for 32% of the farm income. Further at crop level, cash crops gave higher profit and less nutrient mining whereas food crops showed more nutrient mining with less income.

Cho et al. (2000) performed nutrient balance during a period of 1 year to study the flux and balance of nutrients in the rainfall, irrigation water, runoff water and infiltration water in the paddy field of Central Korea. It was found that 68.6% and 16.7% of N and P were lost by rainfall-runoff with more amount of nitrogen during fertilizer application. Also, it showed that loss was more until the reproductive growth of crop. Moreover, the loss ratio in infiltration for N and P were 9.4% and 0.6% respectively.

Bindraban et al. (2000) suggested two indicators for the sustainability of agricultural land. They are the yield gap and soil nutrient balance. The evaluation of soil nutrient balance which is the input/output of nutrients in a system and its change over a more extended period can be used as a sustainability indicator. The yield gap is calculated under three levels: potential, water and nutrient-limited. Results suggested that the rate of soil nutrient change and the soil nutrient stock of an agricultural system should be considered.

Dang (2005) performed soil-plant nutrient balance in the tea plantation system. Various age groups of tea plant are considered in the study. Nutrient N, P, K, S and Mg in the tea stands was more in young leaves than in old stems and no effect of age on tissue concentration of N, Ca or Mg. Results highlighted that though there was no shortage in meeting crop demand for nutrients through fertilizer application, other nutrient losses should be considered for complete nutrient budget calculation.

Aticho et al. (2011) assessed soil N, P and K nutrient balance at farm level for both resource poor and prosperous farmers in Ethiopia. However, the soil depletion rate did not correlate with wealth of farmers but had significant relationship with the rate of N and K application. Thus, sustainable soil fertilizer management practices should be adopted among all groups of farmers depending on the landscape.

Bassanino et al. (2011) identified five Macro Land Units (MLUs), a larger unit of ALUs using GIS in a Po River basin. Euclidean distance was used as the separation method. Calculation of farm-scale characteristics (farm types, stocking rate, land use, and management) and nutrient budget indicators was performed using IRENA European method (GB = fertilizers + manures + others – harvested). The highest positive nutrient surpluses (103, 39, and 95 kg ha-1 for N, P, and K, respectively) were found in the most intensely managed area. N surpluses were due to excess mineral inputs whereas P surpluses were to excess organic inputs.

Phong et al. (2011) evaluated nutrient balance using NUTMON model in 11 farms where integrated agriculture-aquaculture farming took place in Mekong Delta. It was found that N, P, K surpluses were there for all the systems. However, the vegetable fields had the smallest nitrogen surplus while the rice field system saw the most minor excess of phosphorus and

potassium. The positive nutrient balances suggested that soil fertility will be maintained at the risk of environmental contamination in all the systems.

Minhas and Yadav (2015) used nutrient balance approach to monitor nutrient input-output in various production system irrigated with untreated sewage water (SW) and good-quality groundwater (GW). They found that nutrient uptake increased with NP doses and SW though the same uptake was there with reduced NP doses in the case of SW as compared to GW. Further with positive nutrient balance in case of SW improved soil microbial population. Less water-requiring crops are recommended for minimizing groundwater pollution and fertilizer costs.

Carmo et al. (2017) carried out nutrient balance at a national scale in a long term cultivated soil of Potugal. It was found that there was constant negative N balance and positive P and K balance in 1951-56. The negative N balance was rectified through chemical fertilization in 1960s and thus the 1950s is the inflection point from where the change from organic to mineral fertilization took place.

2.5 Optimization techniques

The optimal use of available resources especially land and water is crucially important in the context of the increasing food quantity, fibre, and other crop demands of the rising population worldwide in the face of shrinking resources. These resources can be utilized optimally while increasing the farm economic benefit can be achieved by exercising various optimization techniques. Some of the literatures available on crop planning related to crop diversification are discussed below:

Li et al. (2014) attempted to develop a two-stage stochastic programming model considering randomness in river flow levels. Results gave a real-world picture to the decision-makers allocation of water for crop irrigation under various flow levels while achieving higher farm income, especially in a water-deficit region. In addition, sensitivity analysis helped realize that the trading efforts' trading costs could become ineffective under high trading costs.

Su et al. (2014) prepared a multi-objective optimal allocation model for agricultural water resources with three objectives: maximum net farm income, minimum fairness difference in water utilization by each sector, and full utilization of green water utilization. The results

showed that by decreasing the cultivation of food crops and increasing cultivation of cash crops in the study area, blue water use efficiency for various sectors can be improved in the river basin.

Galán-Martín et al. (2015) developed a multistage linear programming model in each agricultural region to identify the optimal cropping plan to maximize the farmer's net return in each area under three 'greening rules'. Furthermore, the model can estimate the minimum subsidized value that would help apply greening rules and promote adopting more agricultural practices sustainably.

Kumari et al. (2017) developed multiobjective programming to evolve optimal cropping patterns to increase farm income and minimum irrigation water use in eastern Uttar Pradesh. As a result, the cropping pattern has shown an increase of 7 % in farm monetary benefit and a reduction of 6 % in irrigation water use from the existing condition.

Xie et al. (2018) developed an inexact stochastic-fuzzy programming model to consider the uncertainties and limitations in agricultural water management. It includes both stochastic variable in the right-hand side and fuzzy coefficients in the left side of constraints. The model was aimed at water resources and cropland resource allocation. Several scenarios corresponding to the different fuzzy probabilities of violating constraints are investigated to get the best management approach and find trade-offs between varied system profit and risk of system failure.

Ren et al. (2019) presented an improved multi-objective stochastic fuzzy programming method with a planning objective of benefit, maximum agricultural water productivity, minimum irrigation area. Analytical Hierarchy Process (AHP) was used to form the MOP. Chance constrained programming for uncertainty in water supply and fuzzy sets such as irrigation quota and water costs for Wuwei city. It was found that at probability 25% water demand could not be satisfied. Further there is variation of crop area such as potatoes, other vegetables and cucurbit, which have the same characteristics of higher yield with less irrigation than other crops.

Li et al. (2020) developed an integrated MONLP (Multiobjective Nonlinear Programming model) that considers the water-energy-food through two objective functions and constraints. Uncertainties caused by natural conditions and human activities complicate the optimal allocation. The integrated model, AWEFSM (Agricultural Water-Energy-Food Sustainable

Management), could establish interrelationships and trade-offs among system input-outputs, such as water, energy supply-demand, land demand, and food production considering the uncertainty in resources. Further quantification of water and energy footprints was done under various scenarios.

2.6 Climate change impact on temperature and evapotranspiration

Climate change varies temporally and spatially. Change of climatic variable influences the water cycle components such as potential evapotranspiration, soil moisture etc. Several studies assessed IPCC report and various understanding and summaries on climate change response and impact have been published. Few pieces of literatures have been reviewed as follows:

Zarghami et al. (2011) employed the LARS-WG downscaling tool for the General Circulation Models (GCM) in six stations. 3 emission scenarios, A1B, A2 and B1, were assessed for the three periods: 2020, 2055 2090. The research results showed an annual rise in temperature and decline in precipitation of 2.3°C and ~3 respectively in the mid-century. Thus, making the region shift from semi-arid to arid. Further ANN was built to quantify the effect of climate change on three watershed of the region which showed flow reduction drastically.

Mo et al. (2017) utilized the GCM model for the projection of climate change's impact on crop water demand and ET on the North China Plain (NCP). Results showed that by 2050, elevated CWD and ET will reduce moisture due to effective precipitation to about 4% to 24% along with the increase in irrigation water demand during crop growing season. Several possible mitigation options for sustainable agriculture have been identified. Further study findings also suggested that a decrease in winter wheat sowing area by 3% to 15.9% in water-scarce areas can be an adaptation strategy to mitigate water deficit due to climate change.

Li et al. (2020) developed two global warming scenarios of 1.5 °C and 2.0 °C for the rainfed north Kazakhstan and irrigated Fergana regions. Results showed that the average crop water requirement (CWR) raised by 13 mm and 19 mm/year for 1.5 °C and 2.0 °C compared to the 1976-2005. The water supply - demand was analysed to find a magnification of 2.8×10^8 m³ and 1.5×10^8 m³ respectively. However, with increased precipitation the gap in global warming scenario of 1.5 °C could be reduced. Study results suggested that water budgeting of major cultivation areas in water-stressed Central Asia could deliver a science-based sustainable evolution of such areas.

Singh et al. (2021) assessed the irrigation water supply- demand using spatio-temporal and statistical techniques. The mean annual total water requirement for the study area was 7002 ± 852 Mm^3 during 2004–2013 period. Among the crops cultivated, Boro paddy was the highest water-intensive crop. The mean annual dynamic groundwater reserve (DGWR) in the study area was quantified as 5169 ± 782 Mm^3. Results showed that during 'normal,' 'dry' and 'wet' years, 28, 25 and 35 blocks were represented as 'water surplus', respectively. DGWR can be a possible mitigation option in water-limited conditions to lessen the demand–supply gaps in the neighbouring blocks.

2.7 Machine learning methods for hydrological modelling

Hydrologic time series forecasting has been a quite difficult task, requiring an ample amount of data and associated uncertainties due to parameters. Machine learning methods has become quite common in recent decades for the analysis of such non-linear variables in river flow regime forecasting using minimal data. A handful of literatures has been described in brief as follows:

Ahmed and Sarma (2007) generated synthetic streamflow series, using five different statistical methods in the Pagladia River, a tributary of the Brahmaputra River. On comparison with Thomas-Fiering model autoregressive moving average (ARMA) model and ANN model, an ANN based model performed superior to other models.

Sarma et al. (2015) employed the ANN model and SVM for the simulation of daily runoff and sediment yield in a Nepal watershed, Kankaimai with historical data from 1995 to 1999 for runoff prediction and wet season data from 2001–2003 for sediment yield prediction. The model evaluation confirmed that SVM performed slightly better than ANN.

Jimeno-Sáez et al. (2018) developed both ANN and SWAT for generating various levels of flows through flow duration curves in the two watersheds of Spain having contrasting climate. The flow levels were very low, low, medium, high and very high. Results specified that both the models performed equally well for daily runoff modelling. Though SWAT performed better for low flow simulation and ANN was good at higher flow simulation.

Liu et al. (2019) coupled the Climate Forecasting System (CFS) precipitation with the Soil and Water Assessment Tool (SWAT) to predict the short period, 9 months ahead streamflow for the Cascade Reservoir System of Han River (CRSHR). First, CFS precipitation was compared

with the observation and was processed using two machine learning techniques such as random forest and support vector regression. Findings showed that the correlation coefficients processed precipitation and observed one is 0.91–0.96. The developed regional SWAT was calibrated against CRSHR. The efficiency of the model varied from 0.84-0.86 for three reservoir flow simulations. Results also confirmed that prediction for long-term using historical observed value was better compared to CFS. showed that for three reservoirs, long-term streamflow forecast with similar historical observed distribution was more accurate than that with the original CFS.

Hassan and Hassan (2020) employed ANN for the estimation of runoff by integrating the satellite-based Snow cover area (SCA). The performance of models is assessed based on several performance indicators, namely, Nash–Sutcliffe Efficiency, Root Mean Square Error, Variance, and BIAS. Further, the model was compared with the model developed using only gauge discharge data. The findings of the study suggested that the effectiveness of the ANN hydrological model established for mountainous watersheds could be refined by coupling the river gauge discharge with SCA.

Parisouj et al. (2020) developed and evaluated the three widely used machine learning algorithms (Support Vector Regression (SVR), Artificial Neural Network with backpropagation (ANN-BP), and Extreme Learning Machine (ELM) for four river basins of the USA at both monthly and daily scale. Study results suggested that all models performed well at a monthly scale than at daily levels. Further results also showed SVM as the best-performing model except for the snow-fed river of the USA.

Meshram et al. (2021) developed, three AI techniques (ANFIS, GP and ANN) for streamflow projection of the Shakkar watershed, Narmada River, India. As input to the models, precedent streamflow and cyclic terms are utilized to derive the output. Models were evaluated with a range of performance criteria such as RMSE, MAE, CORR and CE. Results showed that the ANFIS has the best performance followed by GP and ANN. Results also showed that models considering the cyclic terms served better than model considering only the precedent streamflow.

Liu et al. (2022) integrated climate variable projections, machine learning and hydrological model simulations to predict hourly runoff in the Yantan catchment, downstream of reservoir.

Results show that the model prepared by hindcast during the rainy season from 2013-17 reduces the probabilistic and deterministic errors by 6% than the traditional approach during the first 7 days. The deterministic error can be further reduced to 6% in 72 hours when combined with Long-Short term memory (LSTM). Nevertheless, the prediction quality of LSTM reduces when using only climate variable projections.

2.8 Climate change impact on hydrology and irrigated agricultural area

Irrigation is crucial for crop production and area expansion for increased productivity with demographic growth. However, climate change has vital importance in affecting agricultural water availability. Literatures reviewed on the management of water resources for people's livelihood are described below.

Saharia and Sarma (2018) investigate the impact of climate change on two tributary river basins of Brahmaputra, Assam, India: Bharalu (urban basin) and Basistha (rural basin). Historical data showed that 98.78% of the generated streamflow was by surface runoff, compared to 75% for the rural basin. Results of the comparison of hydrologic processes showed that urban basin had relatively lesser streamflow, actual evapotranspiration, surface runoff for 2050s and 2090s as compared to rural basin. Further results also confirmed that, there is increase up to 2.20 m^3/s for the rural basin and decrease up to 0.46 m^3/s for the urban basin.

Abeysingha et al. (2020) studied the impact of climate change on Gomti river basin employing the SWAT model. Multiple GCM was used for generating climate change scenarios. Results showed that rainfall in winter season declined, however there was annual increase in rainfall in all the three future periods which increased the streamflow annually up to 18% by the end of the century. Amount and frequency of high flows was found to increase up to 27.3% and 87% respectively for different RCPs.

Kaini et al. (2020) quantifies the climate change response on hydrological behaviour of the Koshi river basin and its subsequent impact on nearby agricultural area utilizing RCPs for near century and mid-century. Results showed that future irrigation supply in the catchment would increase with increase in average flow of the river. Further projection of average minimum monthly flow suggested that winter wheat and monsoon paddy rice crop areas could be increased. Also, late sowing of paddy rice by 1 month was also recommended to avail the most of the river water.

Dutta and Sarma (2021) built on the SWAT model for hydrologic assessment of the data-limited Brahmaputra River basin in three outlet locations along the mainstream. The model showed good results for observed flows at the tributaries with a satisfactory correlation of R^2 = 0.77 at Golaghat station.

Gupta et al. (2021) employed the soil and water assessment tool (SWAT) for the Subansiri river basin for hydrological simulations using the observed period of data for the year 2002–2013.After the training and testing of the model, parameter sensitivity analysis, uncertainty and quantification of parameters were performed with sequential uncertainty fitting (SUFI2) program of the SWAT. Model performed well and precipitation and temperature projections showed an annual rise in maximum temperature (Tmax), minimum temperature (Tmin), and rainfall of the catchment. These projected climatic variables were used as the primary input in the hydrological model for the projection of the streamflow for the period of 2016–2100. The flow duration curve analysis of streamflow projections reveals an increase in the discharge.

Li et al. (2021) utilized the SOBEK model to assess the downstream inundation that occurred by the typhoon event of the 20th century and subsequently project typhoon events for the period 2075–2099 in Taiwan, Arunachal Pradesh. Results showed that Agricultural lands were the worst condition areas and flood affected area raised by 1.89 times. Several adaptation strategies were devised especially for the upland crops using both engineering and traditional methods and these options yielded higher benefit as compared to “do-nothing” option. The benefit to cost ratio was around 1:16.

2.9 Critical appraisal of reviewed literature

From the review of various literature, it has been found that the sustainability of agriculture can be assessed through nutrient balance studies in the agricultural field. Sustainable agriculture guides the safe use of limited natural resources such as soil and water to ensure quantitative and qualitative agricultural production at affordable costs which the burgeoning world population demands. As soil is the major source of the nutrients that helps to grow good and healthy crops it should be enriched with natural fertilizers such as organic, green manure and compost rather than chemical fertilizers. Much of the chemical fertilizers applied to agricultural fields are lost to the environment (Bennett et al. 2001; Galloway et al. 2008; Seitzinger et al. 2010). Various chemical fertilizers are applied containing nitrogen, phosphorus and potassium which increases yield but unbalanced use of these fertilizers can be harmful to

the environment. In most soils more than 50% of the nitrogen applied as fertilizer is lost to the environment through leaching, surface runoff, denitrification and ammonia volatilization (Cho et al., 2000; Anas et al. 2020). Excess phosphorus and potassium get sorbed into the clay particles becoming unavailable to plants and eventually lost to the waterbodies as runoff or leaching. Hence fertilizers when used without the proper prior knowledge of indigenous soil nutrients already present resulted in soil degradation and eutrophication, decreasing resource use efficiency and eventually endangering sustainability. Reviews also confirmed that various fertilization management should be done to optimize fertilizer use by considering the soil texture, indigenous soil nutrient content and prevailing climate of the area.

Additionally, water is a vital part of agriculture that helps sustain life and transport nutrients from soil to plant through transpiration. Along with fertilization, water management practices are followed using water saving technologies like AWD, aerobic rice which is used for paddy cultivation to increase the water productivity. Though there was no interaction between water and N uptake by rice crops, increased fertilization, especially during basal fertilization, can cause nitrate leaching in AWD, thereby decreasing NUE due to nitrification during the drying cycle but it can be reduced to some extent by straw retention. Furthermore, various water conservation measures such as contouring and mulching helps prevent the water flow. Also, it has also been found that for the yield to be increased in AWD treatment, along with shallow groundwater conditions there must be relatively impermeable soil layer below the puddled layer to trap the nitrified N for the plants to uptake (Feng et al., 2007; Tan et al., 2013). Adding to this shallower irrigation in AWD helps develop roots in the deeper layer rather than in the shallower layer of soil (Won et al., 2005). This helps prevent N leaching loss thereby benefitting the crop along with the increase in lodging resistance of the rice plant.

Climate change due to global warming directly affects the global water cycle. The rate of change for the 21st century is expected to be intense for both precipitation and evapotranspiration, consequently the irrigation water demands. The Intergovernmental Panel on Climate Change (IPCC) assessment indicated that global mean temperature is projected to increase by 2.3∘C by the 2090s compared with that of the 2000s under the high emission scenario (A2), while global annual precipitation would increase by 16.9%. The irrigation water requirements of the crops change as a function of climate change. Climate change, high demands for limited water resources, and agricultural goods for food security have highlighted the need for effective water management techniques. Several authors have focused on assessing the impacts of climate change on agriculture and water resources (Batool et al. 2019; Nikolaou

et al. 2020). It has been found that in streamflow forecasting under changing climate, temperature and precipitation are the hydrological model's key components (Berghuijs, Woods, & Hrachowitz, 2014). And to study the effect of water balance components on crop production and to develop various adaptation strategies, models like SWAT, ANFIS, GP, ANN are used.

It has been noticed that rainfall in representing hydrological phenomena related to the soil water storage concept and, finally the construction of the flow at the basin outlet. The second method depends on the precipitation-temperature-elasticity of precipitation on streamflow. For example, a slight increase in rainfall, a large temperature increases while a slight decline in rain, and a significant temperature decrease would reverse the rainfall effect on streamflow. The hydrological modeling with the former approach typically operates on windward side of mountain and can range from conceptual to physically-distributed R-R models. R-R models have been widely used for streamflow in river basins, as they generally provide good prediction accuracy, no orographic influence, and comprehensive data are available. It has also been noticed in the reviews

Data-driven methods are commonly based on regression and machine learning techniques. Neural Network approaches represent nonlinear hydrological processes such as predicting reservoir inflow and rainfall-run-off. Artificial neural networks (ANNs) are Multi-layer perceptron (MLP) techniques, which typically use a backpropagation algorithm for training of the network. More studies evaluate the efficiency of ANN for streamflow simulation compared to other models (Meshram et al. 2021; Parisouj et al. 2020). But there are a few works that have been done in a real irrigated agricultural field in a rain-shadow area where drought-like conditions prevail for rice cultivation and the remaining year remains fallow. Also, there is a need for optimizing the fertilization and water management practices in the downstream part to increase the sustainability of agriculture in a rain-shadow area without affecting the yield of paddy and hence adopting a cropping system that would help in mitigating the adverse effect of climate change.

Chapter 3

Study Area and Input Data

3.1 Introduction

The Jamuna River basin, one of the longest river of North-east India, sub-tributary of the mighty Brahmaputra has been selected as the study area of the present research study. It incorporates the river originating from the Khumbaman hills of the Diphu sub-division (Karbi Anglong) up to the barrage gate and the Jamuna command area. This chapter is presented to discuss the study area including its climate and hydrology. The study area extends from 25º40'N 92º50'E to 26º20'N 93º40'E. This chapter also includes the input data used for the present study objectives for their utilization in various models developed for the research study.

3.2 Jamuna River Basin and Command Area: An Overview

The Jamuna River basin situated in the Nagaon and Karbi Anglong districts of Assam, India, is a tributary of the Kopili river. River and the basin length cover an area of 3903 km^2. The river basin is bounded on north by Mikir hills, east by Nambor Reserve Forest and south by Dhansiri Reserve Forest, forming the eastern and southern boundary of the study area. And on the basin's western side lies the river Kopili, a major tributary of the Brahmaputra. Basin elevation varies from 57 m to 1360 m above MSL. The Jamuna watershed experiences a sub-tropical monsoon climate with some variations due to its location. Most of the catchment is hilly, and forest cover is around 48% of the basin area. The index map of the study area is shown in Fig. 3.1.

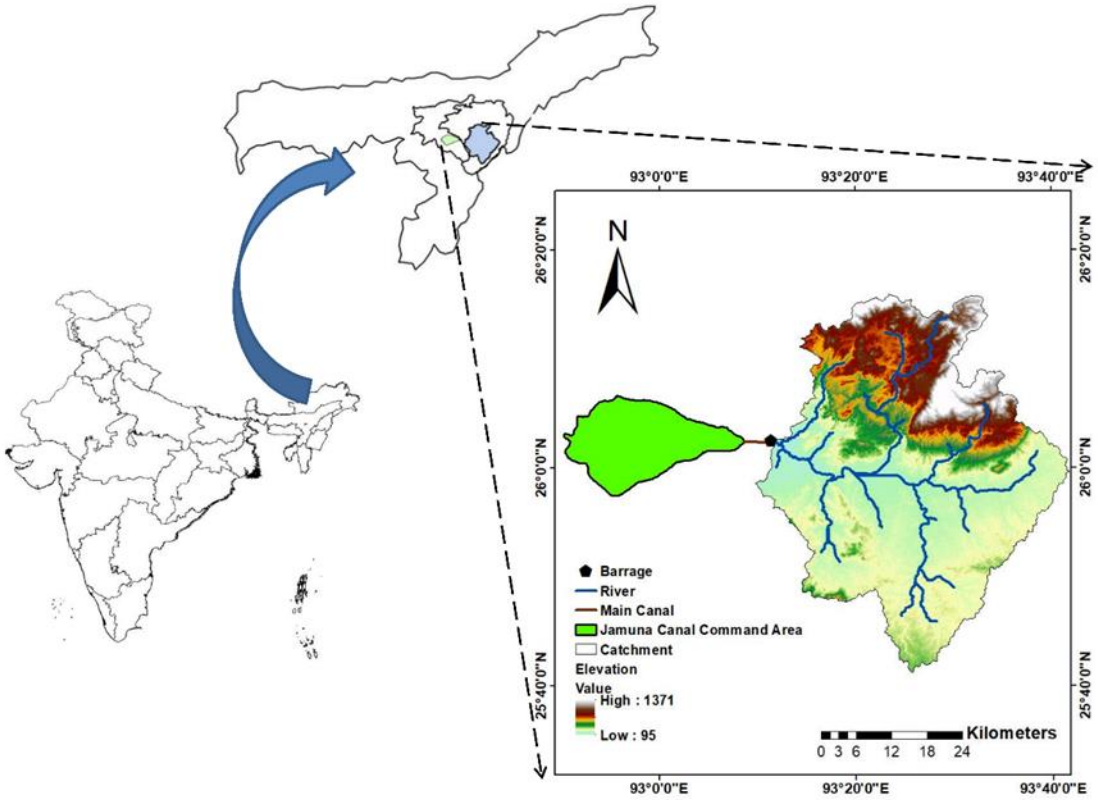

Fig. 3.1 Location map of the catchment area of Jamuna River down the valley up to the Bakuliaghat barrage for irrigating the Jamuna canal command area

The Jamuna command area lies between 25°45′ N 92°48′E and 26°4′N 93°15′E on the left bank of Jamuna River. The river feeds the command area from the barrage outlet situated at Bakuliaghat, Karbianglong. It is bounded by the Jamuna River on the north and by Kopili river on the south west. The Dimorunala, a tributary of the Jamuna River, flows through the command area. The Jamuna command area is uniformly graded and slopes less than 2%. The general elevation of the command area ranges from RL 97.5 m to RL 62 m. It is covered with laterite soil. Early Sali paddy is irrigated in large scale by the farmers living there, during the kharif season and remains fallow for rest of the year. Though, some amount of Ahu and vegetable cultivation is also done in some parts (JCADD Project report).

3.2.1 Climate

The Karbi Anglong plateaus on south and south-east along with Mikir hills on the north bordering the catchment, creates barrier for the moisture-laden winds thereby turning out the area as a rain-shadow zone. Further, the command area, also lies in the rain-shadow area of Khasi Jayantia hills and the Barail ranges. Thus receives an average total precipitation of 118cm

of which around 54% lesser than the state average. 80% of the rainfall is experienced during June to September. The highest amount of rainfall is received during July and August. The post monsoon month from November to February are generally dry. The normal annual temperature in the basin varies from 27°C to 33°C during summer and 16°C to 24°C during winter. The command area's monthly average pan evaporation data is approximately 7 cm.

3.2.2 Hydrology and water supply

A weir fabricated at the Bakuliaghat is used to tap the water of river for diversion to the canal command area as shown in Fig 3.2, for irrigation. An area of 27,705 ha is irrigated through main canal, distributaries, minors and sub minors. The watershed area of Jamuna River up to Bakuliaghat wear is 1869 Km^2.

Fig. 3.2 Diversion weir at Jamuna

3.2.3 Data description

3.2.3.1 Soil data and rainfall data

Soil map of the command area was obtained from the Office of The Assistant Director of Agriculture Soil Survey, Ulubari, Guwahati, Assam. Soil texture information of the study area was collected from the book, published by National Bureau of Soil Survey. The soil map and texture information were used to prepare the digital soil database of the study area. The soil map was scanned and exported to ERDAS IMAGINE 9.1. The boundaries of different soil textures were digitized carefully. The polygons represented by various soil categories and properties were assigned from the collected data in different soil profiles. The soil for the catchment is classified mainly on the percentage of available sand into various texture groups as Fine, Fine loamy, Loamy and Coarse loamy as shown in (Fig. 3.3).

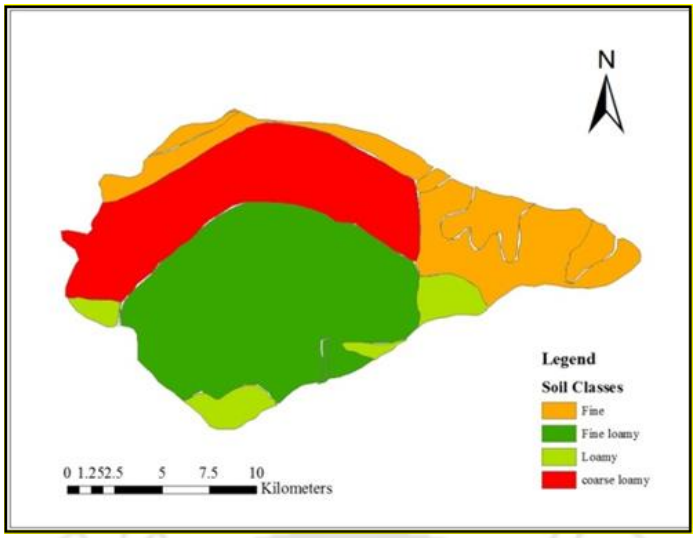

Fig. 3.3 Soil map of Jamuna Command Area

3.2.3.2 Sampling and Analyses

In the downstream part of Jamuna Command Area (JCA), 13 villages were randomly sampled where highly productive paddy fields are supplementarily irrigated with JCA canals. Soil samples were taken from a point in the field at depths 0-10, 10-20 cm using point sampling method (Harrell, 2014) at three points in the field, as shown in Fig. 3.3. Plant sampling was done collecting 3 to 4 plant samples from the same field using Global Positioning System (GPS).

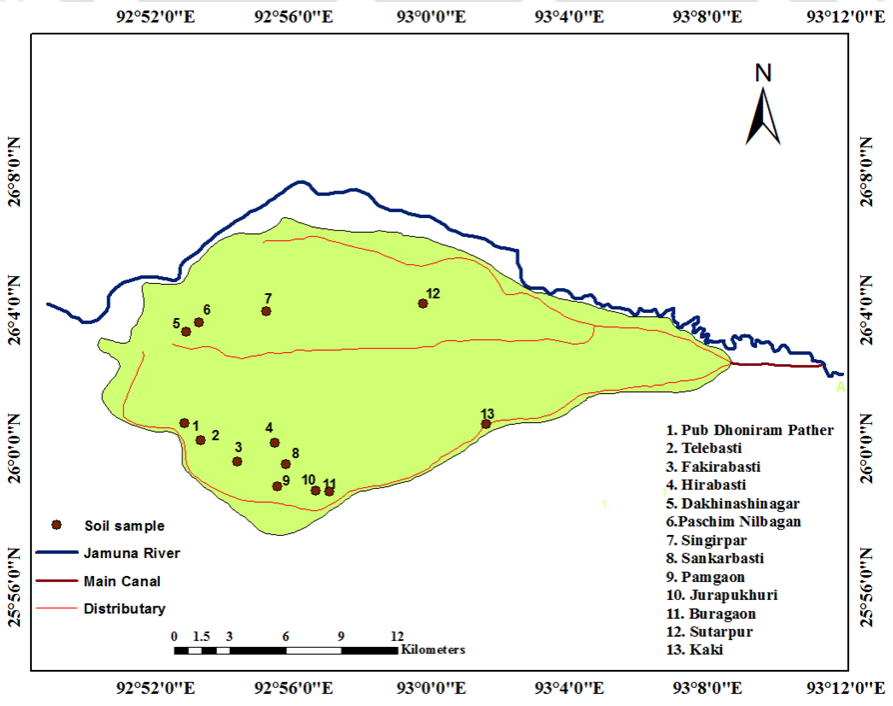

Fig. 3.4 Geographical distribution of sampling villages in the Jamuna Command area of Assam

Water samples were collected from the river and the main canal at 60% depth (Ongley, 1996) using water sampler. The river and main canal were of shallow average depth of approximately 2.5 m and 1.2 m respectively. Various parameters were analysed in the irrigation water as well as the river water that was tapped for irrigation for measuring its chemical properties. The list of parameters along with irrigation standard from FAO is as given Table 3.1 below:

Table 3.1 Chemical properties of irrigation and river water

Parameters	Range	Jamuna river	Irrigation water
EC(µS / cm)	0-3000	90.1	105.8
pH	6-8.5	7.53	7.47
SAR(mmole/l)$^{0.5}$	0-15	0.41	0.44
Ca^{2+}(me/l)	0-20	0.185	0.22
Mg^{2+}(me/l)	0-5	0.15	0.18
Na+(me/l)	0-40	0.17	0.20
CO_3^{2-}(me/l)	0-1	BDL	BDL
HCO_3^-(me/l)	0-10	0.61	0.66
Cl^-(me/l)	0-30	0.08	0.06
$SO4^{2-}$(me/l)	0-20	0.125	0.120
NO_3^--N(mg/l)	0-10	BDL	BDL
NH_4^+-N(mg/l)	0-5	0.155	0.156
PO_4-P(mg/l)	0-2	0.057	0.044
K^+(me/l)	0-2	0.05	0.06

All soil samples were air- dried, ground and passed through 2 mm sieve. Nitrogen was measured by Kjeldahl method and Organic Carbon by Walkley Black rapid titration method.

Bray and Kurtz method was used for measuring available Phosphorus. Exchangeable K, was extracted with 1M NH4OAc pH 7. And then K was measured in Flame photometer.

Plant samples were washed and dried in oven at 70°C. Rice grain, leaf and stem were separately analyzed for total N, P, K. Samples were digested in diacid mixture HNO_3- H_2O_2 except N. For N samples were digested with H_2SO_4. N was measured by Kjeldahl method; K was measured in Flame photometer, Phosphorus was measured in spectrophotometer at 880nm wavelength. Ground water samples were collected from the command area villages at a depth of 30m-100m. The chemical properties of ground water are as shown in Table 3.2

Table 3.2 Chemical properties of ground water

Sl. No.	**EC(µs/cm)**	**pH**	**PO_4-P (mg/l)**	**HCO_3 (mg/l)**	**NH_4-N (mg/l)**	**SO_4 (mg/l)**	**Mg (mg/l)**	**Na (mg/l)**	**Ca (mg/l)**	**K (mg/l)**
1	0.427	6.87	0.33	222.5	0.14	20.40	16.59	49.1	16.65	0.93
2	0.435	7.51	0.39	237.5	0.17	19.83	6.009	103.1	21.57	0.75
3	0.790	7.38	0.23	345.95	0.22	18.95	18.37	106.7	36.44	0.96
4	0.388	7.01	0.25	187.5	0.23	22.50	12.46	50.6	13.42	1.14
5	0.538	7.15	0.16	273.68	0.38	18.13	22.76	53.1	27.77	0.88
6	0.506	7.02	0.18	266.67	0.20	25.29	27.24	35.8	29.96	0.68
7	0.339	6.95	0.33	183.33	0.309	18.42	9.40	47.1	14.10	1.45
8	0.749	6.89	0.18	473.33	0.28	45.14	31.90	115.4	38.34	0.94
9	0.255	6.76	0.58	111.76	0.27	26.77	5.83	37.1	9.71	2.25
10	0.432	6.53	0.23	227.03	0.06	17.79	19.36	36	13.67	1.20

3.2.3.3 Climatic data

Daily rainfall and maximum temperature data of whole year were collected for the Jamuna Command Area (JCA) from Jamuna Command Area Development Division (JCADD), Hojai. Three rain gauge stations are located in the JCA as shown in Table 3.4. The thiessen polygon method was used for deriving weighted rainfall for the JCA. In addition, the temperature and pan evaporation from Hojai station was available for JCA.

Table 3.3 List of rain gauge stations

Sl. No.	Station Name	Source of Data	Period of data	Time step
1.	Hojai	JCADD, Irrigation department, Hojai, Assam	1/1/2000- 31/6/2015	Daily
2.	Nilbagan		1/1/2000-31/6/2015	
3.	Kaki		1/1/2000-31/6/2015	

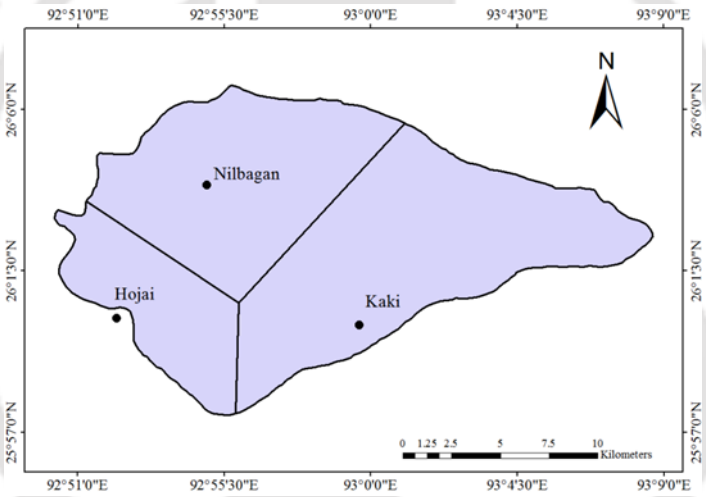

Fig. 3.5 Thiessen Polygon map of the command area rainfall data

3.2.3.4 Discharge data

Discharge data of both the river and main canal were also collected from the same (Table 3.4). The rainfall, runoff data were in mm and m^3/s, respectively.

Table 3.4 List of gauging sites

Sl. No.	Station Name	Location	Period of data	Time step
1.	Jamuna river	2.4 Km upstream of weir site	1/1/2000-31/12/2016	Daily

2.	Main canal	0.6 Km downstream of weir site	1/1/2000-31/12/2016	

3.2.4 Scenario

IPCC defined a scenario as a reasonable, internally consistent, and logical characterization of a feasible future conditions of the world. As a matter of fact, it is not a projection; rather each scenario depicts how a future would be and its vulnerability under various types of emissions. A projection of future delivers the raw material of scenario, but scenarios usually require supplemental details regarding baseline conditions.

3.2.5 RCPs

Several scenarios involving socio-economic and emission related are utilized in climate research to derive numerous possibilities regarding the evolution of future accounting to changes in socio-economic, energy, technological, land use, emissions of greenhouse gases and aerosols. Representative Concentration Pathways (RCPs) have replaced Past Special Report on Emission Scenarios (SRES) in Assessment Report 5 (AR5). It includes a unique set of data for understanding the detail spatially and projection of future through various climate model. An overview of the RCPs is given in Table 3.5.

Table 3.5 Overview of the representative concentration pathways (RCPs) (Van Vuuren, 2011)

Scenario	Description
RCP2.6	Peak in radiative forcing at~3 W/m^2 (ca.490 ppm CO_2 eq) before 2100 and then decline (the selected pathway drops to 2.6 W/m^2 by 2100)
RCP 4.5	Stabilization without overshoot pathway to 4.5 W/m^2 (ca. 650 ppm CO_2 eq) at stabilization after 2100
RCP6	Stabilization without overshoot pathway to 4.5 W/m^2 (ca. ~650 ppm CO_2 eq) at stabilization after 2100
RCP 8.5	Increasing radiative forcing pathway leading to 8.5 W/m^2 (ca. 1370 ppm CO_2 eq) by 2100.

According to IPCC, Radiative forcing (RF) is defined as the quantity of net radiance penetrating the Earth's surface under various climatic factors.

The list of inputs used for various modelling in the present research work has been provided in Table 3.6. Recently in CMIP6 although IPCC has suggested to use combination of RCP and Shared Socioeconomic Pathways (SSP), this has not been considered in this work.

Table 3.6 List of inputs used during the research work for the development of various models

Sl. No.	Dataset		Type	Source	Time period	Scale	Usage				
							Model	Optimization	Hydrological	Water demand	Scenario building
1.	Rice field	Fertilizer type, amount, scheduling	Farmers of command area	Primary	2016-17	Seasonal	✓	✓			
		Paddy grain yield	Farmers of command area	Primary	2016-17	Seasonal		✓			
		Straw yield	Farmers of command area	Primary	2016-17	Seasonal		✓			
2.	Watershed	Discharge	JCADD, Hojai,Assam	Secondary	2001-2016	Daily		✓	✓		
		DEM (SRTM)	GLCF	Secondary					✓		

		Main canal discharge	JCADD, Hojai,Assam	Secondary	2001-16	Daily					✓
4.	Crop	Yield	Directorate of Economics and Statistics, GOI	Secondary			✓	✓			
		Fertilizer and water requirement	AAU and DOA, 2021	Secondary			✓	✓			
		Per capita consumption	Borthakur et al., 2016	Secondary			✓	✓			
		Kc values	FAO	Secondary			✓	✓			
		MSP	Farmers portal	Secondary	2015-16		✓	✓			

		Cost of cultivation	Department of Agriculture and Farmers Welfare	Secondary	2015-16		✓	✓			
		Fertilizer cost	GOI, Department of fertilizers	Secondary	2015-16		✓	✓			
		Nutrient based Subsidy	GOI, Department of fertilizers	Secondary	2015-16		✓	✓			
		Market price	Agricultural marketing board	Secondary	2015-16		✓	✓			
3.	Climate	Maximum Temperature	JCADD, Hojai,Assam	Secondary	2000-12	Daily	✓			✓	
		Minimum Temperature	IMD	Secondary	2000-12	Daily	✓			✓	

		Rainfall	JCADD, Hojai,Assam	Secondary	2000-16	Daily	✓				
		Rainfall upstream	Bokajan, Tea Estate	Secondary	2000-10	Monthly	✓				
		Windspeed at 2m	NASA	Secondary	2000-09	Monthly	✓			✓	
		Relative humidity	NASA	Secondary	2000-09	Monthly	✓			✓	
		Sunshine hours	Jaswal A (2009)	Secondary							
		Pan evaporation	JCADD	Secondary	2000-09	Daily	✓			✓	
	GCM	Historical, future	CMIP5, IPCC	Secondary	2000-12,						

5.	Command area	Population	Census 2011, GOI	Secondary			✓				✓
		Villages	JCADD	Secondary			✓				

3.3 Software Used

ArcGIS 9.1 and ERDAS IMAGINE 9.1 are the image processing software that were used for the study. A brief description of the software is given below.

ArcGIS is a high-end Geographic Information System (GIS) with capabilities for automation, modification, management, analysis and display of geographic information. It creates maps of every aspect of the project with tables and database information. Further it is used for extraction of NetCDF file formats in tabular form.

ERDAS IMAGINE is a raster-based software package developed by Economic and Social Research Institute (ESRI) Geodatabase. The software is specially designed to extract imagery details. ERDAS IMAGINE includes a comprehensive set of devices to create the accurate base image for working on ground. It allows for various tools such as image orthorectification, classification, mosaicking, reprojection, and interpretation. It also allows the user to design image data and present it in formats from printed maps to 3D models. However, the new version of ERDAS IMAGINE 2013 is compatible with Geomedia for GIS processing needs, which is available in Water Resources Engineering Department of IIT Guwahati.

MATLAB stands for Matrix Laboratory and is a platform for programming by engineers and scientists especially for analysing and designing systems and products that represent the present world. The heart of MATLAB is the language which is a matrix-based language that provides the most natural impression of computational mathematics. The platform has the Live Editor, which creates scripts that include code, output, and formatted text in a workable notebook. Various other functions involve creating functions and classes, graphical visualization of data and exploration of data, building desktop and web apps, etc. To work on MATLAB it uses several external language interfaces such as Python, Java, C/C++. Here in this study we have used the NNTOOL for the development of ANN model.

IBMSPSS Statistics is a statistical software developed by IBM for data management, data preparation, multivariate and univariate analysis. The software was initially under SPSS Inc., which IBM finally procured in 2009. It uses to produce regression-based research to provide outcomes and descriptive statistics to comprehend the dataset. Its ease-of-use large data sets, flexibility and scalability provide SPSS as most used statistical tool. Further, the more convenient pull-down menus and command syntax language programming has the asset of handling large and complex data set and its manipulation.

Chapter 4

Fertilization Effect on Nutrient Balance and Plant Biomass in Rice-Fallow Cropping System

4.1 Introduction

Ineffective irrigation systems or water harvesting structures are the leading cause of rainfed cultivation. Rice is one of the major crops grown and consumed in rainfed areas, and rainfed cultivation accounts for about 25% of global rice production. Due to its dependence on climate, rainfed rice cultivation is vulnerable to changes in temperature and rainfall. Further, climate change in these region, aggravates the situation (Datta and Bose 2020). Application of fertilizers are done to increase crop yield. Previous studies have reported on soil fertility management through organic and inorganic fertilizer under rice cropping systems (Saha et al. 2007), but little attention was placed on nutrient management in unsubmerged rainfed rice cultivation areas. This chapter demonstrates the first order of magnitude of nutrient balance (partial nutrient balances). We explored the potential effects of fertilizer doses using primary data collected at plot or farm level in a farmer's field.

4.2 Material and Methods

4.2.1 Study area

The study areas consisted of 13 villages which were situated in a Jamuna command area (JCA), Assam, India, and lies between 25°45′ N 92°48′E and 26°4′N 93°15′E. The villages namely Pub DhoniramPather, Telebasti, Fakirabasti, Hirabasti, DakhinAsinagar, Paschim Nilbagan, Singirpar, Sankarbasti, Pamgaon, Jurapukhuri, Buragaon, Sutarpur and Kaki are located in the rain-shadow area of the Khasi hills and the Barail ranges (Table 4.1). The study area is described in detail in Table 4.1. Thus, farmers of these villages experience rainfed conditions in the command area due to inefficient irrigation infrastructure during rice cultivation while achieving a paddy yield of about 5 – 6 t/ha. As reported in Jamuna Irrigation Project report, winter rice variety is largely cultivated and "Ranjit" (TTB 101-17) variety is popular among the farmers as it is a flood resistant and a high yielding variety. The characteristics of the rice variety is seed to seed duration of 150-155 days. It is a semi-tall (105-110 cm) variety with moderate tillering ability (10-12 tillers). Field experiments were carried out in the study area in the year 2015-16. The farming system is predominantly a rice-fallow cultivation system. Winter rice cultivation has been taking place since the 1960s when the irrigation project began.

Table 4.1 Details of the villages of the command area

Sl. No.	Name of village	Cropped area (ha)	Irrigated area (ha)
1.	Pub Dhoniram Pather	215.74	26.77
2.	Telebasti	244.77	54.88
3.	Fakira basti	285.36	285.36
4.	Hirabasti	183.53	53.54
5.	Dakhin Asinagar	241	107.10
6.	Paschim Nilbagan	87.44	26.77
7.	Singirpar	279.10	207.50
8.	Sankarbasti	164.14	160
9.	Pamgaon	294.45	294.45
10.	Jurapukhuri	124.08	40.83
11.	Buragaon	190.60	120
12.	Sutarpur	186.89	160.46
13.	Kaki	120.08	61.42

4.2.1.1 Soil physical and chemical properties

The physical and chemical properties of the study area's soils are represented in Table 4.2. The soil particle contains mostly silt (ranging 2 to 50 µm). The soil pH ranged from 5.49 to 6.63 depicted the acidity of soils. The EC of soil ranged from 0.42 µS/cm to 1.27 µS/cm. SOC of soil at the start of cultivation was lesser than at the post-harvest in all the villages. SOC at the beginning ranged from 0.50% to 0.20% whereas at the end ranged from 1.55% to 0.37%. Initial soil properties and the amount of K are shown in in Table 4.2 & Appendix, Table A1.

Table 4.2 Chemical and physical properties of the sampled soil

Villages Code	SOC (%)	TKN (kg ha^{-1})	P_{av} (kg ha^{-1})	Exc K	d10(µm)	d50(µm)	d90(µm)	pH (1:2, H_20)	EC 1:2, H20 (µS/cm)
V1	2.4	126.92	6.93	-2.205	3.2	585.51	817.69	5.76	1.27
V2	1.4	162.04	5.43	43.96	2.28	18.77	157.69	6.63	0.94
V3	1.8	122.38	7.53	11.98	1.915	15.56	176.54	5.74	0.82
V4	1.3	121.17	5.74	71.56	1.51	9.95	29.60	5.86	0.71
V5	0.9	107.20	5.90	33.98	1.785	11.18	76.33	5.69	0.42
V6	1.7	203.24	4.05	43.27	1.365	40.06	184.81	6.14	0.75
V7	1.0	54.25	7.65	23.67	1.565	13.12	60.79	6.02	0.81
V8	1.4	52.99	5.87	86.24	1.7	10.65	64.13	6.01	0.78
V9	2.5	32.83	9.37	35.72	3.745	25.72	221.92	5.49	0.72
V10	2.1	87.79	9.57	91.26	3.64	25.87	125.97	5.66	0.54
V11	1.3	98.50	5.49	57.65	2.215	14.23	159.49	6.55	1.27
V12	0.8	87.50	4.93	51.65	1.735	13.23	104.72	6.28	1.17
V13	1.2	169.65	9.81	22.37	1.86	16.86	167.98	5.76	0.49

* TKN denotes Total Kjeldahl Nitrogen, Exc K denotes Extractable K, Pav denotes Available P

4.2.2 Data used

4.2.2.1 Survey

The farm level survey questionnaire was conducted to collect data regarding farm management practices conducted by farmers of the study area. Thus, the survey questionnaire was administered to farmers of each village just after post-harvest operations between February and March 2017. This period was specifically selected to avoid interference with farmers' peak period for agricultural activities. Hence, reaching out to the farmers and interviewing them to collect the required information was easy. About 4 to 5 farmers from each village were surveyed. Most of the respondents were farm owners and rest were tenant farmers. The average farm size of the village field was 3.306 acres. Majority of household held are engaged in full time farm activities. Though, farmers of the villages rely upon the advice of an independent adviser/senior farmer of that area for the quantity of fertilizer application, primarily the small

holder farmers follow same fertilization management practices. Also, command area farmers especially at the tail end, depend on monsoonal rainfall and follow water saving practices such as shallow tillage to prevent water losses, rainwater harvesting in canals and lowland, saturated soil culture. Collected rainwater is then used to irrigate through a bamboo pipe. Further, correct planting time according to the water availability helps in better yield and resistance to weed growth. From the fertilizer input, amounts of N P and K in the fertilizers: Urea, Di-ammonium Phosphate (DAP) and Muriate of Potash (MOP) are 46% and 18% of N, 20.2% of P respectively. The MOP was applied in same amount throughout the villages. Due to variable doses of DAP and Urea, applied N and P doses were ranked (from rank 1=low to rank 4=Very high). Low, medium, high and very high doses for N are 40-60, 61-80, 81-100, 101 kg ha^{-1} and above, respectively, while for P are 0-4, 5-9, 10-19, 20 kg ha^{-1} and above respectively. Field observation was made to validate the information provided by the farmers for the input fertilizer amount, the amount of straw collected, and grains (Table 4.3 & Table 4.4).

Table 4.3 Type and amount of applied fertilizer

Villages	**Tillering Fertilizer (kg ha^{-1})**	**First Panicle Fertilizer (kg ha^{-1})**
V1	29.88(Urea)+59.76(DAP)	37.35(Urea)+29.88(MOP)
V2	29.88(Urea)+59.76(DAP)	37.35(Urea)+29.88(MOP)
V3	37.35(Urea)+82.17(DAP)	37.35(DAP)+29.88(MOP)
V4	74.7(Urea)+37.35(DAP)	37.35(Urea)+22.41(MOP)
V5	112.05(Urea)	59.76(Urea)+37.35(MOP)
V6	74.7(Urea)	37.35(Urea)+74.7(MOP)
V7	37.35(Urea)+74.7(DAP)	37.35(Urea)+22.41(MOP)
V8	74.7(Urea)+37.35(DAP)	37.35(Urea)+22.41(MOP)
V9	29.88(Urea)+59.76(DAP)	44.82(Urea)+29.88(MOP)
V10	74.7(Urea)+149.4(DAP)	93.38(Urea)+29.88(MOP)
V11	74.7(Urea)+149.4(DAP)	93.38(Urea)+29.88(MOP)
V12	29.88(Urea)+59.76(DAP)	44.82(Urea)+29.88(MOP)
V13	74.7(Urea)+168.08(DAP)	74.7(Urea)+29.88(MOP)

Table 4.4 Sample details of the villages, amount of applied fertilizer, grain yield, straw yield

Village Code	N Dose	P Dose	Mean grain yield (kg ha^{-1})	SD	Mean straw yield except the leftover (kg ha^{-1})	SD
V1	Low	High	4856	270.2	2913	162.8
V2	Low	High	4856	372.8	2913	224.5
V3	Low	High	4482	224.1	2689	135
V4	Low	Medium	5528	74.4	3318	44.8
V5	Medium	Low	4183	197.6	2510	119.0
V6	Low	Low	5677	149.4	3406	90
V7	Low	High	5229	186.8	3137	112.5
V8	Low	Medium	5229	149.4	3137	90
V9	Low	High	5080	64.7	3047	38.8
V10	Very high	Very high	5229	393.5	3137	237.0
V11	Very high	Very high	5229	129.4	3137	77.9
V12	Low	High	4781	74.7	2868	45
V13	High	Very high	5603	224.1	3362	135

4.2.2.2 Sample preparation and analysis

Soil samples were air-dried, ground, and mixed thoroughly after removing the plant roots. Finally, the soil samples were passed through a 2 mm sieve and analyzed for plant-available elements: Nitrogen (N) Phosphorus (P) and Potassium (K). Four to five plant samples at maturity stage were collected randomly from each field at the end of the cropping season. They were washed thoroughly with distilled water and dried in an oven at 70° C, after soaking the excess water between filter paper sheets. Dried plant samples were then ground in a grinder to pass through a 40-mesh sieve and analysed for N, P, K. Samples were digested in di-acid mixture HNO_3-H_2O_2 except for N. For N, samples were digested with H_2SO_4. Farmers cut the rice crop at a 1 feet height from the ground during harvest time, and the rest remains as crop residues. Villages are predominantly covered with laterite soil. Soil samples were analyzed for plant-available nutrients. For all the samples, Total Kjeldahl N (TKN) was measured by

Kjeldahl method and Soil Organic Carbon (SOC) by Walkley Black rapid titration method (Walkley and Black, 1934). The Bray and Kurtz method was used to measure Available P (P_{av}) (Bray and Kurtz, 1945). Extractable K (Exc K) was extracted with 1M NH4OAc at pH 7 and was measured in a Flame photometer (Gupta, 2004) (Table 4.5)

Table 4.5 Parameters and methods of analysis for soil, plant samples

Sample	Parameters	Method of analysis
Soil	Texture	Laser diffraction method (Malvern Panalytical Mastersizer 2000)
	Soil pH (H_2O)1:2	Potentiometric phmeter
	Soil EC (H_2O)1:2	Conductivity meter
	SOC	Rapid Titration method (Walkley and Black 1934)
	TKN	Kjeldahl method (Kelplus Distyl em va)
	P_{av}	Spectrophotometer (Spectro-V11D Visible Spectrophotometer VIS ,325)
	Exc K	Flame Photometer (Systronics, Model: 128)
Plant	N	Kjeldahl method (Kelplus Distyl em va)
	P	Photometrically after wet digestion(Thomas et al. 1967)
	K	Flame photometrically

4.2.2.3 Fertilizer N amount and TKN

From the data collected on fertilizer input, it was found that farmers used Diammonium Phosphate (DAP) and urea fertilizer as a source of N, during the tiller formation in rice fields. The corresponding amount of element inputted into the soil is calculated. Analytical results showed that TKN for almost all the villages, were more than the fertilizer N amount as shown in Fig. 4.1. On an average, TKN was more than fertilizer N by about 102%. No correlation was observed between fertilizer N and TKN. TKN was found to be correlated with soil pH as $Y=0.003X+5.693$ ($r=0.31$, $p<0.001$, $n=13$) where Y is TKN in kg ha^{-1}, X is pH.

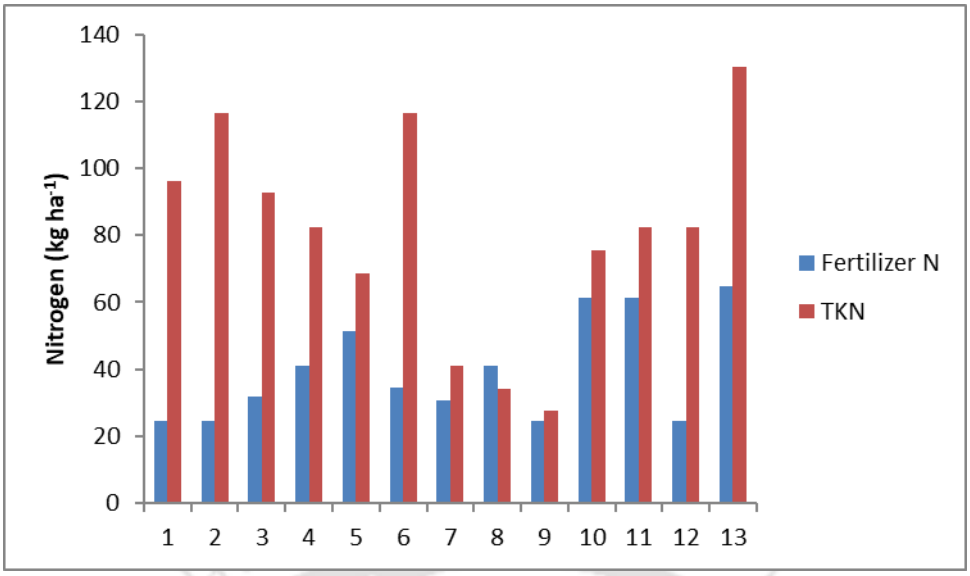

Fig. 4.1 Fertilizer N amount and its corresponding TKN in rice soil of the villages

4.2.2.4 Fertilizer P amount and AP

DAP was used by farmers as a source of P and results showed that P_{av} was less than fertilizer P for all villages except two where no DAP was incorporated into the soil as shown in Fig 4.2. On an average AP was 36% less than fertilizer P. Step regression analysis showed that P_{av} (Y, kg ha^{-1}) had significant correlation with fertilizer amount (X_1, kg ha^{-1}) and with soil parameter, EC (X_2): $Y= 13.979+0.555\ X_1-15.510\ X_2$, R^2 adj= 0.76, $p<0.01$. Fig 4.2. shows that fertilizer P amount ranged from 0 to 34 kg ha^{-1} and AP ranged from 4 to 33 kg ha^{-1}. The coefficient of variation for fertilizer P and AP were 75% and 87% respectively.

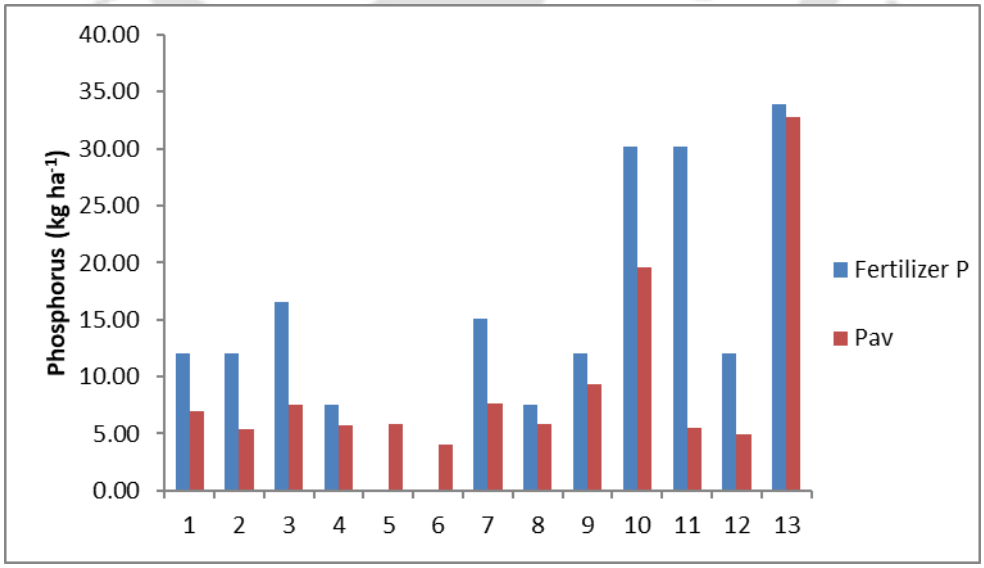

Fig. 4.2 Fertilizer P amount and its corresponding P_{av} in rice soil of the villages

4.2.3 Calculation of nutrient stock and nutrient budgeting

N, P and K nutrient budget in rice crop ecosystem were quantified using field level measurements, survey data from appropriate sources and empirical equations. Nutrient uptake in grain, straw was estimated by multiplying the nutrient concentration (%) with their corresponding yield. To calculate the nutrient budget per rice cropping season three essential components were observed: input in soil (IN_{total}), Output from soil (OUT_{total}), change in soil nutrient pool (ΔS) (Fig. 4.3) (FAO 2003).

$$IN_{total} - OUT_{total} = \Delta S \qquad (1)$$

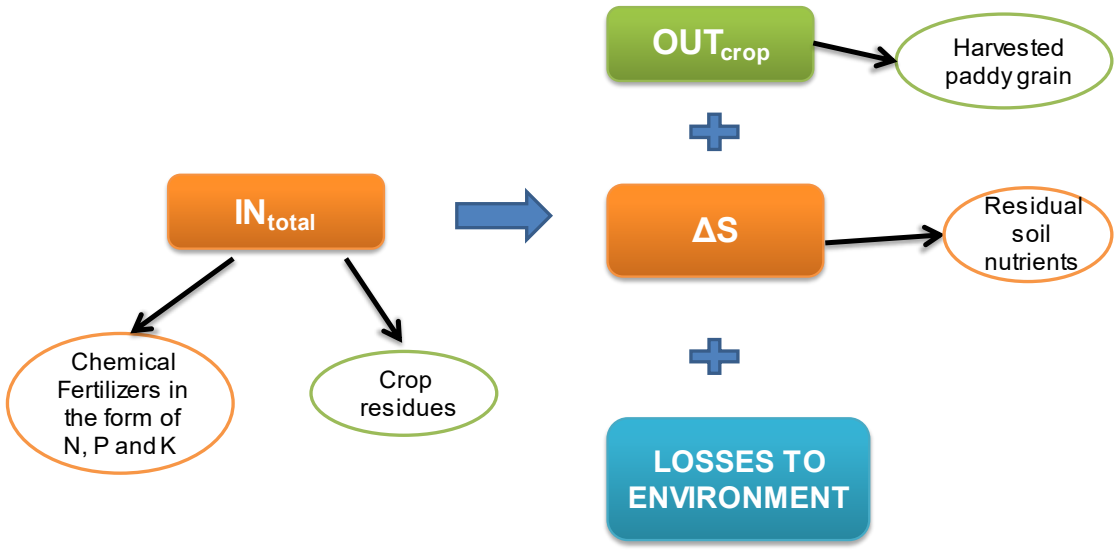

Fig. 4.3 Diagrammatic representation of nutrient budgeting in the rainfed rice crop ecosystem

Eq. (1) can be expanded as the total input in soil and were derived from Mineral fertilisers (MF), Atmospheric Deposition (ADE), Manure (MN), Nitrogen fixation (NF), Sedimentation (SE) and other input flows (IF). The output from the soil were derived from Harvested crops (CH), Crop residues (CR), Leaching (LE), Run-off (RE), Gaseous losses (GL), Erosion (E) and other Output flows (OF).

In unsubmerged/rainfed upland rice cultivation, where inputs from fertiliser and outputs from harvest are significant, omission of variables such as ADE, SE, IF, RE, E and OF is unlikely to introduce much error. Further, after rice harvest (during fallow period), livestock in JCA, feed primarily on stubbles. Hence the two factors MN and CR can interact. Consequently, we can

assume that 100% of the crop residues collected by farmers, is removed temporarily, to be again returned as manure.

Thus, Eq. 1 can be expanded as

$$(MF + NF + MN) - (CH + LE + GL) = \Delta S \qquad (2)$$

Since the loss terms and N-fixing effect of rice were not quantified they are moved to the right-hand side of the Eq. (2)

$$(MF + MN) - CH = \Delta S + (LE + GL) - NF \qquad (3)$$

The right-hand side of Eq. (3) represents the nutrient balance (surplus or deficit) (NB) of the rice ecosystem. So:

$$(MF + MN) - CH = NB \qquad (4)$$

The variable NB can have any value and is likely to differ between individual nutrient on the same plot. Where the NB is positive, the risk of losses (LE or GL) increases and in case of nitrogen, fixing effect is less. A negative NB implies to the mining of soil nutrient.

4.2.4 Soil residual nutrient estimation after cultivation

To quantify the residual storage of nutrients after the cropping season, TKN, Exc K and P_{av} were measured from the plots after the harvest season. Three soil samples were collected from the field of each village at a depth of 0-10 cm and 10-20 cm. We collected 39 samples for each soil layer from thirteen villages. Point soil samples were collected after scrapping away surface litter. Samples were air-dried, ground using a wooden pestle and mortar. Finally, it is passed through a 2 mm sieve to analyze plant-available nutrients.

4.2.5 Fertilizer effect on grain yield using extended Cobb-Douglas Production Function

To achieve the overall production efficiency impacted by fertilizer input factors, an extended Cobb-Douglas production function was designed (Oryani et al. 2021)

$$Y = A \prod_{i=1}^{n} {Z_i}^{u_i}, n = 1,2, \ldots . n \qquad (5)$$

Where Y represents the grain yield; A represents undetermined coefficient; Z_i represents the factor affecting crop yield; u_i is the elasticity; n is the number of factors.

$$Y = AFN^{\alpha}FP^{\beta}orgN^{\gamma}orgP^{\delta} \quad (6)$$

where "A" stands for nutrient uptake through diffusion, "FN" represents N fertilizer, "P" denotes P fertilizer; "orgN" indicates N from previous season, "orgP" indicates P from previous season. The output elasticities of fertilizer N, fertilizer P, Organic N and Organic P are α, β, γ and δ.

The Cobb-Douglas production function is commonly used in economic terms for productivity measurement for minimum cost for producing output using various quantities of input factors (Zhu et al. 2018). The most vital advantages of the production function are : it is best known for its accuracy, it can be applied at the various sectors including agriculture (Zhang et al. 2020). It explicitly includes "the growth accounting factor" by incorporating the A coefficient in the model and production elasticity of output can be obtained from the exponent of each input through logarithmic transformation. The estimated coefficients may help provide the improved input factor measure. Here, an extended production function was developed to determine the effect of nutrient uptake mechanism through root diffusion as total factor productivity in agriculture by utilizing the Cobb-Douglas production function.

Defining the functional relationship between diffusion and nutrient concentration at the root surface can help adjust organic and inorganic fertilization to meet the nutrient requirements for good yield. Diffusion is primary mechanism for nutrient uptake in lesser water condition. According to Fick's law the diffusion is as expressed in Eq (7)

$$F = -D\frac{dc}{dx} \quad (7)$$

Where F is the quantity diffused per unit cross-section and per unit time, dc/dx is the concentration gradient and D is the diffusion coefficient.

A yield curve that can be fitted satisfactorily to these experimental results would make it possible to find the correlation of yield from any quantity of the growth factor in question, here exponential function of concentration gradient in diffusion mechanism have to be introduced, from experimental result for the yield response curve (Harmsen 2000a).

$$A = \upsilon e^{\Delta c} \quad (8)$$

Where υ is a constant and Δc is the concentration gradient.

Replacing the diffusion factor in the Cobb-Douglas function and by substituting Eq (8) in Eq (6), we obtain

$$Y = e^{\Delta C_{FN}\mu} e^{\Delta C_{FP}\tau} e^{\Delta C_{orgN}\omega} e^{\Delta C_{orgP}\varphi} InFN^{\alpha} InFP^{\beta} orgN^{\gamma} orgP^{\delta} e^{\in} \quad (9)$$

By taking natural logarithm on both side of the Eq. 9 and can be linearized as

$$lnY = \emptyset + \mu\Delta C_{FN} + \tau\Delta C_{FP} + \omega\Delta C_{orgN} + \varphi\Delta C_{orgP} + \alpha lnFN + \beta lnFP + \gamma lnorgN + \delta lnorgP + \in \quad (10)$$

where ϕ is intercept, μ, τ, ω, φ are the exponent of concentration gradient of fertilizer N, fertilizer P, organic N, organic P respectively

ϵ is the usual white noise residual. A strict Cobb-Douglas production function, in which sum of output elasticity (E_p) =1, indicates constant returns to scale, E_p>1 indicates increasing returns to scale, and E_p <1 indicates decreasing returns to scale (Besanko and Braeutigam 2020).

4.2.6 Statistical analysis

Analysis of variance (ANOVA) was performed and means were separated using the least significant difference test ($p \leq 0.05$) for N, P uptake of grains and leaf and stem (straw), among villages with different fertilization doses. The soil fertility data were analyzed by combining the data for each fertilizer dose along with each sample depth. Depending on the distribution of data one-way ANOVA was used to compare the differences among different fertilizer doses. The mean values of the data obtained were compared among the various doses using the Tukey tests at a various significance level. In this study, various descriptive statistics such as mean, standard deviation and percent compared with respect to the desired characteristic were used. Statistical analysis was carried out using the software IBM SPSS Statistics 26 version and Microsoft excel 2013.

4.3 Results and Discussion

4.3.1 Nutrient budgeting components

N and P export was most significant for high and low dosed village (78 kg ha^{-1} $yr^{-1}$and 136 kg ha^{-1} yr^{-1}: Table 4.6). The least N and P export was obtained for medium and high dosed villages (33 kg ha^{-1} yr^{-1} and 45 kg ha^{-1} yr^{-1}: Table 4.6). K export was ranging from 7.69 kg ha^{-1} to 40 kg ha^{-1}. Nutrient uptake for N in grains ranged from 0.861g to 0.182g, and P per 100 g ranged from 2.513g to 0.930g across all the fertilizer doses (Appendix, Fig A1). Nutrient uptake in K ranged from 0.6 to 1.1g.

Input in the form of crop residues/straw for N, P ranged from 22 kg ha^{-1} yr^{-1} to 26 kg ha^{-1} yr^{-1} and 0.04 kg ha^{-1} yr^{-1} to 0.6 kg ha^{-1} yr^{-1} and increased with increase in fertilizer doses (Table 4.6). K ranged from 0.4 kg ha^{-1} yr^{-1} to 8.27 kg ha^{-1} yr^{-1}. N uptake in straw (leaf and stem) ranged from 0.576g to 0.281g and P uptake ranged from 0.275g to 0.022 g (Fig. 4.4).

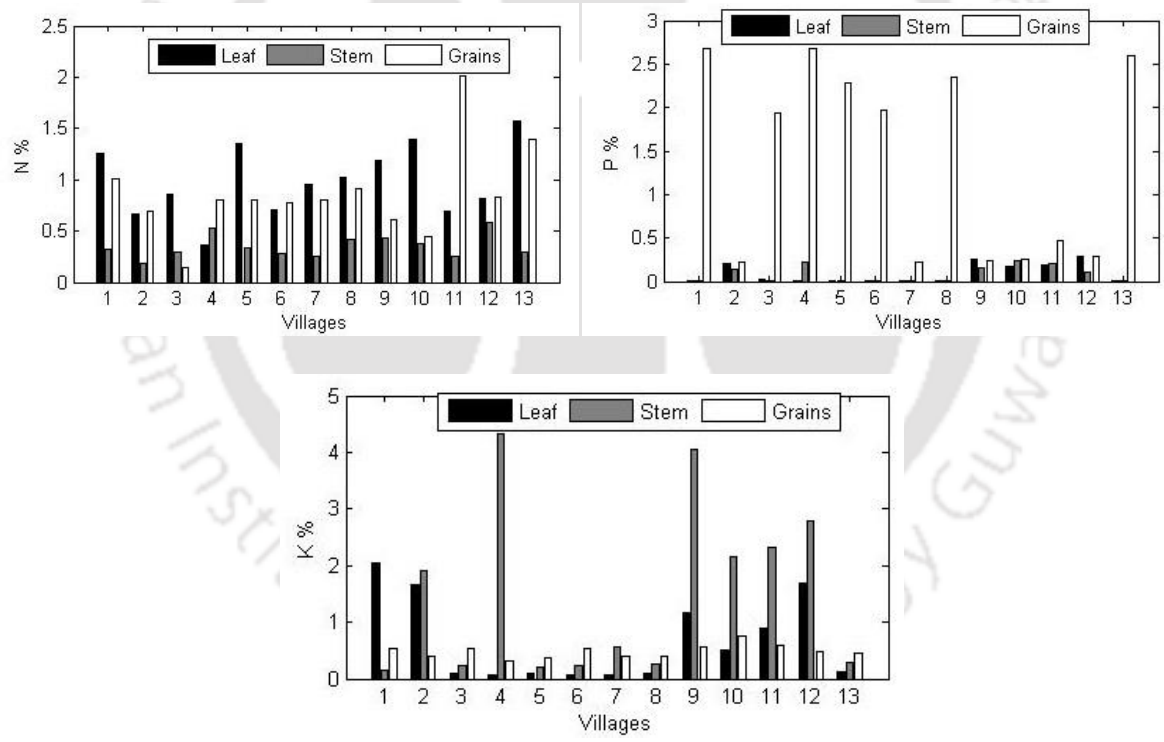

Fig. 4.4 Contribution of the amount absorbed by grains and straw (leaf and stem) of rice crop at maturity as affected by fertilizer application for Nitrogen (N) Phosphorus (P) and Potassium (K)

Results indicated increased N accumulation in rice grain and straw with increased N fertilizer and were consistent after a particular dose up to 100 kg ha^{-1}. Also, the fertilizer N accounted

for the total plant N uptake ranging from 53%–181%. Several studies Aziz et al. (2018) and Kumar et al. (2018) also found increased N use efficiency with increased doses under optimal water conditions up to a specific amount of fertilization (Zhu et al. 2019). Meanwhile, N uptake in rice depends on both inorganic and organic fertilization (Saiz et al. 2021). Likewise, for P, as per speciation, Hedley et al. (1994) found that Resin-P and $NaHCO_3$-Po and solubilizing NaOH-Pi for fertilized soil increased P uptake of rice grains without P application. However, in tested practice, in submerged condition, P uptake was more with increase in fertilizer doses. Results for the N, P uptake in rice plant in tested practice are in line with the study reported by Patra et al., 2018. Effect of fertilizer doses on nutrient removal through harvested grains highlights the detrimental impact of high P use efficiency on soil P fertility. A large amount of soil P uptake, especially in the grains, can ultimately lead to P nutrient depletion without sufficient replenishment. Thus, in many cultivated fields, in case of high P efficiency, the critical value for fertilizer input is equal to the amount removed by the crop to prevent P depletion from soil (Syers et al. 2008). The mean P and N concentrations in grain as estimated by Liu et al. (2003) was (0.29%–0.30%) and (1.13%–1.26%) respectively. However, the proportion of nutrient uptake by grains was consistent with our findings; grains had the most significant P concentrations among all tissues. However due to unsubmerged condition, N were not mobilized from vegetative parts to grains. P absorption by plants, even under water stressed and low fertilized condition, can be found due to the secondary branching of L-type roots. This can be associated with the absorbing capacity of roots via solubilisation (De Bauw et al. 2020) rather than transpiration (Tanguilig et al. 1987). Therefore, the grain yield is affected by ion exchange through diffusion at the root surface rather than the amount of P fertilizer applied. Also, the P accumulated in straw/crop residues is much lesser than in grains; thus, an insignificant amount of organic P is collected in soil.

The amount of K absorbed by harvested part was significantly less as most of the K was concentrated in the crop residues. Moreover, K was relatively less absorbed nutrient because plants uptake relatively immobile K, by mass flow of water, which was minimal in case of the unsubmerged condition.

4.3.2 Residual soil nutrient

In the upper 0-10 cm soil layer, the available N/TKN concentration lowered with increase in doses up to high doses. Most of them remain in upper layer due to unsubmerged condition. It ranged from 54.88 kg ha^{-1} yr^{-1} to 72.03 kg ha^{-1} yr^{-1} (Fig. 4.5). However, in the lower 10-20 cm,

the concentration was lesser and remained almost same for all doses. For P soil nutrient for 0-10 cm and 10-20 cm soil layer ranged from 1.43 kg ha^{-1} yr^{-1} to 0.59 kg ha^{-1} yr^{-1} and 1.41 kg ha^{-1} yr^{-1} to1.15 kg ha^{-1} yr^{-1} respectively. N, P and K at root zone depth at all the doses of fertilizer application was 62.14 kg ha^{-1}, 1.13 kg $ha^{-1}$and 40.26 kg ha^{-1}.

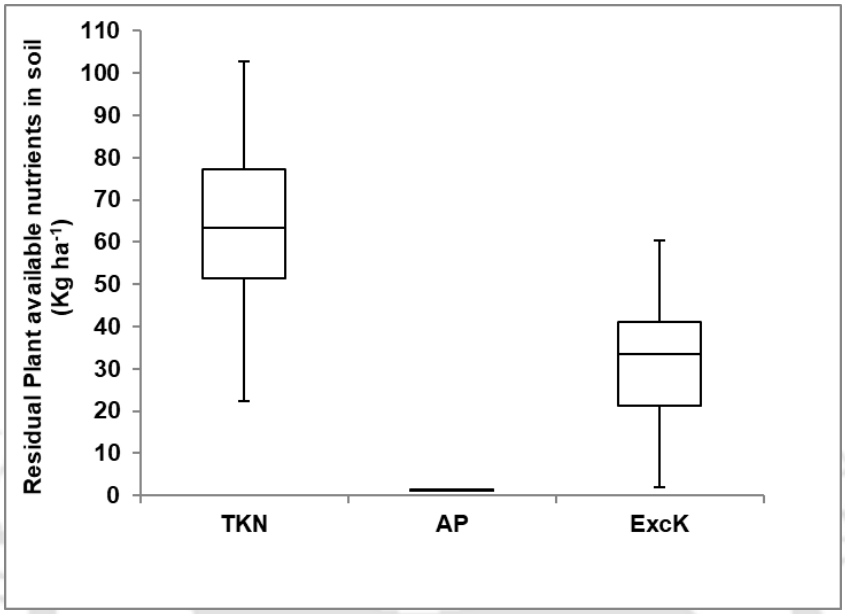

Fig. 4.5 Boxplot of the range of TKN, AP and Exc K for all the villages in Jamuna Command area

Our result suggested that excess N fertilizer input can lead to N retention in the upper soil layer and escape from soil by various means such as leaching or downstream runoff from fields (Verma and Sagar 2020) has predicted a threshold value of 90 kg $ha^{-1}year^{-1}$. Therefore, agricultural researchers, farmers and policy makers should streamline options that minimize nutrient losses with integrated nutrient management. In deficient irrigation, nitrification of most of the NH_4-N in soil to NO_3-N took place during drying, which is lost. SOC increases at the end of cropping season in the top soil layer even without any fertilization due to the addition of root biomass and plant litter (Brar et al., 2013). Statistically, a significant correlation was found between SOC and TKN (r=0.62). According to other studies, a considerable increase of TKN with an increase of SOC was found (e.g., Sakin, 2012; Sofoulaki et al. 2023). The amount of TKN added in the soil after the season could be utilized in the subsequent crop cultivation. As the P accumulated in straw/crop residues is lesser than grains, an insignificant amount of organic P is accumulated in soil. Previous studies showed that paddy rice soils tend to sequester more Organic Carbon than soils under upland crops (Sun et al. 2015; Yan et al. 2013). It was unexpected that SOC increased at the harvest than at the start of cultivation, even in unsubmerged conditions (Appendix, Table A1). However, the differences in SOC between rice

field water management practices are inconsistent in the literature. While some studies found that SOC increased in the moisture-stressed condition and can be associated with the chances of percolating SOC to deeper soil are less than continuous flooded irrigation (Xu et al. 2013). Continuous flooding results in C loss from the surface soil as CH_4 emission (FAO 2020). Other studies (Brar et al. 2013; Pan et al. 2004; Zhang et al. 2012) also reported that SOC at post-harvest is higher than initial values and attributed to the root biomass and plant litter addition due to long term mineral fertilization. Moreover, the selected study area has a long history of rice cultivation with fertilizer, loamy soil characteristics, and soil aggregation thus enhancing SOC sequestration (Wang et al. 2015; Qaswar et al. 2020).

4.3.3 Partial nutrient budgeting

The nutrient budgeting study during the cropping period results showed that there were as such no losses for P. However, plant uptake was very high compared to fertilizer inputs. For N, losses were there for eight out of the thirteen villages for all doses ranging from 12.44 kg ha^{-1} for medium dosed village to 125.05 kg ha-1 for low dosed village. Similarly, there were losses for K up to 32kg ha^{-1} (Table 4.6). Across the thirteen villages, the total plant uptake of N nutrient ranged from 59.35 to 118.30 kg $ha^{-1}season^{-1}$ and similarly, the plant uptake of P ranged from 45.48 kg ha^{-1} to 136.53 kg $ha^{-1}season^{-1}$ (Table 4.6). K uptake ranged from 20.01 kg $ha^{-1}season^{-1}$ to 114.98 kg $ha^{-1}season^{-1}$. N uptake increased in the order low<medium<very high doses<high doses, whereas P uptake increased in the order high<very high<low<medium. Very high doses have no significant effect on N uptake while very high and high doses had almost same effect on N and P uptake (Appendix, Table A2). The post-hoc multiple comparison test results showed that nutrient uptake significantly varied ($P<0.05$) among the doses in all the villages

Table 4.6 Nitrogen (N) and Phosphorus (P) budget in farmers field at the villages of Jamuna Command area. Data are weighted averages based on number of villages of each fertilizer dose

Dose	MF			MN			CH			NB		
	N	P	K	N	P	K	N	P	K	N	P	K
Consistent			29			28			25			+32
Low	49	0		22	0.04		38	104		+33	-104	
Medium	79	8		26	0.2		33	136		+72	-129	
High	99	13		40	0.5		78	45		+60	-31	
Very high	104	31		26	0.6		64	60		+66	-28	

N and P partial budgeting was applied for all the villages with various fertilizer doses based on the farm level analyzed data, survey data and assumptions based on observed field data. The balance was positive for N and negative for P in all the villages. N balance varied between +33 kg N ha^{-1} yr^{-1} for low dose to +72 kg N ha^{-1} yr^{-1} for medium dosed village. N uptake by grains were less for medium dosed village. The balance for P varied between -28 kg P ha^{-1} yr^{-1} for very high dose to -104 kg P ha^{-1} yr^{-1} for low dosed village.

The substantial positive partial nutrient budgeting suggest less nutrient export than input and uncounted nutrient losses through natural processes during cultivation. (Bijay and Bronson 2001) observed that under alternating dry and wet soil conditions, applied N is readily converted to NO_3, which might undergo leaching loss, denitrification loss, or both. Further in contradiction with previous other studies, nitrogen fixation by rice crop up to 19 kg ha^{-1} (Nayak et al. 2019), 15.6 kg ha^{-1} (Rao and Gill 2000) and 22 kg ha^{-1} (Ladha et al. 2016) an insignificant accumulation of TKN with Biological Nitrogen Fixation (BNF) was found. This might be due to less water condition that prevents the growth of nitrogen fixing bacteria (Geisseler et al. 2017; Wu et al. 2020). The calculated positive (surplus) nutrient balances indicate that soil fertility may be maintained at the cost of environmental contamination after rice harvest. The positive value increased with doses indicating the active role of organic fertilization in N uptake. More nitrogen availability in the upper layer can probably be attributed to the increase in mineralization processes by the soil microbes (Ma et al. 2021). It is essential to consider that the decomposition of leaves and stem biomass affected by ecological characteristics can result in nutrient losses from the agroecosystem. Our result suggested that the residual N could be utilized in the subsequent rabi crop cultivation rather than keeping it fallow to increase land productivity and prevent environmental pollution. The partial P balances were negative and significantly higher with doses. This difference might be attributed to the fact that there was high nutrient export through grains in lower quantities. This highlights that along with an increase in mineral P fertilizer input, soil should be amended with fly ash in acidic soil to increase P availability. P can reversibly transfer to readily plant-available from less readily plant-available forms. Thus, ensuring long-term P availability in P fixed grounds that crops can use for many years. Averaging across all the villages an amount of 71 kg ha^{-1} is needed for P replenishment to maintain the yield and enough moisture. However, there is an insignificant change in grain yield due to P fertilizer applied indicating that the rice cultivation is not sustainable in producing higher grain yield by the sole increase of P fertilizer, amendment and

moisture is required at the same time. No correlation could be found between fertilizer N and TKN which indicates that N that is added through fertilizer was lost through leaching or volatilization during the early vegetative growth in these fields and these losses vary depending on variation in management practices of soil (Cassman et al. 1998; Tan et al. 2013). Also, there was more quantity of TKN than fertilizer N amount. Such addition of N in soil can be through various processes like biological N fixation (BNF), atmospheric dry and wet depositions, irrigation water, N mineralization (Cassman et al. 1998). In long term rice cultivation BNF, caused both by symbiotic and nonsymbiotic bacteria, can be the major cause of indigenous N supply from soil (Srestha and Maskey 2005). Therefore, N use efficiency can be increased by decreasing the losses during chemical fertilization and depending more on biological N-fixing bacteria. Some amounts of variation in N fertilization practice were there among the villages though not significant. Similarly, variation in TKN can be attributed to variation in indigenous soil N where N was added through various mechanisms. P immobilization in soil was caused due to the fixing capacity of laterite soil containing Al and Fe and formation of their phosphate compounds. These phosphate compounds are strongly formed in acidic soil thereby preventing the release of soluble P (Meng et al. 2014). Long term P fertilization led to the available P despite no P fertilization. But this type of soil P extraction by plants may eventually deplete the soil P pool or cause P deficiency in rice plants, affecting crop yield (Xu et al. 2007). Therefore, fertilizer P should be applied in large quantity in this type of soil to replenish soil P and increase the AP by decreasing P adsorption capacity of the soil. Exc K was generally dependent on the K equilibrium of soil solution, and hence, there was an erratic behaviour in the concentration of soil K because of the adsorption or release of soil K in relation to its equilibrium (Das et al., 2019). There may be constant input of K through slow release of K from the residual K of the years before, in the soil. Exc K sometimes had negative value, that is, soluble K was more than extractable K, which indicated there was more amount of K in the soil solution.

4.3.5 Input-output analysis of rainfed rice cultivation system

It endeavoured to determine some basic characteristics relating to fertilizer that may influence the system productivity based on survey and nutrient analysis result. Meanwhile, Cobb Douglas Production Function showed that the F statistic and p-value are respectively 4.76 and 0.07, which means that the regression equation passes the significance test.

The regression equation can be obtained as follows:

$$lnY = -4.4 \times 10^7 - (1.4 \times 10^6)\Delta C_{FN} + (0.5 \times 10^6)\Delta C_{FP} - (0.4 \times 10^6)\Delta C_{orgN} + (4.6 \times 10^7)\Delta C_{orgP} + 4.95FN - 0.02FP + 2.00orgN - 3.76orgP + \epsilon \quad (9)$$

Table 4.7 Results of extended Cobb-Douglas production function

Parameter	**Symbol**	**Coefficient**	**Standard error**	**t-test**
Internal N	orgN	2.00	0.61	3.30**
Internal P	orgP	-3.76	1.52	-2.48*
Fertilizer N	FN	4.95	1.42	3.49**
Fertilizer P	FP	-0.02	0.02	-1.42
Return to scale		3.17		
Concentration gradient for Fertilizer N	Δc_{FN}	-1.4×10^{6}	0.4×10^{6}	-3.37**
Concentration gradient for Fertilizer P	Δc_{FP}	0.5×10^{6}	0.2×10^{6}	2.6**
Concentration gradient for Internal N	Δc_{orgN}	-0.4×10^{6}	0.1×10^{6}	-3.34**
Concentration gradient for Internal P	Δc_{orgP}	4.6×10^{7}	1.6×10^{7}	2.75**
Intercept		-4.4×10^{7}	1.6×10^{7}	-2.67**
D-W Test		2.66**		

**, * denotes significance at 5% and10% respectively

The model fit the yield-fertilizer input well with a R^2 value of 0.90. Table 4.7 illustrates the results of the parameters estimation. The fitted equation provides a satisfactory correlation with the field value provided by farmers and thus can be applied to sustainable yield production. To predict the yield, replicating the cross-correlations of output as grain yield and input as elemental nutrient from previous cultivation and fertilizer can provide good result. However, for those moments where there is difficulty to match as there can be other variables such as soil conditions in the form of temperature, soil moisture, other nutrient availability, soil type, compaction. Among the 8 variables, P concentration per unit of root surface (inorganic fertilizer

and organic) and N amount (inorganic fertilizer and organic) positively impacted the grain yield. The return to scale is 3.17, indicating that the overall productivity would increase for the fertilizer applied. The grain yield is affected significantly by variation in N and P nutrient applied, whether external or internal. Durbinwatson test significant at 5%

From the extended C-D function, it was found that concentration gradient and root hairs played the crucial role of in phosphorus uptake through diffusion even in low fertilized P soil. Further, P availability can be increased with increase in moisture (Harmsen 2000b). On the other hand, nitrogen nitrification is highest at field capacity and NO_3^- is a mobile nutrient and is absorbed through mass flow. According to the modified Mitcherlich equation for nutrient-yield relationship in rainfed areas, the nitrogen-use efficiency is assumed to increase with increasing rainfall, followed by phosphorus (Harmsen 2000b). N fertilization was found to increase yield more than internal nitrogen.

4.4 Conclusion

This study investigated the impact of nitrogen and phosphorus fertilization affecting rainfed rice production in a rain-shadow area of Assam using participatory research. The innovation of this research was to blend farmers fertilizer application data and scientific knowledge under water saving practice to perform nutrient budgeting in farmers' field. Nutrient uptake significantly varied among the fertilizer doses of the villages. P uptake for grains was considerably more than straw and increased even with a lower dose of fertilization, mainly due to solubilization by roots under stress conditions. Total N uptake efficiency was limited to high doses of N. The coefficients in the extended C-D model revealed that the amount of Nitrogen application whether external or internal played a crucial role in yield increase rather than phosphorus in moisture-stressed condition. However, phosphorus uptake by diffusion is more prominent than nitrogen. Findings suggested that accurate increase in phosphorus fertilization along with increase in water can still increase grain yield without hampering the environment. Additionally, N remaining after the cultivation can be beneficially used in subsequent cultivation. Jamuna command area has lateritic soil which lowers phosphorus availability in soil and amending with fly ash can help increase in yield. Also, there is an urgent need for combined amendment of acidic soil with increased P fertilizer input to replenish the P removed by grains. Nutrient uptake efficiency was more in case of deficient irrigation and losses of soil nutrient to the local environment can be restrained if fertilizer use can be reduced especially for N.

Chapter 5

Optimal Crop Area Planning in a Canal Command Area Considering Environmental Flow, Soil Residual Nutrients and Farmer's Preference

5.1 Introduction

Legume-based rotation cultivation or Intensive/Multiple cropping is linked with higher food security and soil fertility rather than cereal monocropping (Waha et al., 2020). Also, an increased cultivation of vegetable crops rather than subsequent cereal mono-cropping increase water availability in the face of water stress under climate change [27]. Vegetable cultivation for human food consumption globally not only meets for quantity but quality as well. However, crop yield is dependent primarily on soil and water. Soil is the storehouse of nutrients required for crop growth and replenishment is done through fertilizers. On the other hand, due to prolonged fertilizer input, the overall N-use efficiency is like a Mineral fertilizer equivalent (MFE) ranging from 40%–70% (Gutser et al., 2005). Hence, the fertilizer that builds up due to the excess application can be used in subsequent crop cultivation. Moreover, fertilizers not uptaken by crops during the season are susceptible to hydrologic and volatilization loss in fallow period (Bechmann 2014, Smith and Chalk 2018). Additionally, though there is a huge irrigation potential in developing countries, small-holder farmers are still directly or indirectly dependent on rainfed agriculture. Therefore, government incentives are required to use this irrigation potential effectively to increase and stabilize the country's food production and rural economy. In addition to this, as agricultural water demand has the lions share, its allocation needs to be environmentally sustainable. An environmental flow is the water required in a specific ecosystem, which is necessary for ecosystem restoration. Maintaining environmental flow is an important aspect of reservoir and water resource management (Anderson et al., 2019; Suwal et al., 2020). However, currently, 41% of irrigation water use (997 km3 per year) globally occurs at the cost of Environmental flow release (EFR)s (Jägermeyr et al., 2017). This chapter presents a modelling approach for quantifying crop area planning in fallow areas by considering land and water constraints.

5.2 Model Development

This study developed the Irrigation-Food-Environment Chance-Constrained Programming Model (IFEC), a modelling-based pathway for the sustainable agricultural productivity of crops

while maximizing the economic benefit of farmers according to the available river inflow data. First, a single objective linear programming model was developed to estimate trade-offs in input resources such as land and water resources. Secondly, randomness from fluctuating river inflow and unstable high and low flow levels of river were assessed to learn their indirect effects on crop production. Third, residual soil nutrient from the previous cultivation was incorporated. Fig 5.1 sketches the technical roadmap of this study.

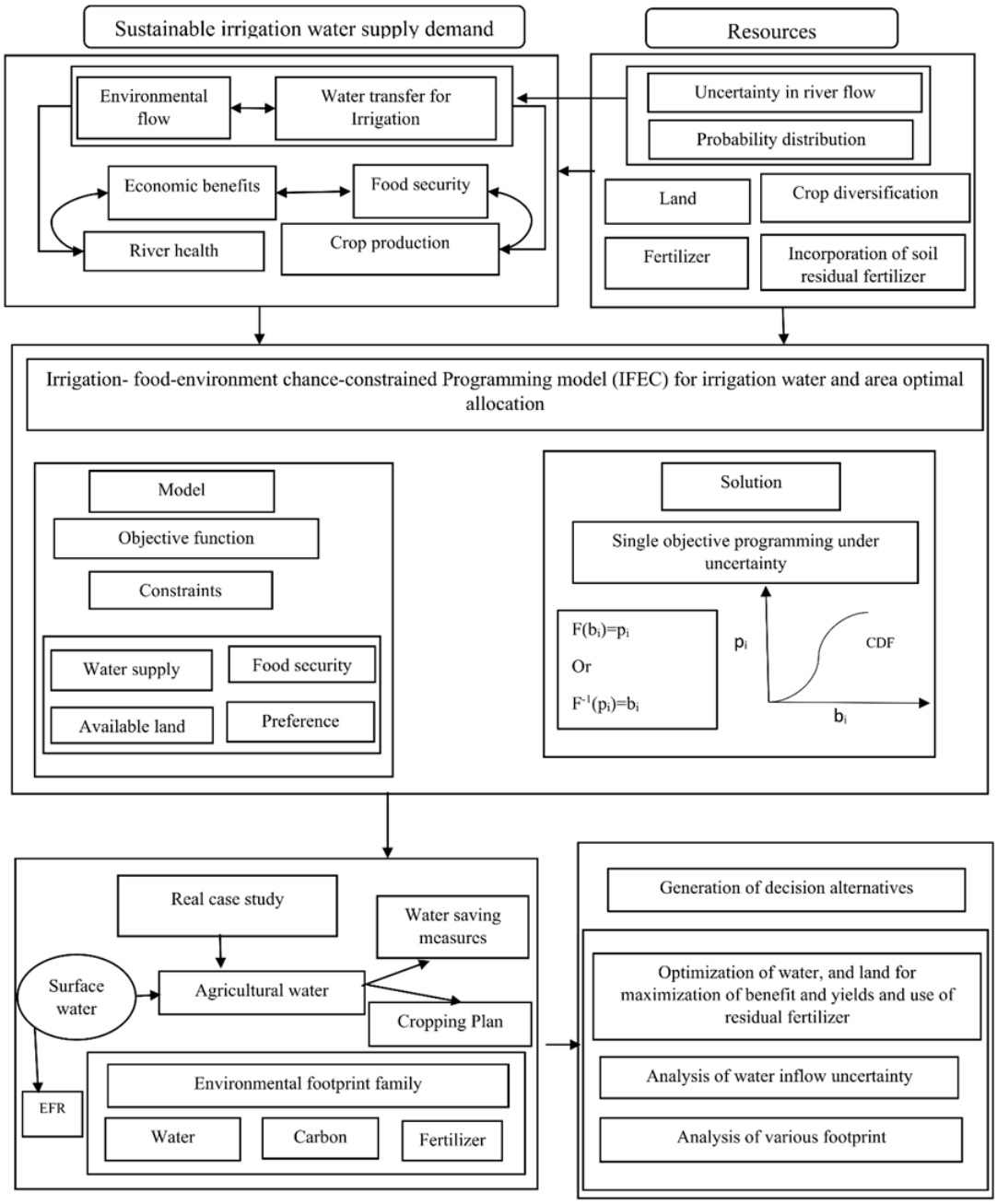

Fig. 5.1 The roadmap of the IFEC optimal model

5.2.1 Chance-constrained optimization model

Random uncertainty in river flow was solved to generate schemes for allocating land and water resources in multiple crop planning. The linear optimization model developed is for administering land for various rabi crops. The model's objective is sustainable crop intensification in the rice-fallow cropping system to manage available land and water for different crop production. For that purpose, high-profit, crop cultivating preference, and eco-friendly plans are proposed and considered in this study. Therefore, farmer benefit maximization criterion considering sustainable use of land and water resources are confirmed for the optimization. These objective functions were subject to constraints for natural resource availability (i.e., water and land), regional food demand, as well as crop diversification (such as perishable, non-perishable crops, and cultivating preference). The model decision variables are harvesting area for each crop. Specifically, crop yield per unit area and associated economic benefit depend collectively on various factors such as land, water and soil nutrients. The Chance constrained Linear Programming (CCLP) model is now discussed in detail as follows.

5.2.1.1 Objective function

Regional economic development and food security are reflected by net profit, which is always a major concern of decision-makers. The concept of food security is outlined, considering both real and economic access to food that combines people's nutritional requirements and food preferences (FAO, 2009). There is a strong linkage between agricultural productivity, household income and regional food security, provided there is sufficient market access (Giller et al., 2021; Kotu et al., 2019). This objective function can ensure food access in the form of economic benefit for the irrigated area from planting winter crops specially, by optimally allocating land and water while reducing N and P fertilizer use and its corresponding cost. The difference between revenues (Rs) and Cultivation costs (CCs) for seasons s, at time t can quantify the Net Economic Benefit (NEB):

$$NEB_t = R_s - CC_s \qquad (1)$$

For an agricultural system, the revenues are from crop production. Hence, crop revenues can be described as a product price per kg. Thus, the revenues of the whole irrigated area are the summation of the revenues of various crops cultivated in the area. R_s is obtained from Eq 2.

$$R_s = \sum_{i=1}^{n}(Y_{is} \times P_{is}) \times A_{is} \quad (2)$$

where Y_i is a parameter that represents the yield of crop i in a particular agricultural region (kg ha^{-1}), P_{is} is a parameter that denotes the price received by the farmer in the market for crop i, A_{is} is the area allocated to each crop in season s.

The total costs for an agricultural production system primarily include fertilizers, pesticides, labour wages, seed cost and other costs such as various machinery, fuel, and irrigation used for food cultivation. However, as all such individual cost is generally not available or difficult to obtain, the average cost of cultivation as reported by Government of India for the similar area is considered in the proposed optimization model (Table S1).

Further, the cost of fertilizer can be minimized by using the residual plant-available-nutrients accumulated in the soil from the antecedent cultivation. This residual fertilizer is deducted from the amount of fertilizer required for growing various crops.

$$FC_i = \left(F_{total,i} - RF_{s-1}\right) \times P_{sub} \times A_{is} \qquad \forall i, s > 1 \ (3)$$

Where FC_i is the fertilizer cost of crop i; $F_{total,i}$ is the fertilizer required for crop i; RF_{s-1} is the residual fertilizer from previous season; P_{sub} is the subsidised price of fertilizer and Ais is the area allocated to each crop in season s.

2.1.2 Constraints

The objective function mentioned above is subject to the following constraints. The maximization of the net economic benefit (Eq. 1) in an agricultural region is subject to a set of criteria that vary as per the surface water availability and type of crops cultivated.

Constraint 1: Water supply. Surface water resources are used for various purposes for humankind's benefit such as drinking water, industrial use and agriculture. Agriculture has the lion's share. Thus, water demand depends on the population's size, level of economic development, and local climate conditions. EFRs are essential for sustainable water resource management. Therefore, we considered uncertainty in water available as in Eq. 4. CCLP models were developed by incorporating uncertainty of inflows at exceedance probabilities (ρ) of 90%, 80%, 50% and 10% (Ren et al., 2019). It was assumed that the whole of the water required for crop growth in an agricultural area must be met from the reservoir release of surface water. Therefore, the water allocation amount for each crop cultivated is focussed on the availability of surface water through the canal network.

$$\sum_{i=1}^{n} CWR_{i,m,s} \times A_{is} \leq b_{jm}^{P_{jm}} \times \gamma - CU_p - R_{jm} \quad (4)$$

Where CWR $_{i,m,s}$ denotes crop water requirement for the month m and season s and crop i; γ is the irrigation efficiency; $b_{jm}^{P_{jm}}$ is the surface water supply for the month m and risk constraint j (Mm^3); Ais is the area allocated to each crop in season s

$$R_{jm} = \emptyset \times b_{jm}^{P_{jm}} \quad (5)$$

Where R_{jm} is the EFR for a particular month m, risk constraint j and ϕ is the percentage release

$$CU_p = \frac{CWR_{p,m,s}}{\gamma} \times (A_{total} - A_r) \quad (6)$$

Where, A_{total} is the total land irrigated with the available water, Ar is the remaining area after preference crop cultivation; CU_p is the gross water use of preference crop; CWR $_{p,m,s}$ denotes crop water requirement for the month m and season s and crop p

$$\sum_{i=1}^{n} CWR_{i,m,s} \times A_{is} \leq F^{-1}(P_{jm}) \quad \forall i, \forall m \ (7)$$

$$F(I_m) = P_{jm} \ or \ F^{-1}(P_{jm}) = I_m \quad (8)$$

Where F is the cumulative distribution function; P_{jm} is the risk probability for risk constraint j and month m; I_m is the inflow for month m.

$$Pr\left[\sum_{i=1}^{n}(CWR_{i,m,s} \times A_{is}) + R_m \leq I_m\right] \geq 1 - P_{jm} \quad (9)$$

$$Pr[I_m \leq F^{-1}(P_{jm})] = P_{jm} \ (10)$$

$$Pr[I_m \leq b_j^{(P_j)}] = P_j \ (11)$$

where P_r is the probability distribution of random variable bj, Pj ∈ [0, 1] illustrates the acceptable risk of constraint j, thus, the constraint j should be satisfied with at least a probability of 1 − P_j or exceedance probability of 1- P_j. Therefore, from the Cumulative Distribution Function (CDF) graph of probability distribution, value of any b_j can be determined with some probability and can be written as in Eq. 9-11.

Constraint 2: Food and nutrition security. The fundamental motive of food cultivation is to ensure food security of the region, which is also the centre point for deciding the type of crop to be cultivated. The important purpose for human food consumption is to meet the demand for

nutrition along with calorie. Grains, pulses and oilseeds are the primary items for calorie intake and to assure food security of the region (Liu et al., 2022; Jayas 2012). Other commodities for food security includes vegetables as vegetables are protective foods packed with vitamins, micronutrients, and essential compounds necessary to prevent multiple diseases and ailments. In addition to this tomato, onion and potato are the largest cultivated and consumed vegetables in India (Gulati et al., 2022).

The crop yield should be able to meet the region's food demand every year.

$$A_i \cdot Y_i \geq FD_{iy} \qquad (12)$$

$$FD_{iy} = A_{pop} \times FD_i^{percapita} \quad (13)$$

Where FD_{iy} is the annual food demand for the local population and is obtained by multiplying the area's population (A_{pop}) and food demand per person ($FD_i^{percapita}$) as in Eq 13.

Constraint 3: Available land. Eq. 14 implements the practice of crop rotations. Similar cereal crops cannot be grown in sequential seasons in the same amount of land area. The total land is the cultivable command area. However sometimes less area is under cultivation due to insufficient water availability for irrigation. The arable land occupied by one crop in season s should be lower than the surface occupied by this crop during the previous season s. The preference crop (i.e., the crop occupying the major area in existing condition) should not occupy a higher than a specific percentage of the total arable land.

$$A_p = \omega \times A_{total} \quad (14)$$

Where, Ap is the remaining area after preference crop cultivation and ω is the percentage of area for preference crop cultivation

$$\sum_{i=1}^{n} A_{is} \leq A_r \qquad (15)$$

Where, A_r is the remaining area after preference crop cultivation and depending on the amount of water left for irrigation.

Constraint 4: Crop diversification. To achieve crop diversification, the farmer must grow at least one crop from cereal, pulses, oilseeds and vegetables in an arable land. This constraint assigns specific land area to the perishable crops during different seasons (Galan Martin et al., 2015; Yigezu et al., 2019)

$$A_{inm} \leq \mu_{is} \times A_r \qquad \forall inm \ (16)$$

$$A_{ip} \leq \vartheta_{is} \times A_r \qquad \forall ip \qquad (17)$$

Where, A_{inm} represents crops with no government support price or non-Minimum Support Price (non-MSP) crops, and A_{ip} represents the higher benefit priced vegetable crop, $\mu_{is}$and $\vartheta_{is}$are the percentage area for perishable vegetable crops and high-priced crops.

Non-negativity constraint

$$A_i \geq 0; A_{inm} \geq 0;\ A_{ip} \geq 0 \qquad (18)$$

Taking the constraints described above as a basis, we describe four models that manifests the potential strategies that the farmer can follow for crop diversification scheme (Table 1). Model I correspond to the situation where demand for the preferred crop is satisfied fully by the previous season's cultivation and therefore, meeting food demand of other crops only remains as constraint. This means the farmer will not go for the same preferred crop already cultivated in previous season. Model II corresponds to cultivation of preferred crop, only when previous season crop is failed due to various unexpected climatic events. Finally, Models III and IV simulate the plan of allowing the farmers to select crop diversification along with preference crops. While Model III goes with the 10% and 20% less EFR flows, Model IV is for the existing condition. To avoid monocropping with preferred crop (summer rice), cultivation of summer rice for Model III and Model IV has been restricted by limiting percentage of summer rice to 20%, 40% and 60%. These are named as Scenario-A, B and C respectively under Model III and IV. With advanced optimization packages, LP models can efficiently solve innumerable decision variables and constraints on a standard computer.

5.2.2 Solution method

This section aims to provide the solution method for the IFEC model. The developed model was solved using Microsoft Excel Solver software. The inputs for the software are target cell, changing cell, constraints and the output are the values of area of per crop selected. In addition, maximum runtime, iterations, constraint precisions, tolerance, convergence for the objective function are also considered.

5.2.3 Case study

5.2.3.1 Study area

The constructed model was applied to the Jamuna command area (JCA), a potential agricultural area in Assam, India. The state of Assam, India is gifted with enormous water resources from

the Brahmaputra River and its tributaries. However the present irrigation area is only 0.85 Mha which is only 20% of existing potential (Singh et al., 2004). The study area covers two districts of Assam; Nagaon and Karbianglong. There are 120 villages in the command area. As per the Jamuna Command area Development Division report, around 90% of the water is released downstream for environmental flows in the existing condition. winter rice is cultivated during kharif season, and land remains fallow in winter after the rice harvest. Farmers apply N, P and K fertilizers for proper growth of rice. Given ample amount of water, the government of Assam is encouraged to improve both the land and water productivity through sustainable crop intensification while increasing producers' profit.

5.2.3.2 Data collection and processing

Water related data

This work considers the agricultural water demand and environmental flow options. We considered uncertainty in water available for irrigation at the barrage from the expected monthly river flows into the weir site at 10%, 50%, 80% and 90% probability of exceedance for the observed data of 2000-2016 (Appendix, Fig. B1). Therefore, the monthly crop water requirement is as shown in (Appendix B, Table B1) at 100% irrigation efficiency (AAU& DOA, 2021). Moreover, as the effective rainfall is insignificant during the rabi season, the crop water requirement is the irrigation water requirement. Further, the irrigation efficiency of the command area is assumed to be 0.35 (Sultana et al., 2017).

Food demand

Foods and water are the major proportion of humans' daily intake of trace elements. Household food consumption patterns included mainly cereals, pulses and vegetables. Food items considered in the study are shown in Table 5.1, and its per capita consumption is shown in Table 5.2. In addition to this, rice is the widely grown cereal covering over 70% of the total cultivable area of Assam. There are four types of rice viz. Ahu, Sali, Boro and Bao. Boro rice has gained more popularity since the last decade because of its better yield potential and area extension due to potential likely irrigation facilities in flood plains of Brahmaputra river (Talukdar et al., 2012)

Table 5.1 Food items considered in the study

Crops considered	Food items
Summer rice	Bhoja bora chaul, komal chaul (soft rice), hurum, korai, sandah guri, puffed rice, popped Rice and flaked rice
Wheat	Broken wheat, flour, chapati
Maize	Corn, yellow corn grains,baby corn , popped maize
Lentil/pulses	Beans (moong bean, chickpea, peas)
Mustard/Oilseeds	Mustard (fresh leafy vegetable, dry seed, seed powder), sunflower,
Vegetables	Tomato, onion, potato, other vegetables

Table 5.2 Per capita various food consumption in Assam. Source: (Borthakur et al., 2016)

Sampled commodity	Average Consumption (g/week)
Rice	2435.74
Wheat	92.44
Maize	9.54
Lentil/pulses	59.25
Mustard/Oilseeds	43.96
Tomato	76.72
Onion	115.07
Potato	383.58

*Food demand is calculated using the consumption and population of the JCA.

The population of JCA is as per the census of the villages lying in the command area

Yield related data

Statistics on the production and yield of crops for each year for 17 years (from 2000 to 2016) were obtained from the Directorate of Economics and Statistics, Department of Agriculture & Cooperation records, Government of India.

Fertilizer data and residual fertilizer

In the upper 0-10 cm soil layer, the available N concentration lowered with increased doses up to high doses. Most of them remain in upper layer due to less water condition. It ranged from 54.88 kg ha^{-1} yr^{-1} to 72.03 kg ha^{-1} yr^{-1}. However, in the lower 10-20 cm, the concentration was lesser and remained almost same for all doses. For P soil nutrient for 0-10 cm and 10-20 cm soil layer ranged from 1.43 kg ha-1 to 0.59 kg ha^{-1} and 1.41 kg ha^{-1} to1.15 kg ha^{-1} respectively. The averaging across two sample depth and villages shows that the value for plant available N and available P are 62.14 kg ha^{-1} and 1.13 kg ha^{-1} respectively. Overall, N and P fertilizer application decreased total soil N and available soil P status after rice harvest. The total N and P due to fertilizer application and plant uptake, soil nutrient decreased by 75% and 500%. This remaining amount of fertilizer is deducted from the required amount. Thus, there is deduction in the total cost of cultivation. The subsidized price of nutrient-based fertilizer for 2015-16 is collected from the Department of Chemicals and Fertilizers.

Economic data

The net return of the farmers from various crops is obtained by deducting the cost of cultivation of the crops from the gross benefit received by selling the produce (Table S1). The average price prevailing in the nearby mandi (Lanka) market is collected from Agricultural marketing board, Government of Assam. As, horticultural crops, including vegetables, spices, and fruits, are yet to receive the minimum price; hence, these crops' prices fluctuate according to the market demand thereby sometimes giving poor farm income. However, for cereal and many other non-perishable crops, a Minimum Support Price (MSP) is fixed yearly by the Commission for Agricultural Costs and Prices (CACP) based on the agricultural production cost. MSP assures farmers fair price to farmers; in case the market price falls below threshold. MSP, market price and cost of cultivation of crops were obtained for 2015-2016. The cost of cultivation was obtained from Department of Agriculture and Farmers Welfare.

5.2.4 Scenario settings and model types

Irrigation demand was estimated under four models (I, II, III and IV) for area coverage under summer rice cropping scenarios (A, B and C) (20%,40%, 60%) and EFRs (70%,80% and 90%). Models were determined using a chance constraint linear programming model (Table 5.3).

5.2.5 Environmental footprint family quantification of food products

The "environment footprint family" consists of water, carbon, and material. These modules present an input-output relationship and help to understand better the performance of the above optimization in the face of changing climate and declining resources. Thus, it allows policymakers to ensure environmentally sustainable production and management of resources. Each of the footprints is discussed below:

Water footprint

The footprint for water (WF) includes blue (irrigation water), green (rainfall) and grey (polluted water) (Hoekstra et al., 2011). The study uses this term because blue and green include the water demand. The unit of WF is $m^3 calorie^{-1}$.

Carbon footprint

The footprint for carbon (CF) includes all the emissions from agricultural input such as fertilizers and pesticides applied, petrol or diesel consumed, and electricity used and they are expressed as carbon equivalent (CE) (Hillier et al., 2009). The calculation was performed based on methods as described in Pandey and Agrawal, 2014. Wherever possible region-specific data was used and the unit for CF was kg CE $calorie^{-1}$.

Material footprint

The footprint for material (MF) includes all the input demand for production. Primarily it is the consumption-based indicator for material use (Dall'Orsoletta and Matthews, 2021). Here in this study, we have considered N, P and K raw material flows for the production of food crops. Unit for MF was $kgcalorie^{-1}$.

Table 5.3 Details of the model types

	Model I	Model II	Model III	Model IV
Description	Not to meet the preference	To fulfil the preference as food demand	To fulfil the preference and	To fulfil the preference at

			environmental flow	the existing release
	Arable land <27705 ha At all release	Arable land <27705 ha At all release	Arable land 11082-22164 ha Available water 70%, 80% released downstream	Arable land 11082-22164 ha
Max [f(x)] s.t. all constraints 4-13,15-18	Max[f(x)] s.t. constraint 4-13,15-18	Max[f(x)] s.t. constraint 4-18	Max[f(x)] s.t. constraint 4-18	Max[f(x)] s.t. constraint 4-18
	F is the objective function which represents the net present value and continuous variables x represent the surface of a crop in the arable land in a specific region			

5.3 Results and Discussion

5.3.1 Model Solution

The CCLP model I have 7 decision variables and 240 equations, whereas models II, III and IV contain 8 and 272, 180 and 60, respectively. Solution time varied according to the instance being solved.

The solution of each CCLP model is given by an optimal cropping plan that maximizes the net benefit of farmers in the command area. Additionally, as a source of natural capital, the water resources system provides for human basic needs and development activities and a solution to the model in a way helps to maintain the riverine stability, health, and productivity. The optimal cropping plan is when the local farmers meet the farmers' preference for food crop in the rabi season. It implies growing summer rice every year in a part of the area as a food crop (summer rice demand as food intake in the command area). And when no summer rice is cultivated (rice demand as food intake in the command area is already met by winter rice). Further, the optimal cropping plans under different risk probabilities and EFRs for each model are detailed in Appendix B, TableB3-B5. The resulting total net returns for the command area in each model

are shown in Table 5.3. As observed, the farmers' net economic return varies for each model and scenario. Among all the models, farmers' net benefit is largest in model I in all releases followed by model II except at existing releases at even 0.5 probability. This is because more profitable crops are grown with the available water in the command area than in the other models. On the other hand, models II-IV involves cultivating summer rice in some part of the arable land, thus giving lesser profit and more water consumed. In model II, vegetable crops occupy a major area of 27% after rice due to higher profit after summer rice. And least benefit was observed for model IV Scenario C. Complying with the preference rules up to 60% area would decrease the profit up to ₹87982 per ha (at up to 70% release) compared to ₹216091 in model I and in existing condition up to ₹212286 per ha at even 0.9 probability. This suggests that the preference crop introduced in the command area might not be economically sustainable, along with over consumption of water leading to no-water-left for other crops. Hence, the farmers' economic net return per hectare is more prominent in model I and/or model II than in model I, the best plan is not satisfying the preference crop (and therefore changing food habit of the localities that consumes more water and satisfy only food demand). Also in model II, insufficient water prevailed except in high flow levels in existing water supply conditions.

Table 5.4 Optimization results in a million ₹

Probability	Release	Model I	Model II	Model III			Model IV		
				Scenario A	Scenario B	Scenario C	Scenario A	ScenarioB	Scenario C
0.1	70%	5986.80	5677.90	4803.45	3620.62	2437.56			
	80%	5986.80	5677.90	4803.45	3620.62	2437.56			
	90%	5986.80	5677.90				4803.45	3560.64	--
0.5	70%	5986.80	5677.90	4803.45	3620.62	2437.56			
	80%	5986.80	5677.90	4803.45	3620.62	--			
	90%	5986.80	--				4707.21	--	--
0.8	70%	5986.80	5677.90	4803.45	3620.62	2437.56			
	80%	5986.80	5677.90	4803.45	3620.62	--			
	90%	5986.80	--				4007.31	--	--
0.9	70%	5986.80	5677.90	4803.45	3620.62	2437.56			
	80%	5986.80	5677.90	4803.45	3620.62	--			
	90%	5881.37	--				3231.23	--	--

--*Denotes insufficient water for crop diversification water demand

Additionally, in the existing condition, model II gives infeasible solution which implies that water is insufficient for a specific month at a risk probability of even 0.5 (Table 5.3). Also, Model III Scenario C shows scarce water even at 80% release. On the other hand, model IV, which is at

existing condition, Scenario B and Scenario C, shows insufficient water except at high flows for Scenario B. For, Scenario A water is sufficient even under current release. This implies that the best strategy is not complying with more than 20% of agricultural area under summer rice.

Table 5.5 Cropping pattern at 80% probability and 80%release and existing release

Crops	Model I	Existing	Model II	Existing	Model III			Model IV (existing)		
				--	I	II	III	I	II	III
Rice			10150	--	5541	11082	16623	5541	11082	16623
wheat	415	415	415	--	415	415	--	415	--	--
maize	12145	12145	1995	--	9375	6604	--	32	--	--
lentil	797	797	797	--	797	797	--	797	--	--
Mustard	495	495	495	--	495	495	--	495	--	--
Tomato	6927	6927	6927	--	5541	4156	--	5269	--	--
Onion	86	86	86	--	86	86	--	86	--	--
Potato	6840	6840	6840	--	5455	4070	--	4187	--	--

--*Denotes insufficient water for crop diversification water demand

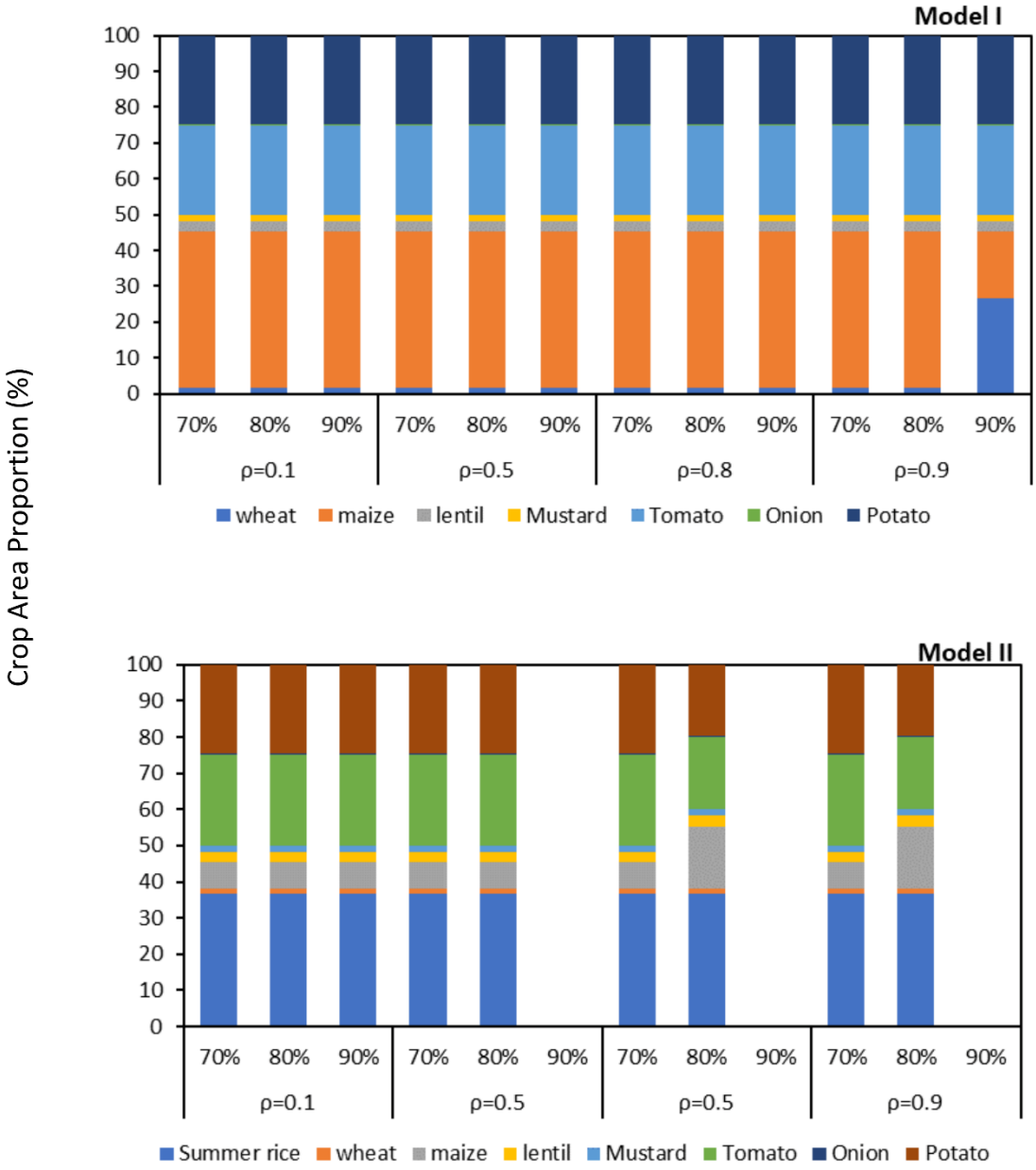

Fig 5.2 Optimal cropping plan in percentage in JCA for arable land under different releases for all probabilities in model I (no summer rice) and model II (summer rice as food demand)

As shown in Table 5.4 and Fig. 5.2, no area (model I) or only food demand area (36.6%) (model II) is under summer rice cultivation in the cropping plan. Summer rice is cultivated according to the food demand of the local people residing in the villages of the command area. In model I, crops such as lentil, mustard, tomato, onion and potato occupy 3,2,25,0.3 and 25% respectively, for different probabilities and all releases. However, in the model I, due to minimal

water under 0.9 probability and 90% release, wheat and maize changes to 27% and 18.5% from 1.5% and 44 %. Area of wheat increases and maize decreases. Thus, along with variation in available water, irrigation area would vary in different crops. Such changes would mainly occur in potato, tomato, and maize, which have the similar feature with higher yield and crop water requirement than other crops. However, in model II, rice occupies the most significant area at 36.6% which is the food demand itself, followed by tomato, potato and maize. However, with a declining water level at 80% release and 0.5 probability, area under tomato and potato slightly reduces from 25 to 20 %, 24.7 to 19.7%, respectively. Area under maize increases to 7.2% to 17.2%. Results showed that vegetable crops that require less water and has more profit, occupied more area of cultivation, and can be cultivated more than the food demand of the arable land, like other food crops. The whole arable land dedicated to producing crops for the food security of the command area year (0.15% cultivated with tomato and 0.78% potato) can be grown in much excess. In model I, the tomato crop is the largest cultivated crop with 25% of area. Therefore, inclusion of vegetable crops for crop rotations involves appropriate farm land management to improve the agricultural sustainability (Ouma and Jeruto 2010). This plan provides profit to the farmer, as it increases total crop yield. Also, an increased cultivation of vegetable crops rather than subsequent cereal cropping, increases water availability in the face of water stress under climate change (Prasad and Chakravorty, 2015). Further, human food consumption globally not only demands for quantity but quality as well. Feeding the rural hunger people globally not only calls for food in quantity but quality as well. Vegetables are protective foods packed with vitamins, micronutrients, and essential compounds necessary to prevent multiple diseases and ailments. Despite, all of the advantages, vegetable crops are more sensitive to soil and environmental factors such as soil type temperature, humidity and their cultivation involves lot of risk for farmers (Prodhan et al., 2018). Notably, even with good yield after outweighing the risk, surplus production might lead to the wastage of crops due to lack of minimum support price and proper market access. In addition to this vegetable marketing facility is subjected to fluctuation depending on supply demand ratio. This attracts less attention of farmers for vegetable cultivation. Kumar et al., 2018 reported that 92.5 % of the farmers avoid vegetable cultivation due to the lack of proper product marketing facilities. Thus, it can be noted that this multiple cropping with major area covered under vegetable crops can only be achieved if the government fixed a yearly minimum price for different crops.

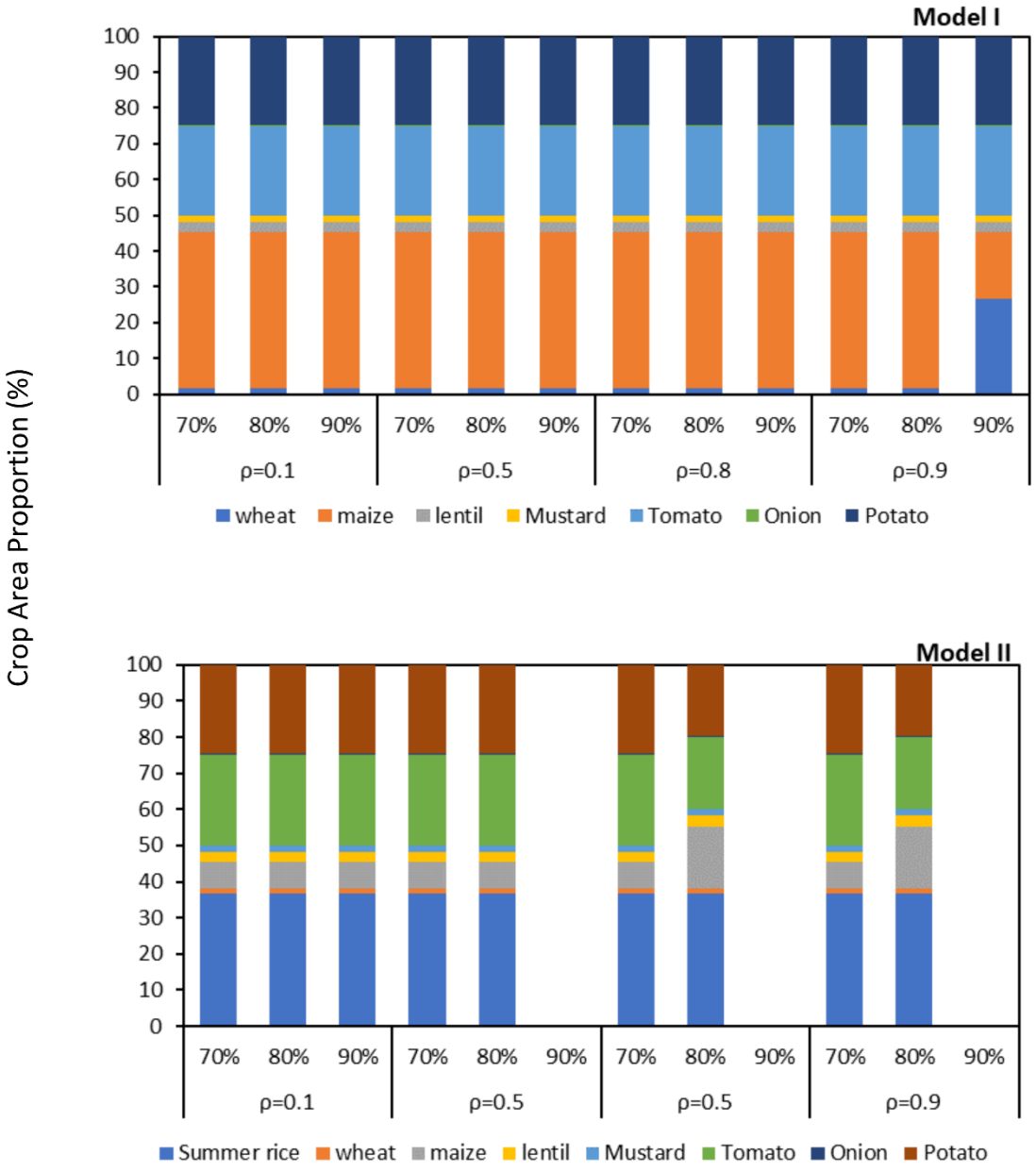

Fig 5.3 Optimal cropping plan in percentage at JCA for model I and model II under different releases for all probabilities for Scenario A (Summer rice area= 20%) Scenario B and Scenario C (Summer rice area=40% and summer rice area= 60%)

The optimal cropping plans in the command area for scenario A, Scenario B and scenario C are shown in Fig. 5.3. In all these models, the optimal cropping pattern for scenarios A, B and C include planting of summer rice at 20%, 40% and 60% of the area. As observed in Fig.4 the cropping plan maximizes more cereal and vegetable crops. For instance, in almost all the scenarios, the cropping area for maize is highest. However, cropping plan is changed at existing

condition, for Scenario A, due to insufficient water even at 0.5 risk probability. Mustard and wheat crop is planted at 17% and 8% compared to 1.5% and 1.8% in other releases. Further, at the existing condition for Scenario A, with further decline in water level at 0.8 probability, area of these crops is devoted mainly to satisfying the local food demand. Principle of optimal use of irrigation water and irrigation areas is that the minimum need should be met first. Hence, the rest of the arable land remains fallow due to water insufficiency. As the extent of boro rice increases the planting area of other crops decreases with more water consumed for growing summer rice crop. For example, tomato and potato in Scenario A, Scenario B and Scenario C decrease as 20%, 15% and 10%; 19.7%,14.7% and 9.7% respectively. Further, the area of maize also reduces 33.8%, 23.8% and 13.8% respectively for Scenario A, Scenario B and Scenario C. Lastly, practical implementation of this suggested optimization results could be obtained primarily through improving and expanding water infrastructure and land management. For increasing field irrigation efficiency, techniques such as border irrigation and surface levelling, must be adopted for maximum usage of available water. Nevertheless, it is worth noting that, attention must be given to proper scheduling of irrigation and uniform allocation of canal water as per crop water needs and appropriate access to marketing facilities of perishable horticultural crops.

5.3.2 Water allocation and EFR sensitivity analysis

In field conditions, water usage in most systems in India varies between 30 and 40 % (Sivanappan, 1994). With better irrigation systems, India can dent the water demand surge by almost 70 %. Further by increasing irrigation efficiency, the total water demand by 2050 can be 8% lower than the current water withdrawals recorded for India (Caldera and Breyer, 2020). The result clearly demonstrates the amount of water used for irrigation considering land and water available. Except for 70 %, the water used for all other releases is 522 Mm3 and covers only 60 % of land due to water unavailability. To further elucidate these results, the maximum possible annual water use of 593.4 Mm3 for Scenario C was calculated for the command area as the sum product of cultivated crops and water used per ha for each crop selected in the scheme. Moreover, the least water used for the Model I considered, uses only 10-20 % of the water available whereas Scenario C would use highest of 30-64 % at 70 % environmental release of maximum water available. Similarly for Scenario A at existing condition, all water is used for satisfying food demand and rest of the area remains fallow due to insufficient water. At the existing release, Model I consume 185 to 167 Mm3 while for Model II, water available at the existing condition is insufficient even at 0.5 exceedance probability. Model IV Scenario

A consumes 321 to 239 Mm3 while water is inadequate for Scenario B and C except at 0.1 exceedance probability for Scenario B. From the results it can also be suggested that identification of the potential groundwater resources is essential for irrigation adequacy in such a canal command area along with increasing efficiency (Singh et al., 2021).

In the present condition, EFR is 90 % of the river flow. Reduction in EFR by 10 % and 20 % from the present condition for each exceedance probability showed that the net benefit would many times increase with decrease in EFR release. For high flows however the benefit was same for each release except for Scenario B and C where the benefit at existing release was less by around 60 M for Scenario B. Complying with the preference rules upto 60 % area would decrease the profit upto ₹87982 per ha (at upto 70 % release or less) compared to ₹216091 in Model I and in existing condition upto ₹212286 per ha at even 0.9 probability. At other possibilities water would be insufficient. However, in other models and scenarios, except Scenario C, the benefit was same for 70 % and 80 % EFR. This reduction in EFR from the existing condition which is 90 % EFR, would increase the profit ranging from ₹3577 M to ₹96 M in various models and scenarios. The model selects the cropping area of each crop keeping in view water availability in such a way inorder to satisfy the model constraints while maximizing the total benefit of the farmers. Moreover, adequate water for cultivation and more irrigated area coverage provides greater profit. Less EFR results in more crop area and more profit for farmers. It was also reported in Jägermeyr et al., 2017, that, globally 41 % of irrigation water consumption occurs at the cost of Environmental Flow Requirement (EFR)s, while water use stakeholders for irrigation supply found that the increasing environmental flows would reduce the area of irrigated agriculture and its farm income.

5.3.3 Crop diversification under various perishable horticultural crop area

We executed the IFEC model with fixation in perishable horticultural crops area ranging from 20 % to 90 % and high-priced vegetable crop (tomato) from 10 % to 55 %, showing that increasing the deviation increases profit. In Model I, the tomato crop is the largest cultivated crop with 25 % of area. In Model I, if no area constraint is available for high priced vegetables and non-MSP priced horticultural crops the benefit is estimated to be maximum around ₹14027 M. However, as the area constraint is given there is a loss. And the loss increases from approximately 23 % to 79 % for all releases and risk probabilities. Similarly for scenario A when sufficient water is available the loss is less as more area is available for vegetable cropping. For example, around 21 % to 79 % loss is incurred as the area of high-priced

vegetable reduces from 55 % to 10 % at 0.8 exceedance probability and 80 % EFR. For Model IV loss is maximum for 0.5 exceedance probability upto 64 % when area under high priced vegetable crop reduces. For Scenario B, depending on water availability loss ranges from 10 % to 76 % at 0.8 exceedance probability of 70 % and 80 % EFR. For scenario C at 70 % EFR release and 0.9 exceedance probability loss ranges from 17 % to 77 %. In general, as the cultivation of preference crop area increases, the area for vegetable cropping reduces and the reduction is further when the water availability is less. Studies showed that because of the dearth of irrigation system in dry tropics cultivation of horticultural crops is reduced during the dry season (Singh et al., 2019; Kandegama et al., 2022). Therefore, the inclusion of vegetable crops for crop rotations involves not only appropriate farm land management to improve the sustainability of agriculture (Ouma and Jeruto, 2010) but also provides higher benefit to farmers. Thus, this strategy benefits the producer, since it increases yield of perishable, non-MSP priced crop and benefit of farmers. Also, an increased cultivation of vegetable crops rather than subsequent cereal mono-cropping, increases water availability in the face of water stress under climate change (Prasad and Chakravorty, 2015). It is also worth noting that, human food consumption globally not only demands for quantity but quality as well. Feeding the rural hunger people globally not only calls for food in quantity but quality as well. Vegetables are protective foods packed with vitamins, micronutrients, and essential compounds necessary to prevent multiple diseases and ailments. Despite, all of the advantages, this fact cannot be denied that, vegetable crops are more sensitive to soil and environmental factors such as soil type temperature, humidity and their cultivation involves lot of risk for farmers (Prodhan et al., 2018). Further even after a good yield by outweighing the risk, surplus production might lead to the wastage of crops due to lack of minimum support price and proper market access. In addition to this vegetable marketing facility is subjected to fluctuation depending on supply-demand ratio. This attracts less attention of farmers for vegetable cultivation. Kumar et al., 2018 reported that 92.5 % of the farmers avoid vegetable cultivation due to the lack of proper product marketing facilities. Thus, it can be noted that this multiple cropping with major area covered under vegetable crops can only be achieved if the government fixed a yearly minimum price or other financial support for such type of crops.

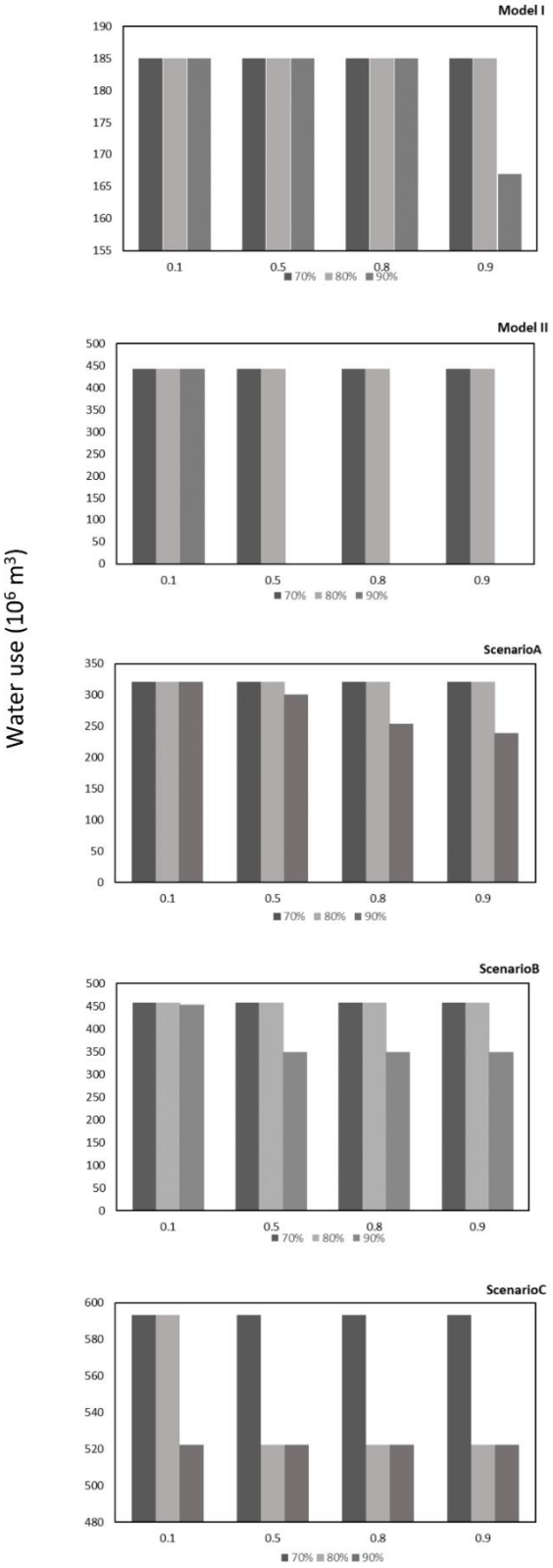

Fig 5.4 Water allocation for different models and scenarios for all probability levels and environmental releases

For the footprint measurement Indian specific data was used. Full details for CF measurement is provided in Sah and Devakumar, 2018. The range is 2.3-1.1 kg calorie-1*10^{-3}, 580.6-167 m^3calorie^{-1},445.3-174.3 kg CE calorie^{-1} for MF, WF and CF respectively for the various optimal cropping patterns under each circumstance.

Based on the analysis performed, the developed IFEC model has shown positive and crucial impact on the overall agricultural sustainability and EFR downstream. The model developed can beneficially utilize the fallow land resources after rice harvest for local food and nutrition security and maximizing the economic benefit of farmers while lowering the fertilizer cost, which has more advantages over the work by previous researchers. However, command area consists of fragmented land holdings and majority of the farmers are marginal or smallholder who cannot invest in improved seed or fertilizer. Further, the practical implementation of irrigated farming in any command area depends on the farming community participation.

On the other hand, in real-world problems, river flow is not stable and complex problem. Hence allocation of irrigation water is a tough problem. The developed model can solve such problem by focusing on the risk associated with varying flows in river. It has an influential effect on the irrigation supply and agricultural sustainability of Jamuna command area which has a water shortage problem. The developed model is integrated with CCP to capture the flow uncertainty of flow in the river. A series of optimal cropping pattern schemes were generated using the model under the different extent of risk associated with the availability of water for supply of irrigation water using the IFEC model. Thereby it will provide the decision-makers to visualize the schemes and make robust decision in selecting the cropping pattern for irrigation in dry season. Therefore, IFEC model is a precise tool for decision making process to ensure livelihood to the farmers and regional food security of the similar command area facing drought-like conditions.

5.4 Conclusions:

This study developed an IFEC model that optimizes cropping patterns under different risk probabilities, maintain EFRs and preference crop cultivation area, along with maximizing the net return for the fallow period in rice-fallow cropping system. Our model allows for decision support for intensive cultivation while considering the residual fertilizer from the antecedent cultivation. This study evaluated three preference crop area (Scenario A, Scenario C and Scenario B) for the best cropping plan. Higher profit shows the best cropping choice under available water. Hence, a suitable optimization approach must be chosen by water managers

based on the nature of problem to get optimal solution. The proposed optimization model was optimized incorporating cropping area variation of perishable and high-priced vegetables ranging from 10 % to 90 %. Further the EFR reduction of 10 % and 20 % was considered during the optimization process. The experimental results show that increasing the vegetable cultivation area and decrease in the area of summer rice increases the crop net return along with sustainable use of surface water resources. Expanding the existing system is necessary to improve the operational management of the irrigation system while establishing an adequate infrastructure to ensure sufficient water among farmers. For each model and scenario, a profitable crop area cultivation was determined, making the preference crop cultivation practically less appealing. The study highlighted the need that, governments should take the opportunity for specific subsidies to be defined for marketing of vegetable crops and ensure agricultural practices by farmers that would foster adaptation and mitigation under changing environments while maintaining the country's rural household food security and economic growth. By allowing the small holder farmers to be aware of the benefit associated with each water availability risk scenarios, they can accordingly plan to avail the crop insurance themselves. Environmental footprint analysis also showed higher profit with less water footprint of vegetable. Tradeoffs between water, economy and carbon emission for crop cultivation can be addressed and accordingly, crop diversification can be modified suitably to sustain food production under changing environments

The development of such an optimization model allows for managing socio-economic requirements efficiently and ensures the sustainable supply of water. The proposed model applies to different areas with similar problems of rice-fallow by calibrating the model for new locations. However, solution provided is based on the water availability explicitly and not on other factors such as stray cattle, availability of quality seed and the risk associated with them. In addition to this, future work could involve the construction of a constraint that involves environmental footprint, which might give a more robustness to the developed model at changing environment.

Chapter 6

Statistical Bias-corrected Models for Climate Change Projection of Temperature and Precipitation

6.1 Introduction

The climate change information for impact studies is of spatial scale consisting of regions of complex topography, coastal or island locations, and highly heterogeneous land cover areas. The General Circulation Model (GCM) is a valuable mathematical model for understanding climate change dynamics. It uses the concept of various physical exercises taking place in the land, atmosphere and oceans, in order to speculate climate changes occurring in the future owing to elevated emissions. However, these variables are archived at the grid resolution of climatic models, with the horizontal resolution generally around 300–500 km. Therefore, a change factor method is required to convert the higher resolution to fine resolution climate change output and derive local climate information.

A statistical model links large-scale climate variables (predictors) to climate variables at the regional scale (predictands). Downscaling is performed because regional climate is influenced by the regional physiographic features as well as the large-scale atmospheric variables. In this chapter, Multilinear Regression (MLR) based statistical downscaling model was utilized automatically to downscale from predictors through model calibration, validation and finally, scenario generation for future projection. The results followed by discussion and conclusions, are presented in this chapter.

6.2 Methodology

At first spatial downscaling method for point observation data was performed for the GCM gridded data. Subsequently, downscaled predictors were inputted into MLR bias corrected model to build the predictor-predictand relationship. The calibrated and validated model was then used to predict the mean monthly air temperature scenarios under two RCP scenarios.

6.2.1 Data

The climate data for the future period were generated from ensembled average of 3 General Circulation Model (GCM)s (Table 6.1). The databases were provided by the Coupled Model Intercomparison Project Phase 5 (CMIP5), from the IPCC Assessment Report 5 (AR5) (IPCC

2013). RCP 4.5 is medium emission scenario that rises and then stabilizes around a radiative forcing level of 4.5 W/m^2 while RCP 8.5 is a business-as usual scenario leading to high emission till the end of 21st century. The GCM data were monthly climate data for the historicalGHG and RCP 4.5 and 8.5 and the GCMs selected for the study area has sufficient historical and future RCP data sets of RCPs and were previously used.

Table 6.1 Representations of the GCM used in the study

Model Name	Model expansion	Resolution	
		Latitude	Longitude
CANESM2	The Second Generation Canadian Earth System Model	2.7906	2.8125
GISS-E2-H	NASA Goddard Institute for space studies-ModelEversion2, HYCOM Ocean model	2.5	1
NorESM1- M	The Norwegian Earth System Model	1.8947	2.5

The predictand is chosen as temperature data (minimum, maximum and mean) and downscaling was applied. The temperature of a region depends upon various factors such as latitude, altitude, the direction of prevailing winds, ocean currents, distance from sea, and the El Nino phenomenon (Mafuru and Guirong 2020; Shukla 1975; Yan et al. 2020) (Appendix, Table C1). Accordingly, 6 GCM predictors were downloaded from the CMIP5 site for 3 GCM models (http://pcmdi9.llnl.gov/esgf-web-fe/) (Table 6.1) for seasonal and monthly variations. Details of predictors are given in Table 6.2. Similarly, rainfall of a place depends on humidity type variable. The GCM outputs of the grid cell were downloaded for individual GCM covering the entire study basin. The base period scenario was obtained from downloading historicalGHG database of the GCM for the year 2000 -2012. The period of 2000–2008 and 2009–2012 are used as training and testing period respectively. For the future scenarios, RCP 4.5 and 8.5 database have been downloaded for the year 2006-2100. The simulated monthly temperature data are then seasonally categorized as winter (December–February), pre monsoon (March–May), monsoon (June–September) and post-monsoon (October–November). The temperature variations till the end of century have been projected for three sub period, namely 2025-40 (early century), 2041-70 (mid-century), and 2071-2100 (end century). Individual GCM projected temperature was then averaged to form ensembled temperature for forecasting future.

Table 6.2 Details of predictors used for temperature projection

Predictors	Description	Unit
prc	Convective Precipitation flux	kg m^{-2} s^{-1}
rsdcs	Surface Downwelling Clear-Sky Shortwave Radiation	W m^{-2}
psl	Sea Level Pressure	Pa
tas	Near-Surface Air Temperature	K
tasmax	Daily Maximum Near-Surface Air Temperature	K
sci	Shallow convective time fraction	1
ci	Fraction of Time Convection Occurs	1
huss	Near surface Specific humidity	1
hfls	Surface upward latent heat flux	W m^{-2}
hurs	Near surface Relative Humidity	%

6.2.2 Spatial interpolation

Many people have carried out the experiment on climate data using different methods from the neighbouring points to a required point (Dhamodaran and Lakshmi 2021, Arowolo et al. 2017). The GCMs chosen for the study area have sufficient historical and RCP data. The downloaded NetCDF files are then extracted in tabular form using ArcGIS 9.1. The spatial interpolation of the tabulated GCM data was performed for downscaling for obtaining regional scale future temperature values. Several processing techniques such as inverse distance weighting (IDW), ordinary kriging (OK), natural neighbour (NN) interpolation and universal kriging (UK) can be used to obtain the required high-resolution or site-specific climate data. GCM predictors for individual GCM model are available at various spatial resolutions, ranging from 1.8 to 2.8° latitude and 1° to 2.8 ° longitude. Spatial interpolation technique for converting GCM gridded large scale data to regional level data was performed. Further the local scale predictor was used to simulate historical and future temperature and rainfall levels through the establishment of predictor-predictand relationship. In this study, we adopted the widely used the inverse distance weighting (IDW) interpolation technique for its simple algorithm and easy implementation (Bayat et al. 2021). Eq. (1) and (2) were used to estimate the climate variables of an unmeasured point using distance and simulated climate values from the four GCM grids point closest to the target (unmeasured) point.

$$T_i = \sum_{i=1}^{N} \frac{w_s(x)}{\sum_{i=1}^{N} w_s(x)} T_i(x_s) \qquad (1)$$

$$w_s(x) = \frac{1}{D^c_{(x,x_s)}} \quad (2)$$

Here, T_i represents the climate variable at the unmeasured point, $w_s(x)$ is the interpolation weight, c is the distance weighting factor, $D^c_{(x,xs)}$ is the distance from the GCM grid to the unmeasured point, and $T_i(xs)$ is the simulated precipitation and temperature from the GCM data closest the aforementioned unmeasured points.

6.2.3 Multiple Linear Regression

The MLR technique is divided into four parts: specification, calibration, validation, and projection. In the specification stage model predictors are chosen. In calibration stage the relationship between predictand and predictor is established. The developed model accuracy is counter checked in the validation stage by comparing the observed and simulated data.

Multilinear Regression (MLR) is widely used types of regression. It establishes the relationship between one dependent variable and two or more independent variables as per the following equation.

$$T = a + b_1x_1 + b_2x_2 + \cdots b_mx_m \quad (3)$$

where "T" is the predictand as temperature (minimum, maximum, and mean temperature), rainfall affected by x_1, x_2, …, x_m spatially interpolated predictors. Like simple regression a, b_1, b_2, ..., b_m are coefficients of regression, which are obtained by minimizing the difference between the plane regression equations and the observation points (predictand) (Bayazıt and Oğuz 1998). During the forecasting stage, the calibrated and validated model is used to derive the future variations. The MLR approach is devised based on the least square method and assumptions are considered where the predictand and predictor relationship is linear and residuals are normally distributed with constant variance. Also, there is no auto correlation among the x variables.

6.2.4 Bias correction

Even after spatial downscaling, bias between the observed and simulated values exists. To remove this, several bias-correction methods are devised. One of them is the adjustment of mean and variance is performed in the correction (Leander and Buishand 2007). This technique of bias correction was also used by (Raneesh and Thampi 2013). It is given as in Eq (4). Finally, the processed outputs for 2000-2012 (baseline), 2025-2040 (2020s), 2041-2070 (2050s) and 2071-2100(2080s) time periods were formed

$$T_{SDCorr} = \overline{T_{obs}} + \left(\frac{\sigma(T_{obs})}{\sigma(T_{gcm})}\right) \times (T_{gcm} - \overline{T_{obs}}) + (\overline{T_{obs}} - \overline{T_{gcm}}) \quad (4)$$

where, T_{SDcorr} is the climatic variables with bias correction; $\overline{T}obs$ is the mean monthly observed climate variable; $\overline{T}_{gcm}$ represents the mean monthly GCM climate output (predicted); $\sigma(T_{obs})$ is the standard deviation showing the observed mean monthly climate output; $\sigma(T_{gcm})$ stands for the standard deviation of the GCM climate output (predicted); T_{gcm} represents the mean monthly climate variable of month i from GCM data (not corrected).

6.2.5 Model evaluation

The capability of the GCMs to simulate the observed rainfall and average temperature values via downscaled approach can be assessed using various measures of model evaluation. However, no individual measure is considered superior to the other, instead combined use of different measures can provide a comprehensive assessment of the model performance. For this study, model results during calibration and validation were calculated using three statistical methods: Correlation coefficient (CC), Nash-Sutcliffe coefficient (NSC), and Adjusted R^2. Nash-Sutcliffe coefficient (NSC) and Correlation coefficient (CC), are used as standard regression and are dimensionless (Moriasi et al. 2007). The equation for the performance index are as shown in Eq. 5-8

$$NSC = 1 - \frac{\sum_{i=1}^{N}(y_i - x_i)^2}{\sum_{i=1}^{N}(y_i - \bar{y})^2} \quad (5)$$

$$CC = \frac{N\sum(x_i - \bar{x})(y_i - \bar{y})}{\sqrt{[N\sum(x_i - \bar{x})^2]\ [N\sum(y_i - \bar{y})^2]}} \quad (6)$$

$$R^2 = 1 - \frac{(1-R^2)(N-1)}{N-p-1} \quad (7)$$

where, y_i and x_i show the observed and simulated predictands. $\bar{y}$ and $\bar{x}$ show average of observed and simulated predictands respectively, p is the number of predictors and the N represents the sample size of the calibrated and validated data. Higher values represent better accuracy.

6.3 Results and Discussion

6.3.1 Performance of statistical downscaling models with GCM predictors

The GCM predictors using the MLR model were trained for the temperature and rainfall data individually for each GCM and tested for the specified period. All the GCM performed satisfactorily, and the performance was measured using NSC, CC and Adj R^2 (Table 6.2 & Table 6.3). The results showed that the NSC and CC range was 0.88–0.94 and 0.94–0.97, respectively for temperature. However, for the rainfall for various input combinations for the GISS model the CC ranged from 0.51-0.54. Therefore, it can be inferred from Table 6.2 that, the performance was good for all GCM in case of temperature. Consequently, it may be concluded that an ensembled CMIP5 model can be used to calculate the monthly mean temperature. Whereas for the rainfall performance was poor and cannot be used for hydrological modelling (Table 6.4).

Table 6.3 Performance statistics for different GCMs for monthly mean temperature

Model Name	**CC**	**NSC**	**NSC**	**CC**
CANESM2	0.94	0.88	0.94	0.97
GISS-E2-H	0.97	0.94	0.92	0.96
NORESM1-M	0.96	0.92	0.92	0.96

Table 6.4 Performance statistics for different input combination of GISS-E2-H GCM for rainfall

Input combination	**R^2**	**Adj R^2**
huss	0.521	0.517
hurs+ps	0.524	0.516
huss+pr+sfc	0.533	0.521
Ps+hurs+huss+pr	0.534	0.517
hurs+huss+pr +sfc +tasmax	0.539	0.519
Hfls+hfss+ps+ hurs+huss+pr	0.534	0.509
Hfls+hfss+ps+ hurs+huss+tasmax+tasmin	0.504	0.538
Hfls+hfss+ps+ hurs+huss+tasmax+tasmin+pr	0.507	0.544

6.3.2 Temperature change projections till the end of 21st century

Changes for future monthly mean temperature for three time slices and two RCP scenarios at the Hojai station of JCA are shown in Fig. 6.1. Under the two RCP scenarios, the mean monthly

temperature for the early-21st century have a decreasing trend in all months, and varies from 0.03 to 1.5 °C. Under the two RCP scenarios, the monthly mean temperature could increase from 0.07 to 0.63°C (0.08 to 1.4 °C) for the 2041–2070 (2071–2100) period, respectively. Similarly, monthly mean temperature could decrease from 0.01 to 0.8°C (0.1 to 0.6 °C) for the 2041–2070 (2071–2100) period, respectively. The greatest monthly mean temperature increase (1.4°C) and decrease (0.01 °C) changes were for February and September month observed for station during the 2071-2100 and 2041–2070 period respectively showing that climate changes is prominent for mid and end of 21st century as compared to the near future.

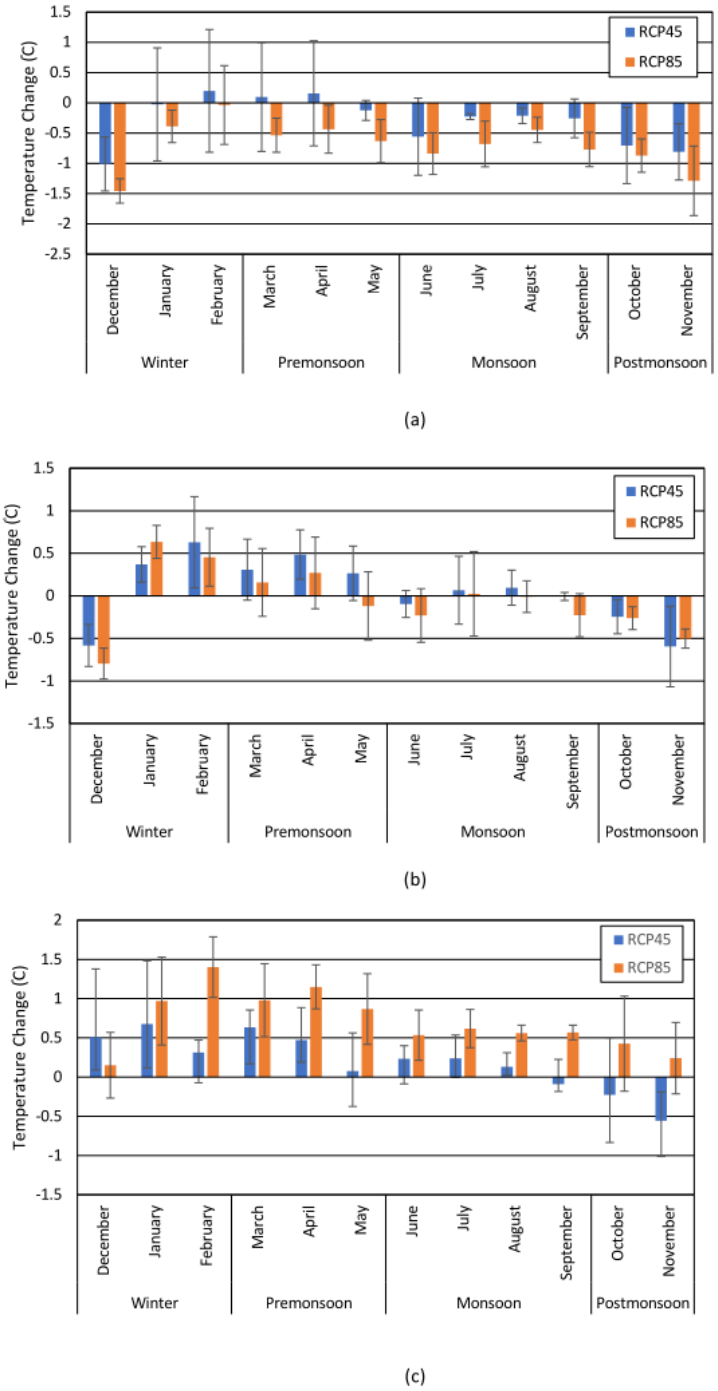

Fig. 6.1 Monthly absolute temperature change due to future emissions in: (a) 2020s, (b) 2050s and (c) 2080s.

February showed an increase in monthly mean temperature for all time period and almost all scenarios except RCP 8.5 in 2020s. It could be due to the rise in minimum temperature. These results are consistent with the findings of Basumatary et al. 2020; Das et al. 2020. In the 2020s all months showed decrease in temperature except for the months of February, March and April

in RCP 4.5. Temperature rise during these months could result in drought and heat stress for the rabi crops (Sehgal et al.,2017). Increasing growing season temperatures will elevate plant transpiration, increasing water consumption (Sadok et al. 2021).

Annually, for the two scenarios increase in mean temperature could be from 0.2 to 0.7 °C for the 2080s period. From the monthly projections as shown in Fig. 6.1, the absolute change in mean air temperature during the future three-time periods for winter, pre monsoon, monsoon, and post-monsoon season was obtained. Winter season increased from 0.09% to 0.13% (0.5% to 0.8%) for all scenarios for 2041-2070 (2071-2100). Pre monsoon season increased from 0.4% to 1% (0.1% to 0.4%) for all scenarios 2041-2070 (2071-2100). Monsoon decreased from 0.1% to 0.6% for all scenarios and time periods except RCP 8.5 in 2041-2070. Post monsoon season decreased from 0.4% to 1.1% for all scenarios all time periods except 2080s RCP 8.5. These findings are consistent with over the twenty-first century trend analysis of Northeast region of India reported by Kumar et al. 2013. Individual RCP scenario analysis indicated that RCP 4.5 showed that temperature increase is more significant in the mid-century than at the end century. Simultaneously, for the RCP 8.5, temperature rises for all the months by the end-century. These results agree with definitions of RCP scenarios.

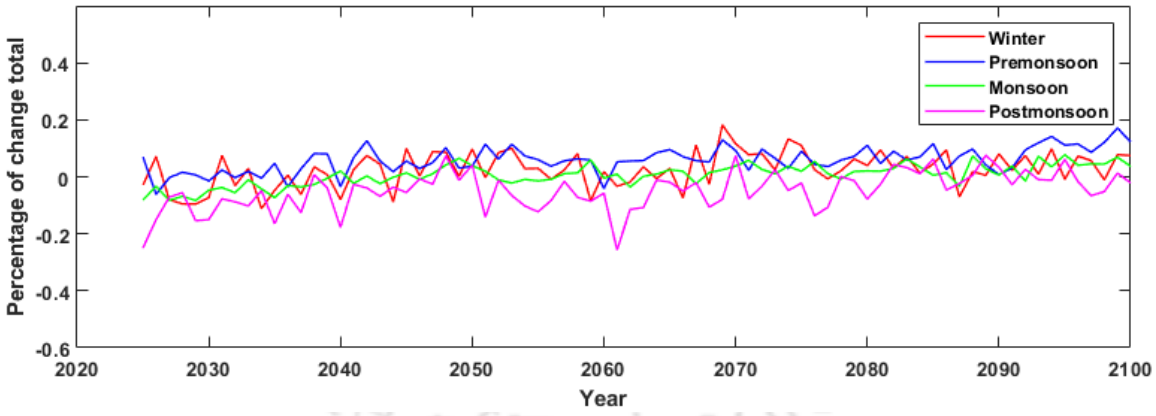

(a)

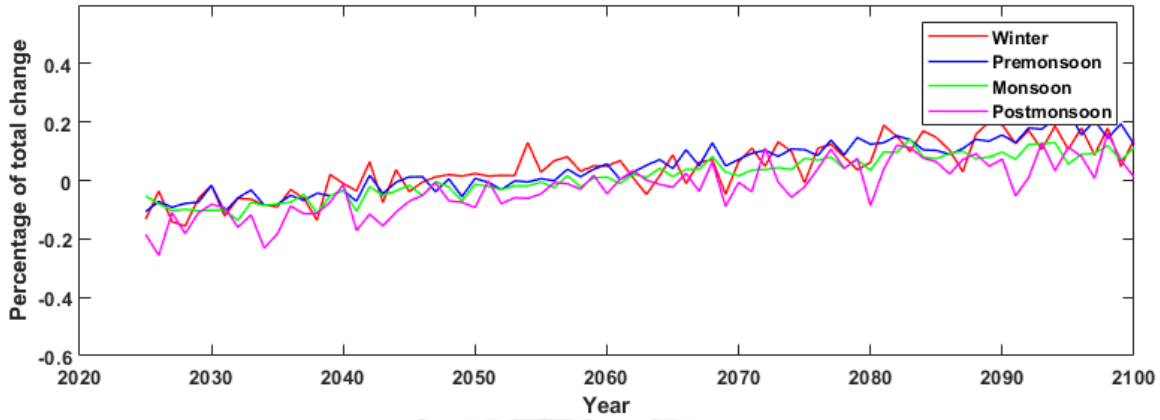

(b)

Fig. 6.2 Percentage contribution of various seasons to the total change after 2025 for: (a) RCP 4.5 and (b) RCP 8.5

Seasonally, the percentage of total change for the future RCP emission scenarios are as shown in Fig. 6.2. Under the RCP scenarios, relative to total temperature change, winter and pre monsoon season added to an increasing fraction of the warming in mid-century and late century. Winter season and pre monsoon contributed to 0.03% to 0.02% (0.05% to 0.12%), and 0.02% to 0.06% (0.08% to 0.14%) respectively in 2040s (2080s). Monsoon season showed increase from 0.01% to 0.08% for 2080s. All the season added to decreasing fraction for both the scenarios in early century from 0.03% to 0.07%, 0.04% to 0.08% and 0.1% in winter, monsoon and post monsoon season respectively. The findings are consistent with other studies covering Northeast India (Soraisam et al. 2018; Goyal and Sarma 2017). Temperature rise in February led to an increase in overall winter season temperature. The post-monsoon season showed a decline in temperature in all scenarios except RCP 8.5 in end century. The decline was from 0.1% to 0.13%, (0.04% to 0.05%) in the 2020s (2050s). The results are in contradiction to previous studies findings, that reported an increase in post-monsoon temperature (Das et al. 2020; Dash et al. 2012; Goyal and Sarma 2017; Jain et al. 2013). However, Vose (2005) reported that an increase in maximum temperature which is relatively lower to the increase in minimum temperature would result in prominent decrease in the overall temperature. October and November months showed a fall in temperature for almost all scenarios and for all periods. The derived lower values during October and November could be attributed to the accumulation of more aerosol particle-laden continental airmass and locally generated pollutant particles over the region (Kothawale et al. 2012). Like the study area, other rain-shadow regions also indicated related temperature variations in the month of post-

monsoon season (Harikishan et al. 2016; Levy et al. 2013). Although an overall projection from 2025-2100, presented a warming trend of 0.20 °C -0.70°C /year for both the scenarios, increase rate was lesser than other places in India (Sanjay et al. 2020; Kothawale et al. 2012).

6.4 Conclusions

MLR model with bias correction was performed for temperature and rainfall of the study area for climate change projection under RCP 4.5 and 8.5 scenarios. Rainfall model showed poor performance with CC value less than 0.65 and could not be projected for future time period. The projections of future monthly mean air temperatures were performed for RCP 4.5 and 8.5 scenarios. The projection showed an increased air temperature in winter and pre monsoon season and decreased temperature during the post-monsoon season under all the RCP scenarios as compared to the base period (2000–2012). The temperature change indicates an overall warming.

Chapter 7

Hybrid ANN Model for Streamflow Projection to Assess Irrigation Water Availability

7.1 Introduction

A robust hydrological assessment is challenging in rural basins with limited hydro-climatological data. This level of uncertainty is further augmented in flood hydrology studies for regions with wide variations in physical and hydro-meteorological characteristics. Mountain barriers create the rain-shadow effect on the river and associated basins, where precipitation is relatively low. The rain-shadow area is characterized by irregular rainfall, water stressed conditions and sometimes prolonged dry spells thus affecting soil moisture for agricultural production and the livelihood of farmers. R-R models have been widely used for streamflow in river basins, as they generally provide good prediction accuracy, where no orographic influence are available (Mohammadi et al. 2022). To use these models in a catchment scale, their parameters should be calibrated for exploring the hydrological dynamics of the catchment. This poses a hurdle in such model development, mainly when data scarcity exists. Further, improved accuracy considering various catchment components is difficult as it contains multiple space and time variability levels, making the hydrologic processes highly complex. As an alternative to regular rainfall–run-off models, data-driven models can be used for hydrological modelling using simple linear regression or nonlinear data driven models, depending on the complexity of the process. This chapter deals with the development of hydrological model with the help of Artificial Neural Network (ANN). Further, the developed model was used to monitor the hydrological response of such river basins, which is necessary for proper agricultural water allocation to avoid agricultural drought-like conditions.

7.1.1 Why ANN?

ANN-BP estimates the flow regime in the Jamuna River basin. Less reliance on quantity of input data and reduced complexity, are the main features of the data-driven methods that are currently drawing attention of the researchers and decision makers (Lima et al. 2022). Due to its highly reliable prediction and flexibility, ANN-BP is one of the most popularly used data-driven methods. The model is based on the concept of human nervous system and multiple neurons. These models do not require careful consideration of the processes underlying a

complex mountain hydrological system. They, thus are not bounded by an insufficient or inappropriate leeward description of the perplexing hydrological response to rainfall transformation exercise. Typically, simple hydrological models require primarily precipitation and potential evapotranspiration input data. Further, due to the limited availability of soil moisture condition data antecedent rainfall generally are used as basic substitute for representing initial moisture condition in ANNs and other statistical streamflow projecting models (Robertson et al. 2013). Meresa 2019 involves the use of soil moisture condition, rainfall present, and antecedent in sufficient moisture condition for hydrological ANN model in their study. Using data related to atmospheric conditions associated with climate change response may let the statistical streamflow forecasting models to characterize changes in the hydrological behaviour of a mountainous catchment on the leeward side.

7.1.2 ANN

An ANN model is made of a collection of nodes and a set of interconnected processing components. ANNs utilize learning algorithms to represent knowledge and store the knowledge in weighted form of connections, thus making a parody of the way a human brain functions (Pradhan and Lee 2010). They are considered as heuristic method of learning where they gain knowledge from previous experiences using samples and are subsequently applied to recognize completely new form of sample (Kavzoglu and Mather 2002). The parallel distribution of information within the ANNs allow the model to summation of complicated, nonlinear, interrelated processes between various input and model output. Finally, ANN models imitate the environmental systems without prior knowledge of the algebraic relationships between variables.

7.2 Methodology

A flowchart in Fig. 7.1 shows a diagrammatic representation of the steps to estimate extreme streamflow quantiles under changing climate (i) development of initial state using a handful of predictors from large scale climate variables and processing into local hydrological regime (ii) selection of potential input matrix using iterative input selection approach for the ANN-BP model calibration and validation (iii) simulation of future scenarios with the suitable ANN-BP model (iv) quantile estimation for the ensemble members of GCM. Five GCMs namely CanESM2, CNRM-CM5, CSIRO- Mk3-6-0, GISS-E2-H and NorESM1-M from Coupled Model Intercomparison Project 5 (CMIP5) were selected for acquiring climate data based on the predictor availability for each RCP scenarios and independence of the models. (Table 7.1).

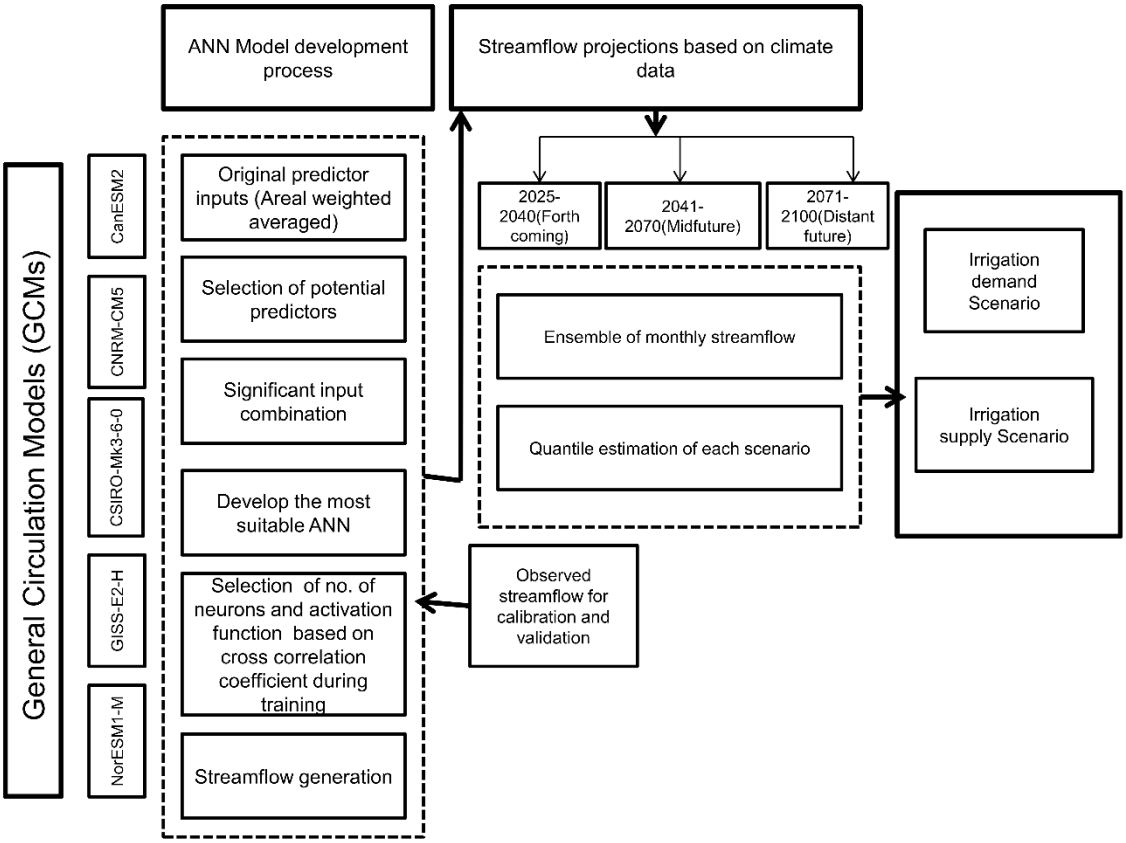

Fig 7.1 Flowchart for streamflow forecasting using artificial neural network and CMIP5 model data for adaptation strategy in the agricultural area of river catchment

Table 7.1 Representations of the Global Circulation Models from CMIP5

Model Name	Model expansion	Resolution		Experiment	Ensemble Member
		Latitude	Longitude		
CanESM2	The Second Generation CANadian Earth System Model	2.7906º	2.8125º	historicalMisc	r2i1p4
				rcp45	r2i1p4
				rcp85	
CNRM-CM5	Centre National de Recherches Météorologiques	1.4008º	1.40625º	historicalMisc	r1i1p1
				rcp45	r1i1p1
				rcp85	
CSIRO-Mk3-6-0	The Commonwealth	1.8653º	1.875º	historicalMisc	r1i1p1
				rcp45	r1i1p1

	Scientific and Industrial Research Organisation			rcp85	
GISS-E2-H	NASA Goddard Institute for space studies-ModelEversion2, HYCOM Ocean model	2.5º	1º	historicalMisc	r1i1p1
				historicalExt	
				rcp45	r1i1p1
				rcp85	
NorESM1-M	The Norwegian Earth System Model	1.8947 º	2.5º	historicalMisc	r1i1p1
				rcp45	r1i1p1
				rcp85	

7.2.1 Global change variables of the hydrological regime

Investigating the processes using the large-scale GCM model outputs, related to hydrological characteristics in the rain-shadow area will form the background for evaluating its projection and provide reliability in prediction while using simulation model. It is easy and desirable to consider the thermodynamical (circulation-induced) and dynamical (temperature-induced) components for diagnosing physical procedures.

7.2.2 Iterative Input variable selection

7.2.2.1 Potential predictor matrix

Selection methods for Input variable is of three types: model-based, model-free and hybrid approaches. The model-based approach is based on calibration and validation of various models with different input data sets and finally choose the best set. Model-free method engages in input selection based on interdependence of input-output values and is devoid of any predefined threshold value, thus leading to recognizing numerous input variables with risk of repetition involved. In a hybrid approach a rank-based prominent variables changes theoretical and information-based selection criterion of model-free methods. Finally, the rank-

based input variables are put into a supervised, stepwise forward selection model-based technique to be assessed by cross-validation.

Iterative Input variable Selection (IIS) algorithm, is used in the study for selection of input. It is executed in three steps as described in Galelli and Castelletti, 2013. During the input ranking (IR) step, from a set of D datasets, the most relatable inputs are selected in a forward selection method. The relative prominence of the first p-ranked selected variables is evaluated for the given output in the form of Single Input Single Output (SISO) model. Thus, from p number of SISO models, the best ones are placed (set p′) based on some performance evaluator. A model building approach is then executed to recognize a multi-input single-output (MISO) model. The process is iterated by employing the new input variable from SISO model till the point either the best input variable combination returned by the IR method is already in the set X_i. Also, the performance of the underlying model as evaluated by several performance criteria such as coefficient of determination and mean-squared error etc.

7.2.2.2 Construction of global predictor matrix and input selection process

Before the development of hydrological model, a whole set of global change variables as potential predictors related to discharge are chosen as predictand over 13 years. Notably, any data-driven approach must recognize the patterns and trends in both the predictors and predictand. As predictor fields, near surface specific humidity, convective precipitation, surface upwelling longwave radiation, fraction of time convection occurs, air temperature, precipitation rate, wind speed, maximum air temperature, minimum air temperature, surface upward latent heat flux, surface upward sensible heat flux, surface temperature, surface air pressure, relative humidity, cloud area fraction, evaporation and specific humidity are used, all defined on the grids which is covered in the study area. The choice of predictors is based on dynamic and thermal and humidity factors affecting temperature and precipitation. This produced a pool of 12 predictors.

Table 7.2 Step-by-step procedure with an algorithm for hybrid ANN

Algorithm		
1	Input dataset: A=(a_1, a_2…a_s)	
2	Output: Potential input parameter p for ANN	
3	STEP 1	Data preprocessing

4	Extract the first q-ranked variables based on the SISO model	
5	Evaluate the selected variables based on MISO model	
6	While error> Threshold	
7	While n<q	
8	Add inputs from SISO model	
9	STEP 2	Initialization
10	Initialize its free synaptic weights and biases in a random manner	
11	STEP 3	Training
12	Present inputs and compute outputs in a forward manner using eqn (2)	
13	Calculate error using eqn (3)	
14	While error> Threshold	
15	While iter < maximum iter do	
16	While error> Threshold	
17	Adjust weight and biases during backpropagation	
18	Return W, b	

7.2.2.3 ANN model development for Basin

The multilayered ANN model which is structured in MATLAB consisted of three layers: an input layer with the input nodes or predictors (Fig. 7.2). The second layer is the hidden layer with several neurons. Each hidden node/neuron transforms the input nodes nonlinearly into another dimension through a weight and a bias term shown and activation function as Eq (2). The last layer is the output layer that contains the output node, such as streamflow, which was the case in this study. The activation function used in the first hidden layer is the logistic function, while the weights were determined in the training procedure through successive

weight adaptations. Three widely used transfer functions, tangent sigmoid, linear, and log-sigmoid, were evaluated in multilayered ANN-BP construction trials. Equations for tangent sigmoid, linear sigmoid, and log sigmoid are as given below:

$$\left.\begin{array}{l} f(z) \approx \frac{2}{1+e^{-2z}} - 1 \\ f(z) = z \\ f(z) \approx \frac{1}{1+e^{-z}} \end{array}\right\} \quad (1)$$

The final neural network was formed with the Levenberg-Marquardt feed forward-back propagation algorithm

$$logy_k = f_2\left(\sum_{j=1}^{k}\left\{f_1\left(\sum_{i=1}^{n} x_i w_{ij} + b_j\right)\right\} w_{jk} + b_k\right) \quad (2)$$

Where, w_{ij}=weight of input x_i; b_j= bias term; f_1=activation function at the hidden layer; f_2=activation function at the output layer; k=no. of neurons at the output layer; w_{jk}=weight of neurons at the output layer; b_k=bias term.

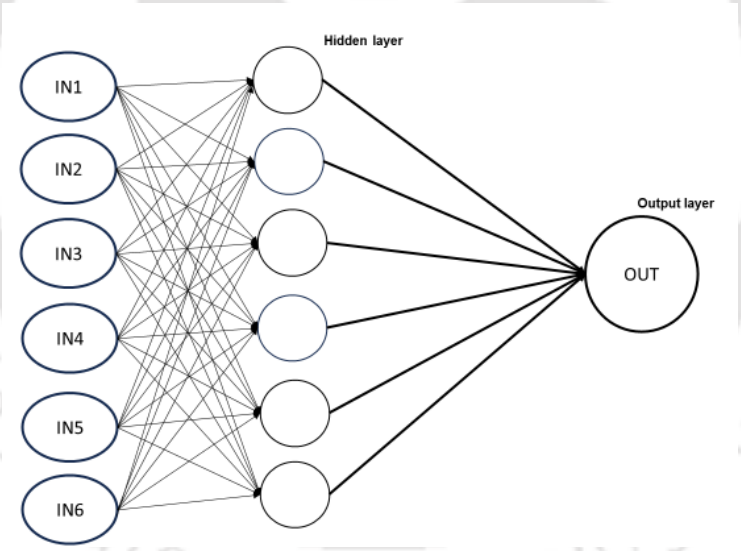

Fig. 7.2 Structure of the multilayered Artificial neural network with back propagation

Streamflow as a single output node and two intermediate nodded layers created the model. In the training process, inputs were passed forward through the network to result in the outputs, then compared to the observed data. The performance was measured based on mean squared error (MSE).

$$MSE = \frac{1}{n}\sum_{i=1}^{n}(X_i - Y_i)^2 \quad (3)$$

Where, n is the no. of samples, X_i is the observed and Y_i is the simulated values

The type of activation functions was chosen based on training trials. If the error was higher than the desired value, it was passed backward through the network, and once the comparison error was lowered to an acceptable level, the training phase ended. This was the structure of the ANN-BP that was subsequently used for each GCM. During the training phase 70:30 of the observed data was used to train and test the model through calibration and validation using a logarithmic representation of historical observed streamflow data. This is because more minor observed data were represented with a greater distance between them, whereas more extensive data were more compacted in the log graph. Thus, these absolute differences between quantities would become increasingly smaller on a log scale of representation as amount increased. However, if the term would be linear in case of variability is scalar and increases in proportion to the size of the number. Therefore, logarithmic representation of historical streamflow data as target is used during ANN development for each GCM model. The algorithm for the developed hybrid ANN model is in Table 7.2.

7.2.2.4 Model performance evaluation

For a more complete evaluation, the accuracy and ability of streamflow estimation models was also established separately for each ANN model based on their performance. Correlation coefficient (R) and root mean square error (RMSE) are performance indicators used to evaluate ANN-BP model efficiency for each model. In this case, the study was an exploratory analysis of the power of ANN models for monthly streamflow simulation. Model performance were considered satisfactory if R>0.65 and RMSE < 0.5. R provides a numerical estimate of the statistical co-variation between monthly observed streamflow data Q_m and monthly simulated streamflow data Q_s. $\bar{Q}_m$ and $\bar{Q}_s$ are the average of monthly observed and simulated streamflow data respectively. e is the error in prediction and n is the number of observations.

$$R = \frac{\sum(Q_m - \bar{Q}_m)(Q_s - \bar{Q}_s)}{\sqrt{\sum(Q_m - \bar{Q}_m)^2 \sum(Q_s - \bar{Q}_s)^2}} \quad (4)$$

$$RMSE = \sqrt{\frac{1}{n}\sum_{i=1}^{n} e_i^2} \quad (5)$$

The results were also analyzed graphically using scatter plots. In addition to these model efficiency measures, we evaluated the effects based on the flow duration curves (FDC) to help visualize the differences between observed and estimated streamflow graphically. In this study,

FDCs were divided into low and high flow measures to assess different phases of the hydrograph.

7.2.3 Uncertainty Analysis

Uncertainty in model projection is primarily caused by traditional uncertainty by any hydrological model and climate prediction uncertainty due to uncertainty arising from models, scenarios, or other internal variability due to their interaction (Hawkins & Sutton, 2011). Climate models produce different output even for the similar radiative forcing. While scenario led uncertainty can be caused by an inappropriate understanding of the climate change process, such as greenhouse gas emission. Internal variability (IV) depicts the climate system's natural variability even without any external radiative forcing. It includes processes ingrained in the land, atmosphere, the ocean, or ocean-atmosphere system. Also, all the form of uncertainties do not contribute equally hence segregation of each form of uncertainty is required (Chawla and Mujumdar 2018; Lehner et al. 2020). Several approaches are developed for quantification of uncertainty associated with climate projection with hydrological model. These include Analysis of Variance (ANOVA) (Yip et al. 2011), fourth order polynomial fitting' (Hawkins &Sutton 2011), 'maximum entropy theory' (Lee et al. 2017) and 'cumulative uncertainty approach' (Kim et al. 2019). ANOVA is a simpler and robust method for uncertainty partitioning. According to Yip et al. 2011, ANOVA requires very few assumptions compared to other methodologies. Thus, ANOVA is used here in this chapter for assessing the climate related uncertainty. The difference between future simulated and reference values is considered as the input in the ANOVA method for partitioning uncertainty due to individual sources in high and low flows. The two-way ANOVA is used to segregate total uncertainty in the projection of flow quantiles. These variance components depict uncertainty contribution of two main effects: GCM models (factor A with I=5 levels) and climatic Scenario (factor B with J=2 levels).
The ANOVA technique is defined as follows:

$$\Delta Y_{ij} = \mu + \alpha_i + \beta_j + \alpha\beta_{ij} + \varepsilon_{ij} \qquad (6)$$

ΔY is the difference between predicted and observed quantile values a given variable Y and the error term (ε_{ij}) is the internal variability. $\alpha\beta$ shows the interaction between contributing terms in uncertainty analysis. μ is the average due to contributing terms and their interaction

In ANOVA decompositions the total variance into additive component due to various sources of variation. The total variance in predicted future streamflow is given by the sum of squares from individual contributions and their interactions is given as follows:

$$SS_T = SS_A + SS_B + SS_{AB} + SS_E \quad (7)$$

Where SS_T is the total sum of squares, SS_A, SS_B is the sum of square of individual factor A and B, SS_{AB} is the interaction of two factors and SS_E is the sum of square error.
Uncertainty caused by individual factor is the ratio of individual factor sum of square to the total sum of square.

7.2.4 Processing of climate data for future streamflow simulation

Simulation of the future river flow regime scenarios under climate change in Jamuna River was done based on IPCC recommended climate change scenarios. RCP 4.5 and 8.5 (representing medium stabilization and very high emission scenarios, respectively) were utilized to project future climate scenarios. The RCP 4.5 is a lower medium stabilization scenario that stabilizes the radiative forcing level at 4.5 W/m^2 by 21st century and RCP 8.5 is a business-as-usual scenario that leads to high emissions. Three future climate scenarios have been projected, namely 2020s (2025-40) (forthcoming), 2050s (2041-80) (mid future) and 2080s (2081-2100) (distant future) time periods were used to generate climate change scenarios for the future. Streamflow calculated using the procedure described previously from individual GCMs was then ensembled for final forecasting.

For instance, one of the five GCMs selected was Goddard Institute for Space Studies (GISS-E2-H) (Source: http://pcmdi9.llnl.gov/esgf-web-fe/). The GCMs outputs of the grid cell containing the entire study basin were downloaded. The base period scenario was obtained from downloading historical data for the year 2000 to 2012 has been downloaded.

7.3 Results and Discussion

7.3.1 ANN Model Results

7.3.1.1 Selection of potential input matrix from GCM outputs

The credibility of GCM model projections is confirmed by exploring the larger-scale dynamical, thermodynamical circulations and its associated large feedback such as

temperature, water vapour, cloud cover processes that drive the local-scale future changes in the hydrological simulations. A substantial dynamical force is always exerted by topographic arrangement, on the atmospheric circulations. The land surface interchanges energy, water, and momentum with the atmosphere. Hence, land–atmosphere interactions potentially impact climate variable patterns (e.g., Blumsack 1971; Zhou et al. 2019). Precipitation change is related to various forms of atmospheric circulation patterns and atmospheric pressure (Aizen et al. 2001). Sea surface temperature and sea level pressure also vitalize precipitation depending on the geographic location (Peng and Mysak 1993). In a recent study by Nourani et al. 2018, to have a complete idea of regional changes in precipitation, precipitation was downscaled based on linear relationship with humidity type predictors such as specific humidity, water evaporation flux and nonlinear relationship with temperature based predictors representation such as air temperature, surface temperature.

The IIS model selected, the most significant and non-redundant inputs from a large real-world data set characterized by several redundant variables. Here, the potential input data matrix of the GISS-E2-H model have been used for other GCM models. NorESM1-M model uses the second-best possible input data matrix of GISS-E2-H due to non-availability of input GCM data. Correlation coefficient (R) values of 0.67 (0.66) and Adj R^2 values of 0.66 (0.65) for other model four models (NorESM1-M). Five different ANN models with two sets of input data: precipitation rate, specific humidity, wind speed, maximum air temperature, minimum air temperature, surface upward latent heat flux, and surface upward sensible heat flux, surface air pressure, maximum air temperature, minimum air temperature, surface upward latent heat flux have been proposed to predict the streamflow at the weir site. The log transformed MLR model was applied to estimate the exact effect of climate change variables contributing to the variations in streamflow estimates. Table 7.3 presents our IIS results. While positive coefficients indicate the effect of physical components on increasing streamflow, negative values suggest the effect of physical components on decreasing streamflow (Fig 7.3). This further implies that our predictors have a multiplicative relationship with predictand and not additive relationship. Results indicated that for 1 unit increase in discharge, hfls decreases by 1% for both 1st and 2nd sets and tasmax decreases by 24% and 34% for 1st and 2nd set respectively. On the other hand, for 1 unit increase in streamflow, tasmin increases by 34% and 61% respectively for 1st and 2nd set.

Table 7.3 Results of IIS method for two sets of Potential Predictors matrix for the streamflow simulation

Variables	Symbol	Coefficient	Standard error	Coefficient	Standard error
Surface upward latent heat flux	hfls	-0.01	0.003***	-0.0077	0.002***
Surface upward sensible heat flux	hfss			0.0075	0.006
Surface air pressure	ps				
Specific humidity	huss	109.34	75.72		
Precipitation	pr	-0.00	0.0002		
Wind speed	sfc	0.05	0.24		
Maximum air temperature	tasmax	-0.27	0.07***	-0.42	0.05***
Minimum air temperature	tasmin	0.29	0.1***	0.47	0.04***

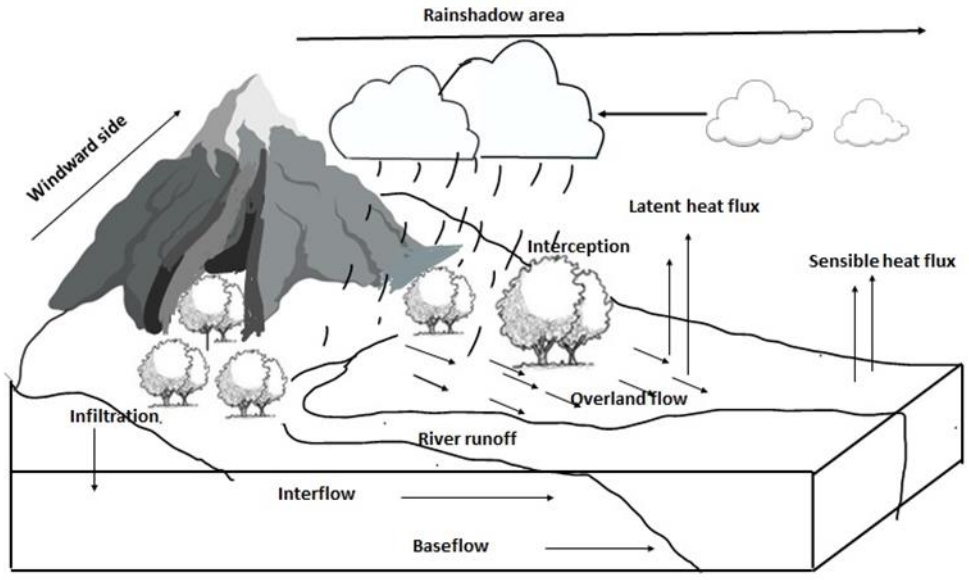

Fig. 7.3 Schematic diagram of rain-shadowed hydrological cycle

7.3.1.2 ANN model performance evaluation

The ANN statistics for each GCM model comply satisfactorily for both the calibration and validation period except for NorESM1-M in validation period due to overestimation during the simulation. Also, all the models showed good agreement and followed well the patterns of the observed data during the simulation (Fig. 7.4) Though the models produce good R value ranging from 0.91 to 0.87 and 0.81 to 0.65 during calibration and validation period respectively, the RMSE value was more in validation period than calibration period (Table 7.4). Validation period gives more emphasize for extremes due to log-transformed streamflow as evident from Fig. 7.5.

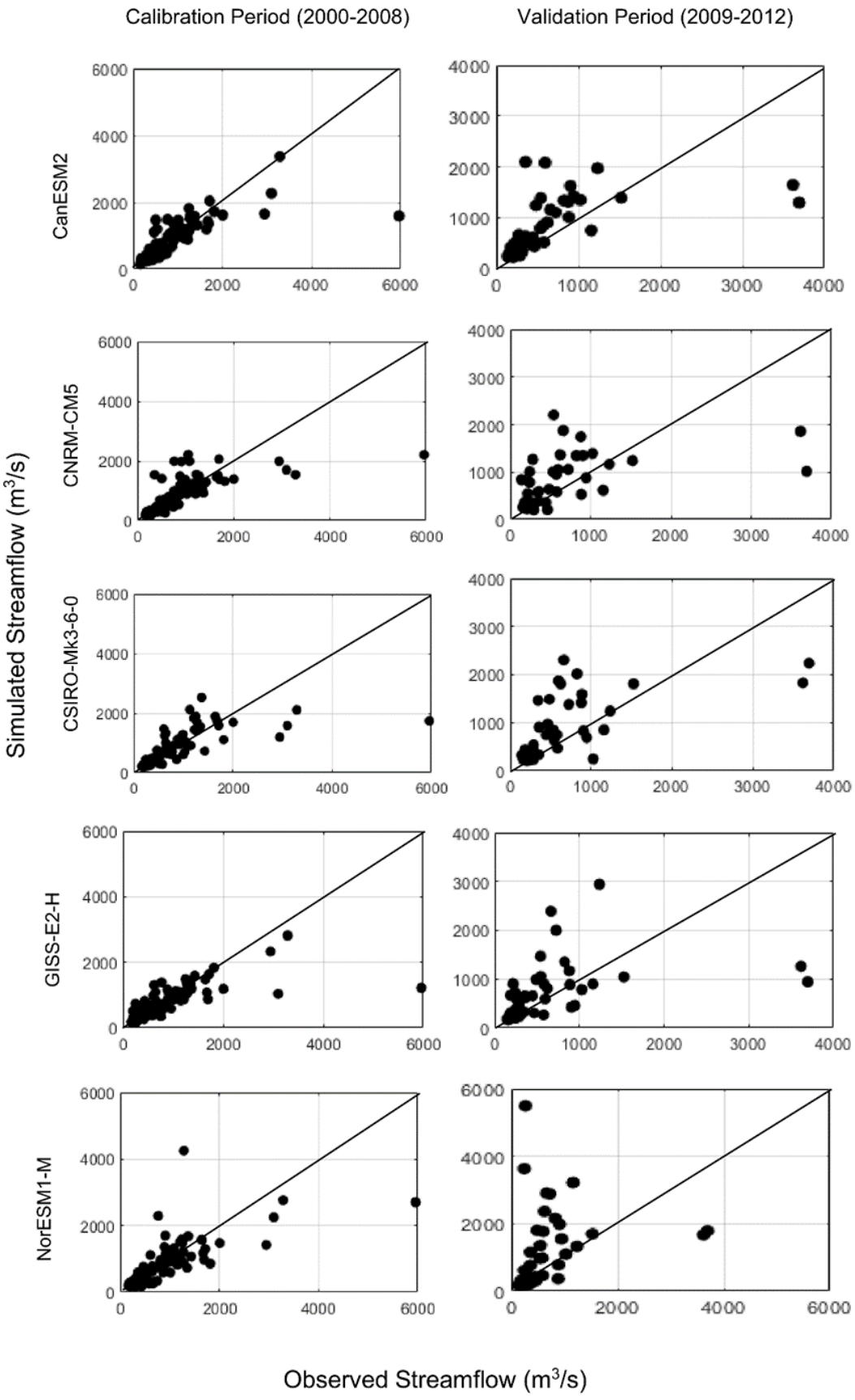

Fig. 7.4 Monthly observed vs monthly simulated streamflow at the barrage gate

Table 7.4 Performance indices calculated for the models for the calibration and validation sets at monthly scale

Model Name	Calibration		Validation	
	R	RMSE	R	RMSE
CanESM2	0.91	0.3	0.81	0.6
CNRM-CM5	0.89	0.3	0.67	0.7
CSIRO-MK3-6-0	0.90	0.3	0.76	0.6
GISS-E2-H	0.87	0.4	0.67	0.6
NorESM1-M	0.88	0.4	0.65	0.9

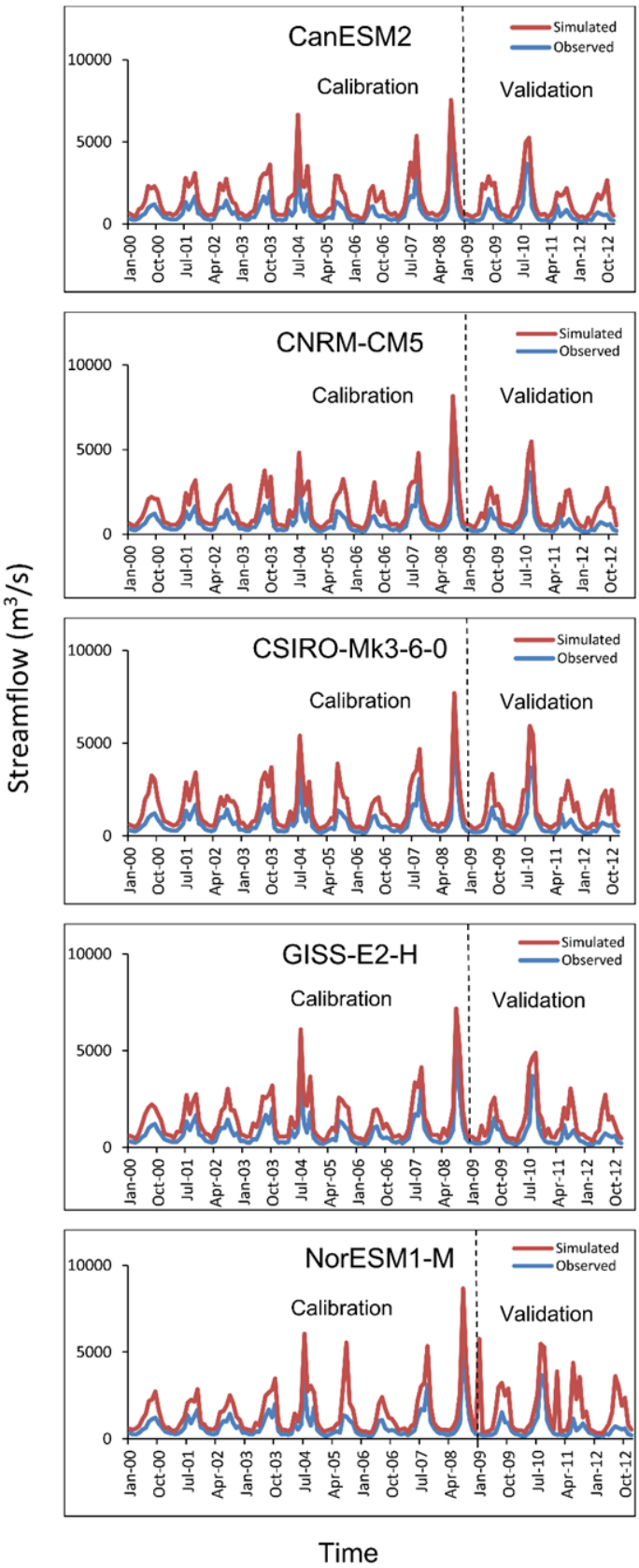

Fig. 7.5 Simulated and observed monthly streamflow at the barrage gate

7.3.2 River flow projections till 21st century

The monthly flows are seasonally categorized as winter (December–February), pre monsoon (March–May), monsoon (June–September) and post-monsoon (October–November). Over the respective three time slices (forthcoming, mid future and distant future) monthly streamflow are simulated for each separate GCM model and ensemble of GCMs (Fig. 7.6). Error for the simulated GCM values is shown in Appendix, Fig. C1. Individual GCM projections showed that during mid future and distant future, NorESM1-M showed shift in high streamflow towards postmonsoon months for all scenarios. In RCP 8.5, CanESM2 showed shift towards pre monsoon months for all time slices and GISS-E2-H in distant future (Appendix, Fig C2). Ensembled monthly flow in distant future for RCP 4.5 showed more increase than RCP 8.5. For all periods, the average winter flow under RCP 4.5 and RCP 8.5 increased by 29.04%, 100.72%, 181.89% and 22.47%, 20.91, 32.20%, respectively for forthcoming future, mid future and distant future. Streamflow also showed an expected increase during the pre monsoon months by 30.56% to 52.5% and 30.011% to 98.6% for RCP 4.5 and RCP 8.5 respectively for forthcoming future, mid future and distant future. Decrease in monsoon precipitation is expected for all periods by 5.1% to 6.91% and 3.85% to 9.95% for RCP 4.5 and RCP 8.5 respectively. The postmonsoon flow is expected to decrease more than the monsoon and likely to decrease up to 26% in distant future for RCP 8.5 and the decrease is lower in RCP 4.5. The decrease in monthly streamflow from August to November ranged between -47% to -6%, while the increase in monthly streamflow from Dec to July ranged from 202% to 9% (Table 7.5)

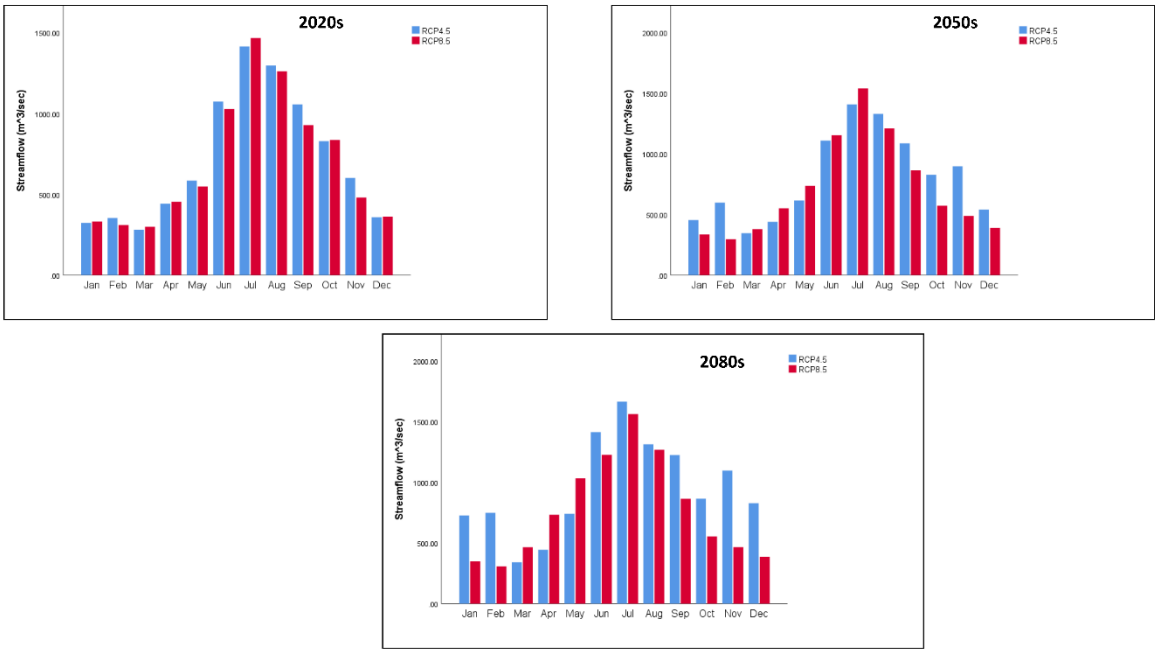

Fig. 7.6 Monthly ensemble streamflow at Bakuliaghat barrage from emission scenarios RCP 4.5 and RCP 8.5

Regarding climate change impact studies on annual streamflow alterations, the average annual river flow is projected to increase under all scenarios and in all study periods except in forthcoming future where slight decrease is projected of 0.1 % and 4% respectively for RCP 4.5 and RCP 8.5 respectively (Table 7.6). Under RCP 4.5 there is a gradual increase by 12% and 32.46% respectively for the mid and distant future. Under RCP 8.5, there is a slight decrease in flow for the mid future and increase to 7% for distant future.

Table 7.5 Absolute value and relative changes percentage in annual and seasonal flows of the Jamuna River at Bakuliaghat barrage based on average of 5 GCMs/ensembles

	Forthcoming				**Mid future**				**Distant future**			
	RCP 4.5		**RCP 8.5**		**RCP 4.5**		**RCP 8.5**		**RCP 4.5**		**RCP 8.5**	
	Absolute value (m^3/s)	**% change**	**Absolute value (m^3/s)**	**% change**	**Absolute value (m^3/s)**	**% change**	**Absolute value (m^3/s)**	**% change**	**Absolute value (m^3/s)**	**% change**	**Absolute value (m^3/s)**	**% change**
Annual	718	-0.1	692	-4	805	12	710	-1.2	952	33	769	7
Winter season	338	29	321	23	526	101	317	21	738.2	182	328	25
Pre monsoon	436	31	434	30	467	40	556	66	509	53	744	123
monsoon	1211	-7	1172	-10	1235	-5	1193	-8	1406	8	1232	-5
Post monsoon	597	-6	557	-11	755	20	484	-23	931	48	469	-26

Table 7.6 Percentage change in monthly ensembled streamflow relative to the observed streamflow in Jamuna river

Seasonal Flow		Winter			Pre monsoon			Monsoon				Postmonsoon	
	Scenarios	Dec	Jan	Feb	Mar	Apr	May	June	July	Aug	Sept	Oct	Nov
Forthcoming future	RCP 4.5	9	17	42	24	30	33	40	13	-25	-28	-21	17
	RCP 8.5	10	20	25	33	35	25	34	17	-27	-36	-20	-7
Mid future	RCP 4.5	63	65	141	53	30	41	45	13	-23	-26	-21	74
	RCP 8.5	18	21	20	68	63	68	50	23	-30	-41	-45	-6
Distant future	RCP 4.5	151	164	202	52	31	69	84	33	-24	-16	-17	113
	RCP 8.5	17	26	24	106	117	136	60	25	-26	-41	-47	-10

Distributed physical models and conceptual models which are commonly used to represent hydrologic processes, require ample input data (Pellicciotti et al. 2012; Thampi et al. 2010). Like other rain-shadow river basin, this river is influenced by orographic-induced variation in rainfall distribution (Terry and Wotling 2011). These results in difficulty and underestimating of temperature-related flow regime in climate change studies by GCM or Regional Climate Model (RCM) in rain-shadow river basins (Damseaux et al. 2020; Vandana et al. 2019). Hence, ANN was used to establish a direct relationship coefficient of the logarithmic value of observed discharge with the areal-weighted averaged GCM input data of the river catchment area. On the other hand, ANN, saves the cost and time of developing tools for streamflow simulation and require a relatively smaller amount of input data for hydrometeorological variable simulation

Streamflow is affected by several variables such as precipitation, overland flow, evaporation, infiltration, soil moisture and net precipitation (i.e., precipitation minus evapotranspiration). Further cloud formation and aerosol in rain-shadow area is dependent on specific humidity and wind speed (Varghese et al. 2021) which uses aerosol as layer for scattering solar radiation (Wei et al. 2018). An increased streamflow during the winter and pre monsoon season, than the base period was found instead of the monsoon season (Fig 7.5) contrary to most of the climate change studies on river stream flow projections of northeast India. They noted an increase in streamflow due to increased rainfall during the monsoon season (Dutta et al. 2021; Gupta et al. 2021; Patil et al. 2018). Streamflow during the monsoon season was relatively less than the base period in almost all time periods for both the RCP Scenarios (Table 7.5) because of lowered precipitation during the monsoon season (Bandyopadhyay et al. 2015). For example, previous studies in the basin reported decline in rainfall amount during monsoon season (Das 2004; Deka et al. 2016). Regarding scale of measurement, overland flow is more dominant than channel storage in a medium-sized catchment and are highly sensitive to high-intensity short-duration precipitation (Karimi et al. 2018), however, land use affects the streamflow in the river. Jamuna catchment being a forest catchment and a rainfed river, the rain water is held by the trees through interception and the ground cover facilitates to infiltrate thereby the subsurface flow becomes dominant and there are times when there is little to no overland flow (Ahirwar and Shukla 2018; Borah and Deka 2020). There is greater recharge of groundwater which can be associated with increased streamflow in winter season (Table 7.6) (Chappell et al. 2007). The increase in winter flow varied in all time periods, possibly because of the differences in rainfall in the catchment. The discontinuity in overland flow is also generated by

evaporation which is governed by latent heat flux (Priestley and Taylor 1972). Increasing net precipitation increases river discharge. The precipitation is governed by upward sensible heat flux (Myhre et al. 2018), which increases streamflow. The postmonsoon season was drier and far lower than the previously reported values in Maharjan et al. 2021; Vandana et al. 2019. The clear difference between the results of our study and those of previous studies could be related to the lower rainfall associated with rain-shadow region. Moreover, water withdrawal rates from storage built up depend on the fan shape of catchment (Subramanya 2013). Also, Mudbhatkal et al. 2017 reported a declined postmonsoon and attributed it mainly to weakening monsoon.

In line with our results other studies (Lotfirad et al. 2021; Negewo and Sarma 2021) reported more increase of streamflow in RCP 4.5 than RCP 8.5 (Fig. 7.5). They attributed it to the increased rainfall and temperature in future under RCP 8.5. Further, annual total runoff in future showed decrease from the present condition (Table 7.5) till mid future which might be associated with lowered precipitation in monsoon season (Shah and Mishra 2018). Highest increase of streamflow is projected in distant future in RCP 4.5. Other studies also reported (Dutta and Sarma 2021; Anand and Oinam 2019; Sarkar 2015) 11%, 13.06%, and 28% increase in streamflow and attributed it to increased precipitation in monsoon season.

7.3.2.1 Alterations in monthly flow extremes

The annual simulated values of Q_{95} and Q_{10} for low and high flows, in the calibration and validation periods were compared to those estimated from the observed time series. The results are presented in Fig. 7.6. Individual analysis showed that 3 out of 5 models showed good performance for low flows in the calibration period and 3 out of 5 models showed good performance in the validation period. The high flow (Q_{10}) bias ranged from -19.25% to 174.94% and bias for the low flow condition (Q_{95}) ranged from -15.26% to 43.55%. NorESM1-M showed maximum bias for high flow and CSIRO-MK3-6-0 showed a minimum bias of 1.46. CanESM2 showed maximum bias in low flow and minimum bias (Appendix, Table C2)

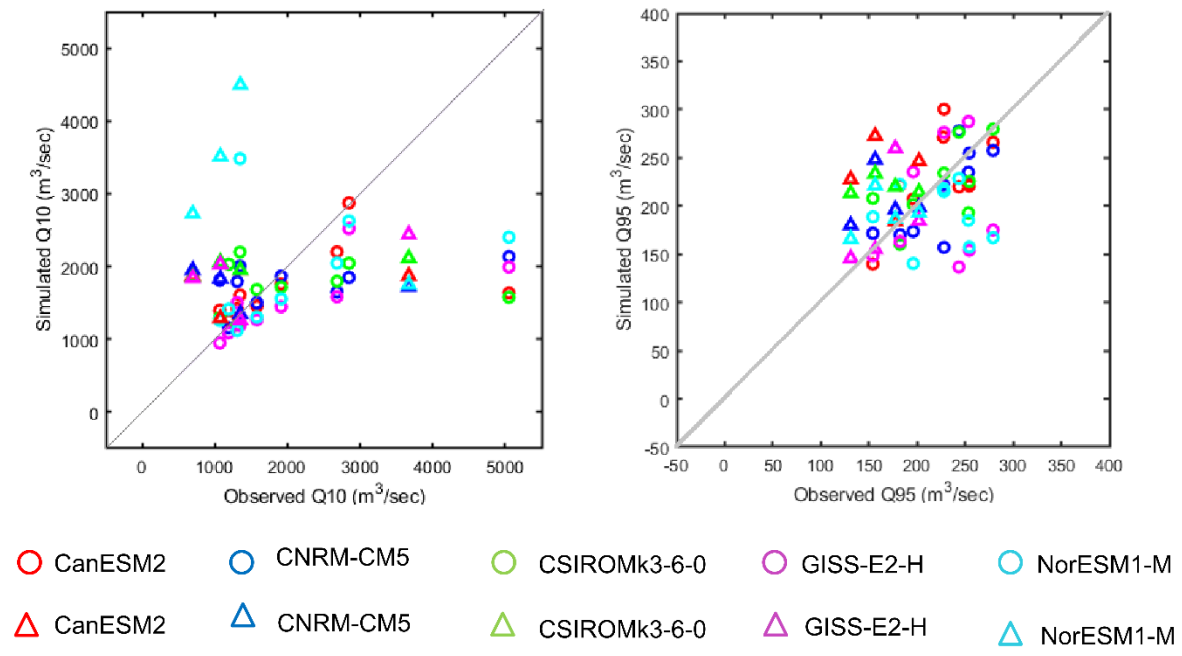

Fig. 7.7 Comparison of simulated and observed annual values of Q_{95} and Q_{10} in the calibration and validation periods for RCPs. Circle denotes calibration result and triangle denotes validation result.

The results presented in Fig. 7.8 indicate an increase in low flows under both RCP 4.5 and RCP 8.5 during all three future periods. The increase in low flows were in the range 35-45%, 49–79% and 53–73% during the 2020s, 2050s and 2080s, respectively. Further, the increase in low flow was highest for RCP 4.5 than RCP 8.5 during all three future periods except 2020s. 2020s showed least increase in low flows in both the scenarios. Similarly, analysis of high flows showed minimal increase under both RCP 4.5 and RCP 8.5 during all three future periods except 2020s of RCP 4.5 scenario The increase ranged from 0.20-2%, 15-11% during 2050s 2080s respectively. It is also to be noted that increase in high flows is greater during the 2020s followed by the 2050s and 2080s.

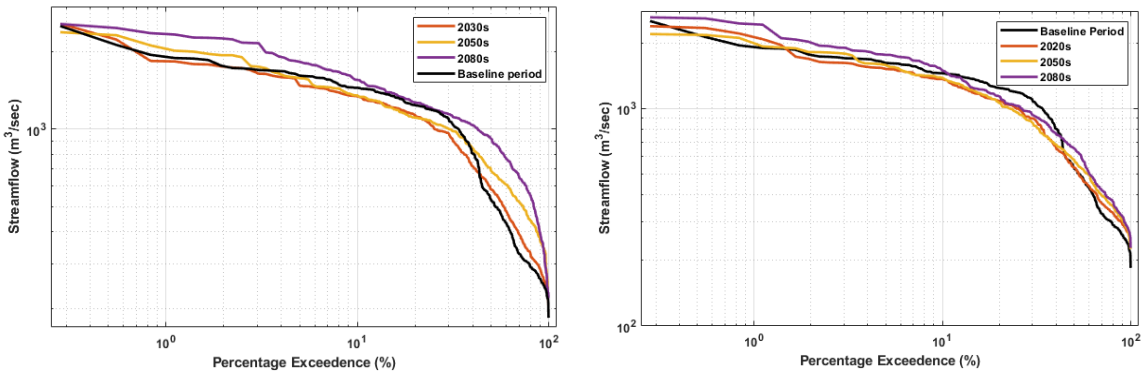

(a) (b)

Fig. 7.7 Flow Duration Curve (FDCs) at base period (2000-2012), 2020s, 2050s and2080s for (a) RCP 4.5 and (b) RCP 8.5

The FDCs thus revealed an increase in magnitude of low flows while there is a minimal increase in magnitude of high flows under all scenarios (Fig. 7.7). A slight decrease in high flows in the forthcoming future during the monsoon season, implies that greater attention may be needed for water management strategies in rice cultivation. A comparison of relative changes in high and low flows indicated a more significant increase in low flows than the high flows. The low flow increase will provide a chance to provide water for irrigation supply in the basin for meeting crop water requirements even during the low flow period. It is also to be noted that increase in both low and high flows is greater during the 2080s followed by the 2050s and 2020s except 2020s which showed lower high flows. These results confirm changes in annual streamflow of basin as a greater streamflow increase is projected during the 2080s, followed by the 2050s and 2020s.

Model evaluation result showed that different models showed different range of variations in annual as well as seasonal streamflow. This is supported by the fact that Jamuna River being a sub tributary of Brahmaputra, there is high variations amongst the monthly streamflow as tributaries are expected to have a much higher temporal variability than the main river (Döll and Schmied 2012). Further, the result for Q_{10} is weaker than Q_{95} in terms of correlation coefficient for the GCM models. Q_{10} values were 10 times higher than Q_{95}; therefore, low flow got small weights in the calibration process, leading to simulation bias.

7.3.2.2 Uncertainty analysis

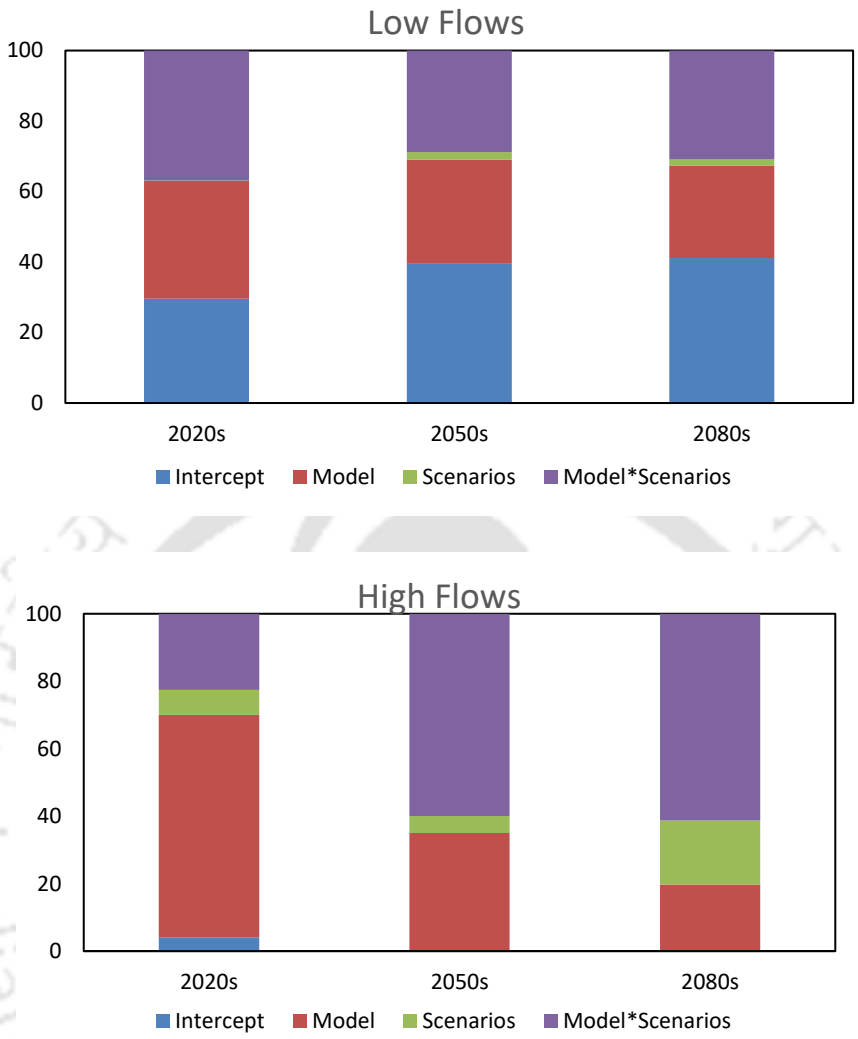

Fig. 7.8 Uncertainty analysis for low and high flows

ANOVA is used to segregate the total uncertainty in future streamflow projections for high and low flows as well as contribution of each source of uncertainty, which includes GCMs, RCPs, interaction of GCM and RCPs and IV. GCMs are the primary source of uncertainty for both the flows, followed by the internal variability for low flows and interaction effect for high flows (Fig 7.8). It can be inferred that uncertainty in the climate projections mainly lies with the selection of GCM. Several other studies also showed agreement with our findings (Chawla and Mujumdar 2018; Gaur et al. 2021; Hawkins and Sutton 2011).

The contribution of uncertainty due to IV was significant and implies its importance in regional level. Smith et al. 2020 suggested that the contribution to uncertainty could be slightly less by careful and proper initialization of climate projection and observed data sets. Further,

interaction of models and scenarios showed significant contribution of uncertainty along with GCM models which indicated towards appropriate choosing of models for climate prediction.

7.4 Conclusions

This study aimed to comprehend the impacts of climate change and its responses for irrigation supply in the Jamuna River catchment, a prominent catchment in Northeast India. For this purpose, a systematic integrated approach based on data from five different GCM CMIP5 models, IIS and using ANN-BP model for the first time in Jamuna irrigation project. All the RCP scenarios for all time periods showed an increase in winter and pre-monsoon seasons. The ANN model outputs projected an overall decrease in the streamflow values in the forthcoming future and eventually increase in the mid future and distant future for RCP 4.5 and RCP 8.5. Moreover, the winter and pre monsoon seasons showed increased streamflow than the base periods for all periods and scenarios while the monsoon season flow decreased. These results suggested that in order to acquire the positive effects from the possible impacts of climate change, the timing of cultivation of crops and opening of gate for irrigation are likely to be modified. In addition to this, crop intensification in the command area can be promoted for sustainable agricultural development. This study further highlights that a specific examination by water resources organizations is necessary to mitigate the increased flow pattern in the river as with present main canal capacity, only negligible portion of water is diverted through main canal. In particular, the current study concluded that IIS-ANN serves as a tool for agricultural planning under changing climate by quantitative streamflow estimation in similar rain-shadow regions once an appropriate set of predictors are quantified. To reduce the uncertainty in the ANN-based streamflow projection, all the sources of uncertainty in the modelling system must be considered. GCM model showed highest uncertainty.

Chapter 8

Model Selection and Assessment of Future Irrigation Demand under Climate Change

8.1 Introduction

Water allocation and management practices in most countries are challenging for water managers in the face of socioeconomic growth and climate change. Therefore, agriculture of these countries, relies on rainfall in rainfed agricultural areas (Mishra and Aayog 2019). However, climate change risk is an integral part of rainfed agriculture. Supplemental irrigation helps in reducing the risk. Moreover, freshwater resources are required to satisfy the need of water-demanding sectors such as domestic uses, industry, navigation, including establishment of irrigated arable area (UNDP, 2006; Dolan et al., 2021). Thus, the appropriate evaluation of the irrigation water demand of crops cultivated in a canal command area is necessary for the decision-making process under changing climate. In this chapter, we have presented the development of crop water demand model to understand the irrigation water demand round the year. Finally, after evaluation, the model was used for future projections of ET.

8.2 Methodology

An ensembled average value of the temperature was used for projecting future evapotranspiration under two RCP scenarios using the ET_0 method. The integrated modeling approach incorporates crop water demand model developed using Temperature based ET_0 estimation technique . The flowchart of the integrated modelling adopted in this study is shown in Fig. 8.1.

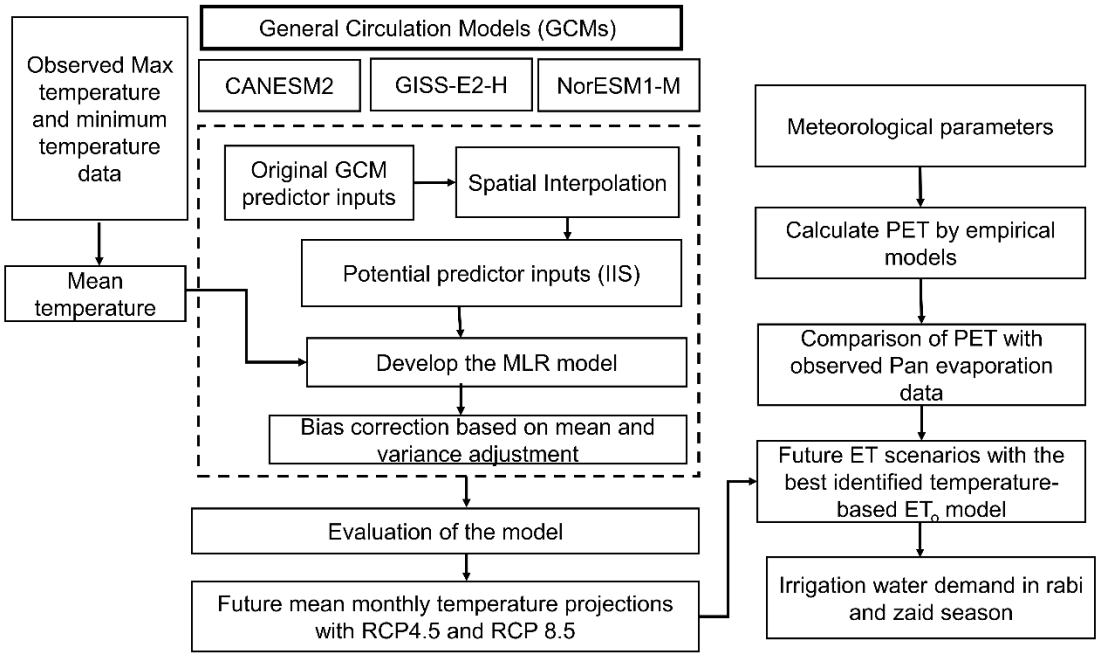

Fig 8.1 Flowchart of the methodology adopted for estimation of future agricultural water demand through integrated modelling concept

8.2.1 Temperature-based Reference Evapotranspiration assessment equations

Reference evapotranspiration (ET) assessment methods that involve only temperature climate data are viewed as temperature-based techniques The temperature methods are some of the earliest methods for estimating ET. This study used four TET methods, FAO 56 Penman-Monteith (PMT), Modified Penman (MP), Thornthwaite (TH), Blaney-Criddle (BC), to assess ET_0. The ET_0 from various model is calibrated with Pan evaporation method of ET_0 estimation (Nourani et al. 2019, Kisi et al. 2022). They have been selected to represent a sample of ET estimation methods usually used for hydrological evaluation, as presented in Table 8.1. Pan evaporation data is measured in USWB class A pan. Pan coefficient is calculated according to the relative humidity and wind speed of the area to derive reference evapotranspiration.

Table 8.1 List of Temperature based ET_0 models used in the study

Proposed by	Source	Equation
FAO 56 Penman monteith	(Allen et al 1998)	$[PT \times TT \times VPD] + [DT \times R_n]$
Modified Penman method	Doorenbos and Pruitt (1975)	$[W \times R_n] + [(1 - W) \times f(u) \times VPD]$
Blaney Criddle Method	Blaney Criddle (1950)	$\frac{T \times p}{100}$
Thornthwaite Method	(Brookeld 1948)	$1.6 \times \left(\frac{10 \times T}{I}\right)^a$

Where, R_n is the net radiation at the crop surface, TT is the temperature term, PT is the psi term, DT is the delta term, VPD is vapour pressure deficit, W is the weight for radiation term, 1-W is the weight for aerodynamic term, f(u) is the wind related function, T is the mean monthly temperature in Farenheit and p is the monthly daylight hours expressed as a percentage of daylight hours of the year. I is the annual heat index, T is the mean monthly temperature, and a is an empirical exponent**.**

8.2.2 Evaluation criteria for selection of best ET model

The ET by various methods investigated and compared using linear correlation coefficient (R) (Eq. 1), normalized standard deviation (σ*) (Eq. 2), and centralized root mean squared deviation (CRMSD) (Eq. 3) (Taylor 2001). The Taylor diagram allows to rank the multiple models by using these three different performance evaluation criteria,

$$R = \frac{\frac{1}{N}\sum(x_i - \bar{x})(y_i - \bar{y})}{\sigma_x \sigma_y} \quad (1)$$

$$\sigma_* = \frac{\sigma_y}{\sigma_x} \quad (2)$$

$$CRMSD = \sqrt{\frac{1}{N}\sum[(x_i - \bar{x}) - (y_i - \bar{y})]^2} \quad (3)$$

Where y_i = simulated values and x_i = observed values and $\bar{y}$ = mean of simulated values and $\bar{x}$ = mean of the observed values and σ_x = standard deviation values of observed values and σ_y =

standard deviation of simulated values of predictands respectively and the N represents the sample size of the training and testing data

8.2.3 Calculation of future irrigation water demand based on cropland water balance

Water required by crops refers to the amount of water needed during its growth period to develop into a full-fledged crop. The water required is related to the water from various sources, and the balance equation is as follows:

$$WR = ER + IR + \Delta SW + \Delta GW \quad (4)$$

Where WR is the net water demand of different crops (mm), ER is the effective rainfall, IR is the irrigation requirement; ΔGW is the groundwater contribution during the growth of the crop (mm), and ΔSW is the soil moisture storage contribution (mm). To assign net water required, ground water and soil water contribution is considered as 0. It can be observed from the groundwater monitoring well data that the groundwater level below ground in the irrigation area is usually more than 10 m, which cannot be utilized by crops and minor changes in soil moisture occur during the crop growth period because of the well-timed irrigation. The effective precipitation in the formula refers to the amount of rainfall that cannot be utilized by crop for full-fledged growth and development as seasonal effective precipitation contributes less than 9% of effective rainfall during the non-monsoon period and it is insignificant to cause any error (Sethi et al. 2019)

In this study, we selected major food crops (cereals, pulses and oilseeds) based on the household food consumption pattern in Eastern India and cultivated during rabi and zaid season after rice harvest in multi-cropping system. List of crops includes summer rice, lentil, mustard, maize, wheat as the rabi period and ahu rice, sunflower, moong, urad during zaid season (Directorate of Economics and statistics (DES), 2018). Therefore, these crops are proposed in this study for intensive cultivation and area augmentation of rice-fallow cropping system. The rabi season starts from post monsoon and finishes in mid-pre monsoon season while zaid season is of short duration between rabi and monsoon season. The crop water demand/requirement (CWD) of each cropping season for individual food crops was estimated by multiplying the crop coefficient of individual crop by ET_0 as irrigation demand in crop lands. The crop coefficient was obtained from FAO 56 paper (Allen et al. 1998). Then, the derived CWD was multiplied by crop harvested area for agricultural water demand.

8.3 Results and Discussion

8.3.1 Performance of evapotranspiration

The Taylor diagram in Fig. 8.2 depicts the statistical patterns and similarities in distributions of Pan evaporation data with each temperature-based ET_0 model (PMT, MP, TH, BC). Surprisingly, detecting model relationships and deviation with the observed data is more straightforward. For instance, correlation coefficient (R) ranges from 0.75 to 0.45. It conveys the percentage of variation explained by the models. The lower R values represent weak goodness of fit. The highest R values are observed for BC followed by TH model. The CMRSD value represents the error in the model, and the TH has a higher value of CMRSD with a higher standard deviation. However, in Taylor plot, the PMT, BC which are near each other should be realized as being distant from the observational data set rather than necessarily adjacent to one another. The Blaney Criddle equation had the best performance among all the TET models, featuring a lower CRMSD and higher R value (Fig. 8.2). Furthermore, while some studies suggested that the FAO 56 methods could be a potential evapotranspiration estimating method, with only maximum and minimum temperature, this may not be the case for this study (Jensen and Haise 1963, Jabloun and Sahli 2008). In a survey carried out by, Liu et al (2017), they compared, 16 temperature-based models for the estimation of monthly ET_0, in a semi-arid site in China to find that the FAO-ppp-17, Penman and 1963 Penman model had the best overall performance than FAO-56. It was reported that FAO-56 showed large error in high evaporative environment. Later, Pandey et al., (2016) study conducted in several stations of northeast region of India for the identification of a suitable alternative to the FAO-56. It is essential to highlight that the BC equation conserves part of its physical base, which probably makes it more ideal for TET method in northeast region as the temperature is the driving factor while wind speed has a negligible effect. High humidity conditions, as are characteristic in northeast India. The Taylor diagrams also establish that the substitute data set is in better correspondence with the primary observations than are any of the models selected. The agreement is significant because, for any given observation, the two estimations may be derived from different energy balance equations, which resulted in substantial differences in the simulations of ET_0 models. These diagrams convey strong evidence for higher prediction skill of BC model, with better or nearly equal deviation than other TET models used in this study. Overall, the performances of the evapotranspiration methods depended on various conditions, including, but not restricted

to, the transformation function and the topographic situation of the region. The variation in model structures and involved variables caused differences from region to region.

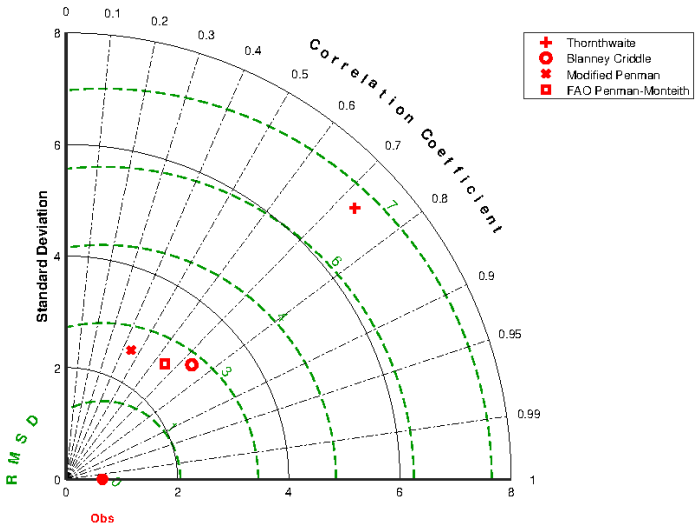

Fig. 8.2 Taylor diagram for statistical comparison of station monthly Pan evaporation (Observed) with 4 ET estimation methods for the period (2000-2009)

8.3.2 Climate change impact on evapotranspiration

Table 8.2 Absolute value and relative changes in annual and seasonal ET values of the Jamuna Command area based on 3 GCMs/ensembles

	Forthcoming				**Mid future**				**Distant future**			
	RCP 4.5		**RCP 8.5**		**RCP 4.5**		**RCP 8.5**		**RCP 4.5**		**RCP 8.5**	
	Absolute value (mm)	**Relative change**	**Absolute value (mm)**	**Relative change**	**Absolute value (mm)**	**Relative change**	**Absolute value (mm)**	**Relative change**	**Absolute value (mm)**	**Relative change**	**Absolute value (mm)**	**Relative change**
Annual	195.61	-1.02	193.70	-2.93	197.17	0.54	196.63	0	197.83	1.20	200.1	3.45
Winter season	37.1	-0.19	36.7	-0.57	37.5	0.23	37.5	0.16	37.3	0.30	38.2	0.90
Pre monsoon	52	0.12	51.3	-0.59	52.4	0.49	52	0.18	52.5	0.64	53.2	1.26
monsoon	77.1	-0.47	76.5	-1.06	77.6	0.08	77.5	-0.11	77.9	0.33	78.6	1.01
Post monsoon	29.3	-0.49	29.1	-0.72	29.6	-0.25	29.5	-0.23	29.7	-0.07	30	0.27

Table 8.3 Change in monthly ensembled ET relative to the observed ET in the Jamuna Command area

Seasonal Evapotranspiration		**Winter**			**Pre monsoon**			**Monsoon**				**Postmonsoon**	
	Scenarios	**Dec**	**Jan**	**Feb**	**Mar**	**Apr**	**May**	**June**	**July**	**Aug**	**Sept**	**Oct**	**Nov**
Forthcoming future	RCP 4.5	-0.31	0.09	0.07	0.09	-0.03	-0.22	-0.09	-0.08	-0.08	-0.28	-0.24	-0.25
	RCP 8.5	-0.47	-0.11	0.01	-0.18	-0.15	-0.25	-0.34	-0.28	-0.17	-0.28	-0.30	-0.41
Mid future	RCP 4.5	-0.17	0.16	0.23	0.14	0.21	0.13	-0.03	0.04	0.05	0.01	-0.07	-0.18
	RCP 8.5	-0.25	0.24	0.17	0.08	0.13	-0.03	-0.08	0.03	0.01	-0.07	-0.08	-0.15
Distant future	RCP 4.5	-0.16	0.21	0.25	0.15	0.27	0.22	0.05	0.11	0.11	0.06	-0.02	-0.05
	RCP 8.5	0.07	0.35	0.48	0.40	0.47	0.39	0.24	0.28	0.25	0.23	0.17	0.10

Spatial and annual variations of ET_0 study are of keen interest to climatologists and meteorologists. Still, as an agriculturist, seasonal or even monthly calibrations are of great importance to crops (Nouri et al. 2018). ET_0 during the season was relatively less than the base period in the early century for both the RCPs except pre monsoon in RCP 4.5. Under the RCP scenarios 4.5 and 8.5, the seasonal changes over the study area have been shown in Table 7.2. The winter season ET_0 increased from 0.4 to 0.6% (0.8 to 2.4%) in 2041-2070(2071-2100). Pre monsoon season ET_0 over the command area was increased from 0.3-0.9 % (1.23–2.43 %) in 2041-2070 (2071-2100). Monsoon season increased from 0.4 to 1.3% in 2080s (Table 8.3). However, postmonsoon showed decrease in all scenarios and all time period except RCP 8.5 in late century. Postmonsoon showed a decrease from 1.6% to 2.4% (0.7 to 0.8%) in 2025-2040 (2041-2070). Seasonally, water demand in the command area was highest for pre monsoon 147 Mm^3 and 146 Mm^3 in the distant future for RCP 8.5 and RCP 4.5 respectively. It is followed by winter and post-monsoon months. Though there was a gradual rise, the months of September, October, November, December and June showed less value in RCP 8.5 in the forthcoming future than the base period up to 1.6%, 1.9%, 3%, 3.7% and 1.7%, respectively (Table 8.3). At the same time, January to May showed an increase in ET_0 for RCP 8.5 up to 3.9% in February. Accordingly, the rabi crop evapotranspiration over the command area was increased by about 0.6-1 %, and 0.4–2.5 % during mid and distant future periods under RCP 4.5, and 8.5 scenarios, respectively. The zaid crop evapotranspiration 0.5-1.3% and 0.1-2.4% during mid and distant future periods under RCP 4.5, and 8.5 scenarios, respectively.

8.3.3 Future irrigation water demand estimation using climate change scenarios

Table 8.4 Crop water requirement of candidate crops along with kharif rice in intensive cultivation

Season	Crop type	Total water requirement (m^3/ha)					
		Forthcoming		Mid future		Distant future	
		RCP 4.5	RCP 8.5	RCP 4.5	RCP 8.5	RCP 4.5	RCP 8.5
Rabi	Summer rice	7351	7262	7418	7395	7431	7543
	Lentil	6246	6173	6305	6290	6314	6416
	Mustard	2785	2756	2815	2810	2820	2866
	Maize	6282	6205	6338	6319	6350	6445
	Wheat	3637	3594	3671	3663	3676	3736

Zaid	Ahu Rice	7147	7076	7204	7175	7231	7301
	Moong	2933	2896	2956	2936	2968	2998
	Sunflower	4072	4031	4107	4085	4124	4164
	Urad	2933	2896	2956	2936	2968	2998

October is the start of rabi crop growing season starting from October and is extended up to April/May. The season sets about with the quite dry months of October and November, where scanty rainfall is received in the country. Due to the dry and drought like conditions in these months, sowing is usually shifted towards late November or in the start of December to avail soil moisture gained from rainfall which is required for germination and initial crop establishment However, winter rains (December to March) are insignificant in rain-shadow areas of the mountains. Also prolonged dry spell during the critical stages of crop growth results into lower than the potential yield. Therefore, estimation of irrigation demand for proper irrigation is likely to reduce risk associated with rainfed cultivation. Table 8.4 shows the projected crop water demand in the command area's rabi and zaid cropping season under two scenarios in three future time slices. It can be noticed that the quantity of water required in each cropping season of the command area is dependent on the crop cultivated. The overall rabi crop evapotranspiration demand was determined for the study area, which increased gradually from 7351 to 7431 m^3/ha and 2785 to 2820 m^3/ha under RCP 4.5, and 7262 to 7543 m^3/ha and 2756 to 2866 m^3/ha under RCP 8.5 scenarios for summer rice and mustard crop respectively till the end century. Summer rice and mustard crop are the highest and least water-demanding crops among the selected crops in the rabi season. Summer rice water requirement is up to 206 Mm^3 and 292 Mm^3 respectively for RCP 4.5 and RCP 8.5. Crop water requirement for mustard crop is up to 78 Mm^3 and 127 Mm^3 respectively for RCP 4.5 and RCP 8.5. Similarly, for zaid crop, ahu rice had highest water demand varying from 7147 m^3/ha to 7231 m^3/ha and 7076 m^3/ha to 7301 m^3/ha in RCP 4.5 and RCP 8.5 respectively. Ahu rice crop water requirement increased up to 200 Mm^3 and 202 Mm^3, respectively. Further rabi crop demand increased significantly, followed by zaid and kharif in RCP 8.5, whereas increase in CWD was highest for zaid crop for RCP 4.5. The maximum utilizable is only 206 Mm^3 for rabi and 154 Mm^3 for zaid. The findings suggested that, the existing water diversion infrastructure is insufficient in terms of single crop and it will be hard to satisfy the irrigation water demand of water-intensive crops like rice (Table 8.4). This water shortage implies either expansion of water diversion structure or reduction in crop cultivating area or crops under deficit irrigation must be followed. For

instance, crop diversification would lead to consumption of 147 Mm^3 and 120 Mm^3 for rabi and zaid crops, till the end of century. Except for the forthcoming future, other simulated scenarios showed an increase in evapotranspiration. For both the scenarios summer rice, lentil, mustard, maize, wheat increased from 0.5% to 0.8% (1% to 2.5%), 0.5% to 0.7% (0.8% to 2.5%), 0.4 to 0.6% (0.8% to 2.4%), 0.5% to0.8% (1% to 2.5%), 0.5% to 0.7% (0.8% to 2.5%) in 2041-2070 (2071-2100). Similarly, ahu rice, moong, sunflower, urad increased from 0.1 to 0.5% (0.8% to 1.8%), 0.2 to 0.9% (1.3% to 2.4%), 0 to 0.6% (1 to 2%), 0.2 to 0.9% (1.3% to 2.4%) in 2041-2070 (2071-2100). Moreover, this underlines the need to improve water use efficiency by adopting modified irrigation techniques such as drip irrigation in the face of demographic growth and demand for more food crops. Additionally, developing alternative water sources within the command area will meet the crop water demands through the water supply. Alternative sources include rainwater harvesting and recycling (Yuan et al. 2003, Velasco-Muñoz et al. 2019). Further, the excess water during the monsoon season can be stored in, on-farm irrigation ponds for crop cultivation in the subsequent season (Vico et al. 2020). Summer rice demands more water than other crops such as maize, and mustard. Thus, crop diversification with lesser water-requiring crops instead of monocropping help reduce the irrigation demand and thus increases water availability (Sarker et al. 2021). Overall, to achieve sustainability in the agricultural catchment, the adoption of science-led water management strategies needs to be practiced under probable climate change scenarios. Infrastructural changes and enough access to water through booster pump could be made for more water availability. This study confirms that climate change will greatly impact agricultural water demand of rice-fallow crop land areas of Eastern India. However, these scenarios indicate that agricultural areas can potentially enhance water use efficiency, either through improved irrigation system or depending on the type of crop selection. For example, with lower water requirements, summer rice can be replaced by maize and wheat. A study in the odisha district suggested a diversification and cropping pattern based on water availability which would balance the water supply-demand (Brahmanand et al. 2021). Further, in their study, Hao et al.,2018 developed optimal cropping patterns based on water availability and saving potential for increased water use efficiency and maximization of benefit of farmers. Nevertheless, rice being the water-loving crops, several technologies are developed for mitigating water-scarce conditions under climate change (Enriquez et al. 2021, Parthasarathi et al. 2012). Land productivity and food security are threatened by climate change if the basic water conservation measures such as crop diversification, crop breeding and types, and innovative technologies

are not practiced, especially in rice-fallow cropland areas. The present study necessitates the vital points to be considered to jointly remove water insufficiency under traditional irrigation system while increasing regional agricultural productivity in response to climate change. It can be summarized as modifying to multiple cropping, cultivating crops requiring relatively less water; more efficient irrigation systems, and expanding infrastructure to avoid unnecessary loss while given environmental flows. Furthermore, emphasis should be given to integrating small farms to increase irrigation efficiency in an agricultural area. Suitable adaptations while reducing the current area under cultivation for water-intensive crops such as rice, onion, etc., changing practices (using favourable sowing dates according to climate, and high-yielding cultivars for the particular agro-climatological region). The present situation in eastern India is unacceptable as they cannot fulfil the required demand for food for people and depend on exported food. The continued use of current water utilization systems and cultivation practices argues for an urgent need to shift towards scientific solutions that would then be seen as a rational approach to decision-making on a pragmatic evaluation of alternatives available. In addition, the sustainability recommendations for using water resources should be popularized to agricultural water consumption based on demand. Stakeholder engagement is crucial for bringing in the firm technically feasible policies and regulations, and advocating balanced water consumption per available water resources. However, such policies should be able to deal with farmers' choice and consumer needs along with market access (Burchfield and de la Poterie 2018). In a nutshell, the level of implementation of water demand calculation for future water management will change depending on trends in farmers choice, CO_2 induced crop physiology and agricultural management systems.

8.3.4 Irrigation water management for rice-fallows under changing climate and demographic growth

The agricultural water management model for future climate change scenario was prepared by the combined impact of demographic growth and outcomes of optimization, hydrology and crop water demand model on EFR. Future streamflow data generated for two RCP scenarios were utilized for providing inflow volume to the reservoir. The reservoir optimization model was used for crop planning in irrigation command area, and the crop water requirement of the crops were estimated from the developed crop water demand model. Based on the ideal cropping plan, future food demand was evaluated through a conceptual approach of demographic growth and crop water requirement scenarios under climate change. Future projection of increased population was assessed from the linear equation prepared from census

data of 2011 and subsequent 1.5% increase rate every year. The command area comprises of 21 villages and encompasses major portion of Nagaon district of Assam. A schematic flowchart of the integrated modelling approach for irrigation water management in a river basin under changing climate and demographic growth is shown in Fig 8.3. Climate change brings in additional stress to existing stressed water systems due to burgeoning population and socio-economic development in developing countries. Climate change is intrinsically related with the hydrological cycle and is expected to cause significant changes in local level water resources systems for practical implementation necessitating adaptive strategic measures and mitigation. Increasing temperatures, for example, are likely to introduce change in precipitation patterns resulting in variations in regional water availability as well as evaporative water demand of crops. An extensive assessment of local scale hydrological impacts of climate change is thus mandatory for practical implementation.

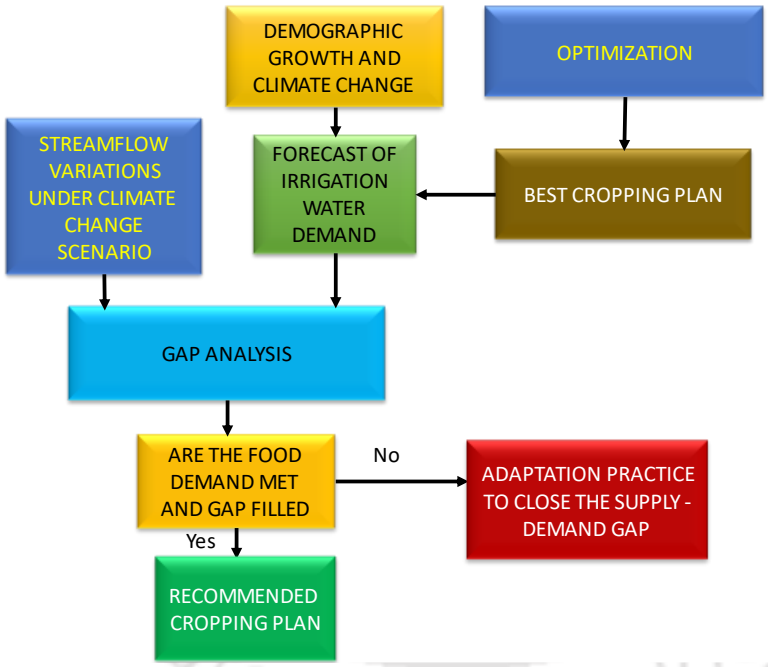

Fig. 8.3 Road map to assess the water gap in intensive cultivation

Water is sufficient even at 90% release of water and 0.9 probability with the ideal cropping plan however there is need for expansion of cropping area with population growth along with cultivation of high yielding variety (Table 8.5).

Table 8.5 Water supply-demand assessment for 2020s, 2050s, 2090s

Crops	2020s					2050s					2080s				
	Food demand in area (ha)	**Water Demand (Mm^3)**		**Water available (Mm^3)**		**Food demand in area (ha)**	**Water Demand (Mm^3)**		**Water available (Mm^3)**		**Food demand in area (ha)**	**Water Demand (Mm^3)**		**Water available (Mm^3)**	
Total	3209	RCP 4.5	RCP 8.5	RCP 4.5	RCP 8.5	5016	RCP 4.5	RCP 8.5	RCP 4.5	RCP 8.5	7840	RCP 4.5	RCP 8.5	RCP 4.5	RCP 8.5
Wheat	638	179	146	282	288	998	186	186	399	304	1560	194	196	399	353
Maize	49					77					120				
Lentil	1228					1919					2999				
Mustard	762					1191					1861				
Tomato	66					102					160				
Onion	132					207					323				
Potato	334					522					817				

8.4 Conclusions

The impact analysis of the projected temperature in irrigation water demand in a command area indicates that water demand for the rabi and zaid is going to be increased. Therefore, the water demand of each crop in crop diversification provides a synoptic view for the total water demand for crop intensification due to increase in temperature. Further, under changing climate and demographic growth, adequate water is available to meet the demand of crops selected for crop diversification. This chapter underlines the need to improve crop variety to produce more yield per hectare efficiency by adopting irrigation service as abundant surface water is available for irrigating cropland areas. Additionally, expanding irrigated areas in the river basin will meet the food demand of the growing local population residing in the command area and increase the farmers' benefit, provided other inputs are available along with market access. These will also help manage the water supply to minimize imbalanced water release such as insufficient water or waterlogged condition and affecting the environmental flow release in the future.

Chapter 9

Summary and Future Scope

9.1 General

This study presents a framework for the cultivation of crops to achieve sustainable agricultural under changing climate. The framework was developed using the basic concept of nutrient balance and agricultural water demand-supply. Several cropping patterns was developed at various levels of irrigation water available in a command area. The best cropping plan was tested by considering the impact of climate change. Further, a detailed analysis of field nutrient balance was performed at village level. The impact of climate change on the agricultural water demand-supply in the command area of the river basin was quantified using climate models and ANN. Different combinations of GCMs and RCPs were used to evaluate the changes under the projected climate.

9.2 Summary and Conclusion

A brief summary along with some concluding remarks are presented below on various research topics taken up under this study.

9.2.1 Nutrient balance and Cobb Douglas model

The nutrient balance for the rice-fallow cropping system was for non-submerged rice soil conditions. Hence, considerable information on the leaching and runoff losses for the budgeting of nutrients was not taken into account. In this work, a farmers' participatory approach is proposed for the nutrient balance study. The lab analysis data and farmers' data were linked to form the Cobb-Douglas model. The model was developed using with experimental data of 13 villages of the command area. The investigation into the nutrient balance for residual nutrient agreed with other studies (Sakin, 2012; Geisseler et al. 2017; Meng et al., 2014). Presence of the residual nutrient in soil was considered in the subsequent cultivation in fallow lands to prevent excess or less fertilizer use. The performance of the cobb-Douglas model is found satisfactory.

9.2.2 Optimization

The fallow lands after the cultivation of rice can be beneficially utilized by farmers for crop diversification. Hence, the prior information of soil quality and available water resources is

necessary for crop planning and maximization of the benefit of farmers along with food security. In this work, a chance constrained approach is proposed for crop diversification by linking PDF with linear optimization model. The environmental flow release rates in the realm are realized from FDC methods. From FDC method, flows ranging from Q_{90} to Q_{10} are used as various level of indicators. The several risk probabilities are formed in water constraints. Also, the influence of EFR on water is also considered. The residual nutrient into the optimization model is considered for soil quality and fertilizer requirement. Both, the food demand and cultivation preference of the farmers are taken into account. Various model scenarios were generated to form the best optimal cropping pattern. The model was then applied to the command area. Results showed Scenario A as the ideal cropping plan at all probabilities and preference food crop area cultivated should not be more than 20% of the total area. Cultivation of vegetable crops with proper market facilities are recommended.

9.2.3 Temperature change

To study the effect of climate change on various crop water demands in the Jamuna command area during the rabi fallow season, temperature-based ET model was developed. For that, mean temperature data were statistically downscaled using Multiple Linear Regression, which was further bias corrected. The downscaling result from the ensemble of 3 GCM showed increase in winter and pre monsoon temperature while there is a decrease in post monsoon season. The post-monsoon season showed a decline in temperature to 0.25% in the mid-future for RCP 4.5 and RCP 8.5 showed a significant decrease in post-monsoon temperature to 0.26% in the near future. Contrary to our findings, previous studies reported an increase in the trend for post-monsoon temperature. The lower mean temperature values during October and November could be mainly due to more aerosol particle-laden continental airmass present over the region and locally generated pollutants which is a characteristic of the rain-shadow area.

9.2.4 Irrigation demand

With prior knowledge about crops to be cultivated and temperature projections, the proposed model is integrated with the crop water demand model for its application in fallow lands of South Asia under changing climate. A crop water demand assessment is carried out to estimate the overall irrigation demand in the command area. The temperature change analysis was used for ET estimation using the Blaney-Criddle ET model based on comparison with the observed Pan evaporation data and Taylor diagram. The developed model was used for ET projections for 2025-2100. The results from the developed model indicate that lower mean temperature

values during October and November. Further, rabi crop evapotranspiration over the command area was increased by about 0.6-1 %, and 0.4–2.5 % during mid and distant future periods under RCP 4.5, and 8.5 scenarios. Based on study results, it can be suggested that there is a possible increase in crop water demand in the basin due to an increase in temperature. Further, it will increase the need for water supply from the river for irrigation under changing climate in the future.

9.2.5 Hydrologic modeling

Reviewing the different studies on the hydrological models and climate change impact, rainfall-runoff relationship is mainly established. In an undulating topography, especially in rain-shadow areas, the irregular pattern of rainfall and temperature affects the reliability of such hydrological models. However, the data-driven method has emerged as widely used model to understand complex processes with meagre amount of data for some of the otherwise important physical parameters of hydrological process. Thus, for the climate change scenarios, Artificial Neural Network model was developed from spatially interpolated selected GCM model outputs from CMIP5. The selection of potential predictors was based on the IIS algorithm. Results indicated that for 1 unit increase in discharge, hfls decreases by 1% for both 1st and 2nd sets and tasmax decreases by 24% and 34% for 1st and 2nd set respectively. On the other hand, for 1 unit increase in streamflow, tasmin increases by 34% and 61% respectively for 1st and 2nd set. Model evaluation result showed that different models showed different range of variations in annual as well as seasonal streamflow. Jamuna river being a sub tributary of Brahmaputra, there is high variations amongst the monthly streamflow as small tributaries are expected to have much higher temporal variability than the main river. The developed model was used to project river inflow at upstream of the barrage for 2025-2100. Results showed that towards end of the century, there is a possibility of annual increase in streamflow up to as high as 33% and 7% for RCP 4.5 and RCP 8.5 respectively. However, there is a considerable decrease in monsoonal flow and even more decrease in post-monsoon season for both the scenarios. Interestingly winter flow has shown an increasing trend.

9.2.6 Coupling of demographic growth within the developed model

Demographic growth and increased food demand are an integral part of the food security and influence the land and water resources required for crop production in addition to the climate change. The agricultural water management model for future climate change scenario was prepared by combined impact of demographic growth and outcomes of optimization,

hydrology and crop water demand model on EFR. Future streamflow data generated for two RCP scenarios were utilized for providing inflow volume to the reservoir. The reservoir optimization model was used for crop planning in irrigation command area, and the crop water requirement of the crops were estimated from the developed crop water demand model. Based on the ideal cropping plan, future food demand was calculated through a conceptual approach of total population increase and crop water requirement scenarios under changing climate. Water is shown to be abundant as compared to land in future time periods even at the mid of century, thus emphasizing on urgent need for land expansion or cultivation of high yielding variety.

The limitations and future extension of the current research work are as discussed below:

9.3 Future Scope

The scopes of future study may be recommended as follows:

1. The nutrient balance study in the command area provides a tool for avoiding inadvertent fertilizer abuse for nitrogen and phosphorus and more accurate trends should be possible with database expanded over years.
2. The GCM models that were selected for simulating the historical regional climate showed variation in climate change impact studies which therefore brings changes in ensembled projections. The upcoming CMIP6 model archive from the IPCC can be used for climate change studies using socio-economic scenarios.
3. Irrigation water demand model for the projections of crop evapotranspiration is based only on projected temperature using 3 GCM models and 2 RCP scenarios. However, the proposed model does not take into account changes in crop phenology under changing climate
4. In optimization model, for maximizing benefit through agricultural practices was done for a small agricultural area of the river basin considering household food security. However, the model can be used for maximizing benefit considering expansion of cropland area through deforestation in the basin.

Appendix

Appendix A

Table A1 Soil Organic Carbon (SOC) at the start and end of cultivation

Villages Code	SOC at the before of cropping season (%)	SOC at the end of cropping season (%)
V1	0.50	0.60
V2	0.39	0.37
V3	0.37	1.55
V4	0.28	0.86
V5	0.29	0.66
V6	0.21	0.41
V7	0.20	0.49
V8	0.24	0.63
V9	0.50	0.72
V10	0.45	0.60
V11	0.31	0.79
V12	0.22	0.50
V13	0.25	0.39

Table A2 Nitrogen (N) and Phosphorus (P) uptake by rice for various doses of N and P fertilizer applied.

Fertilizer doses	Plant N uptake	Plant P uptake
Low	59.35 ± 3.00^{a}	103.82 ± 6.02^{a}
Medium	59.59 ± 7.15^{ac}	136.53 ± 6.63^{a}
High	118.30 ± 4.85^{b}	45.48 ± 11.32^{b}
Very high	90.45 ± 14.79^{bc}	60.60 ± 21.52^{ab}

* Means within a column followed by different letters are significantly different at $P\leq0.05$

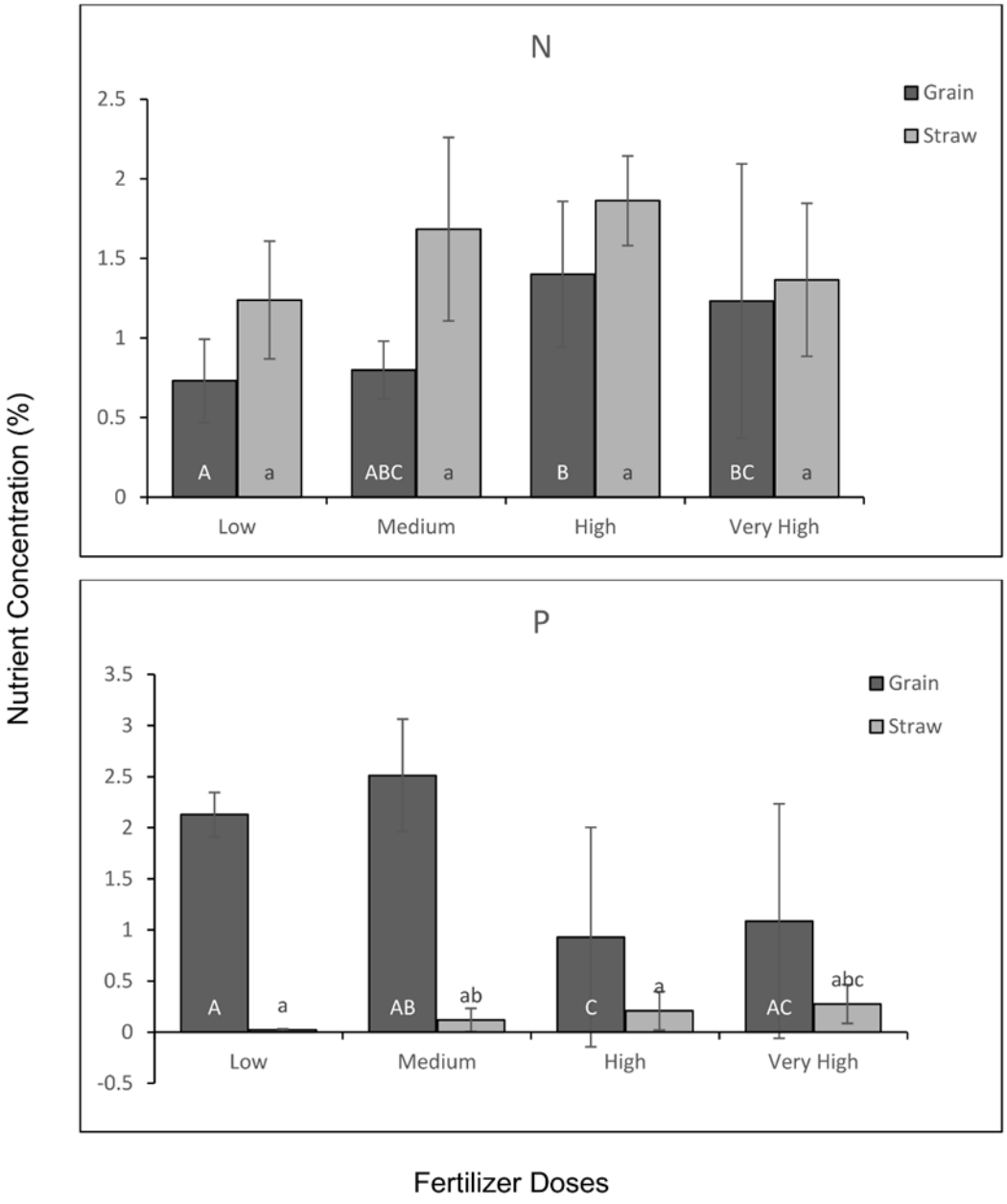

Fig. A1 Contribution of the amount of absorbed by grains and straw of rice crop at maturity as affected by various fertilizer doses for Nitrogen (N) and Phosphorus (P). Data presents means over three locations and three replications at each location. Bar graphs with different letters a–c and A–C denote significant difference ($P \leq 0.05$) among the fertilizer doses. Error bars indicate standard error of the means

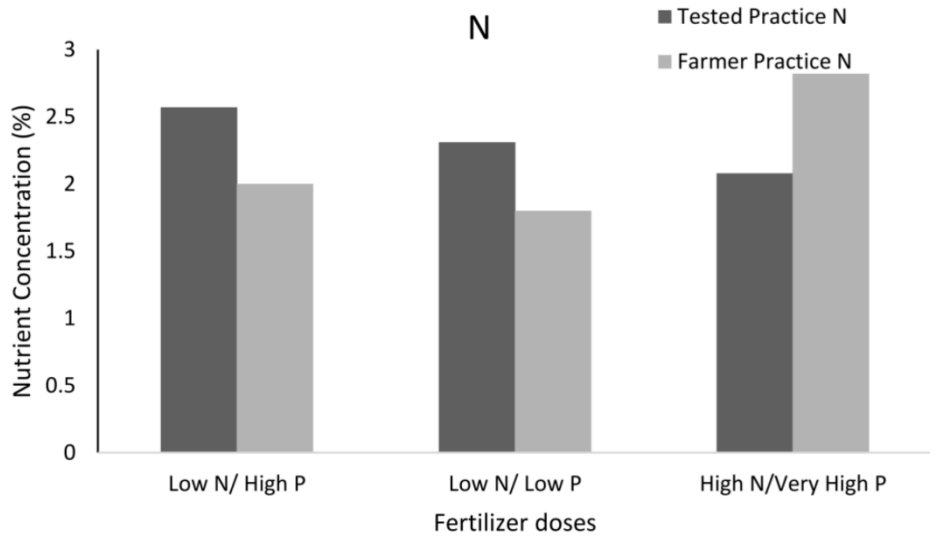

(a)

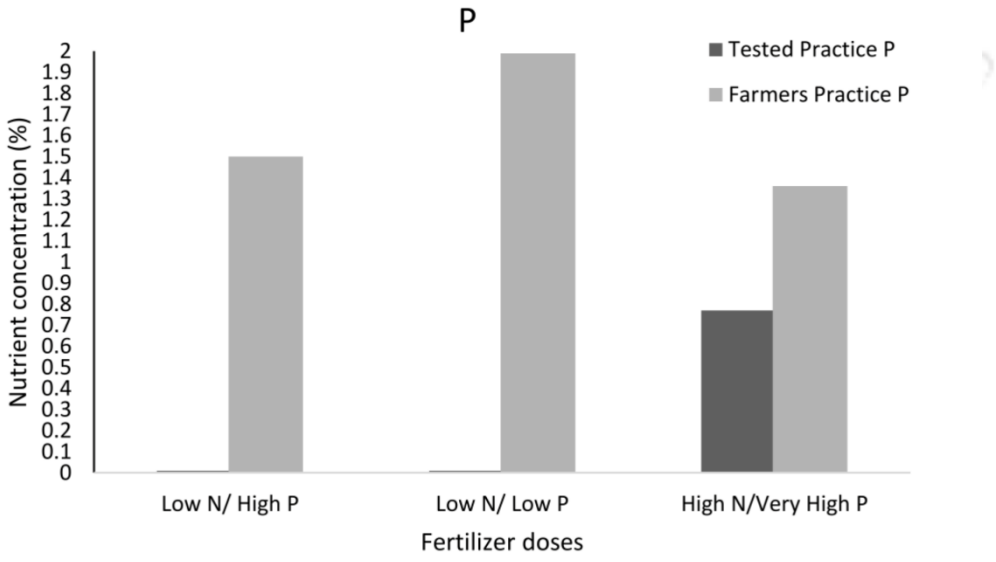

(b)

Fig. A2 Nutrient uptake under Tested practice and Farmer practice for (a) N and (b) P (Source: Ahmed et al., 2014)

Appendix B

Table B1 Monthly crop water requirement of crops (Source: AAU & DOAA, 2021)

Month / **Crops**	**Nov**	**Dec**	**Jan**	**Feb**	**March**	**April**
Summer rice	2000	2000	2000	2000	2000	1000
Lentil	-	250	250	-	-	-
Mustard	-	250	-	-	-	-
Maize	-	700	700	700	-	-
Wheat	600	-	600	-	-	-
Tomato	600	1200	1200	-	-	-
Onion	2400	2400	2400	2400	1200	-
Potato	1200	1200	-	-	-	-

Table B2 Cost of cultivation and revenue generated for various crops (Source: Department of Agriculture and Farmers Welfare; Agricultural marketing board, Farmers Portal)

Operational Cost of cultivation (₹/ha)	**Rice**	**wheat**	**maize**	**lentil**	**Mustard**	**Tomato**	**Onion**	**Potato**
Fertilizer/manure cost	8218.15	5489.06	4853.83	1258.81	2210.41	6179.23	13660.07	9384
Seed cost	2004.99	4086.84	2195.27	3726.25	593.52	10789.69	23128.87	44952.09
pesticides	3102.19	39.81	-	9.80	43.60	1440.12	3162.21	1783.53
Machine labour	9505.37	3441.69	3857.67	3803.55	2164.09	10720.67	9215.15	3437.35
Bullock labour	499.46	2427.33	-	2685.84	6788.68	-	1517.07	6936.03
Miscellaneous	95.91	-	-	-	-	-	25.45	316.44
Interest on working capital	1291.86	926.49	636.59	598.13	418.16	583.06	2939.74	2285.25
Human labour	26647.54	16655.81	13420.44	13152.20	14521.16	8827.51	50617.28	36364.60
Mandi Price (₹/Quintal)	1450	1525	1325	3400	3350	2300	1700	1450

Table B3 Optimal cropping pattern for 70% release for all probabilities

Crop	**Model I**	**Model II**	**Model III**											
			Scenario A				**Scenario B**				**Scenario C**			
			0.1	0.5	0.8	0.9	0.1	0.5	0.8	0.9	0.1	0.5	0.8	0.9
Rice		10150	5541	--	--	--	11082	--	--	--	16623	--	--	--
wheat	415	415	415	--	--	--	415	--	--	--	415	--	--	--
maize	12145	1995	9375	--	--	--	6604	--	--	--	3834	--	--	--
lentil	797	797	797	--	--	--	797	--	--	--	797	--	--	--
Mustard	495	495	495	--	--	--	495	--	--	--	495	--	--	--
Tomato	6927	6927	5541	--	--	--	4156	--	--	--	2771	--	--	--
Onion	86	86	86	--	--	--	86	--	--	--	86	--	--	--
Potato	6840	6840	5455	--	--	--	4070	--	--	--	2684	--	--	--

*-- Denotes insufficient water

Table B4 Optimal cropping pattern for 80% release for all probabilities

Crop	**Model I**	**Model II**	**Model III**											
			Scenario A				**Scenario B**				**Scenario C**			
			0.1	0.5	0.8	0.9	0.1	0.5	0.8	0.9	0.1	0.5	0.8	0.9
Rice		10150	5541	--	--	--	11082	--	--	--	16623	16623	16623	16623
wheat	415	415	415	--	--	--	415	--	--	--	415	--	--	--
maize	12145	1995	9375	--	--	--	6604	--	--	--	3834	--	--	--
lentil	797	797	797	--	--	--	797	--	--	--	797	--	--	--
Mustard	495	495	495	--	--	--	495	--	--	--	495	--	--	--
Tomato	6927	6927	5541	--	--	--	4156	--	--	--	2771	--	--	--
Onion	86	86	86	--	--	--	86	--	--	--	86	--	--	--
Potato	6840	6840	5455	--	--	--	4070	--	--	--	2684	--	--	--

*-- Denotes insufficient water

Table B5 Optimal cropping pattern for 90% release for all probabilities

Crop	Model I				Model II				Model IV								
									ScenarioA				ScenarioB				Scenario C
	0.1	0.5	0.8	0.9	0.1	0.5	0.8	0.9	0.1	0.5	0.8	0.9	0.1	0.5	0.8	0.9	0.1-0.9
Rice					10150				5541	5541	5541	5541	11082	11082	11082	11082	16623
wheat	415	415	415	7419.62	415	--	--	--	415	4818.2	415	415	1813.9	--	--	--	--
maize	12145	12145	12145	5140.38	1995	--	--	--	9375	3291.4	32	32	5205.1	--	--	--	--
lentil	797	797	797	797	797	--	--	--	797	797	797	797	797	--	--	--	--
Mustard	495	495	495	495	495	--	--	--	495	2175.4	495	495	495	--	--	--	--
Tomato	6927	6927	6927	6927	6927	--	--	--	5541	5541	5268.6	4393.7	4156	--	--	--	--
Onion	86	86	86	86	86	--	--	--	86	86	86	86	86	--	--	--	--
Potato	6840	6840	6840	6840	6840	--	--	--	5455	5455	4187.2	3020.7	4070	--	--	--	--

*-- Denotes insufficient water

Table B6 Environmental footprint family results

Crops	MF (kg/calorie *10^{-3})	WF (m^3/calorie*10^{-3})	CF (kg CE/calorie*10^{-3})
Rice	0.008222467	2.58	1.33
wheat	0.007098844	0.30	1.43
maize	0.013593606	1.36	3.64
lentil	0.004117531	0.39	4.38
Mustard	0.009571332	0.11	2.56
Tomato	0.016640043	1.90	3.57
Onion	0.009813411	4.61	2.16
Potato	0.00317505	0.36	0.85

* MF denotes Material Footprint, WF denotes Water Footprint, CF denotes Carbon Footprint

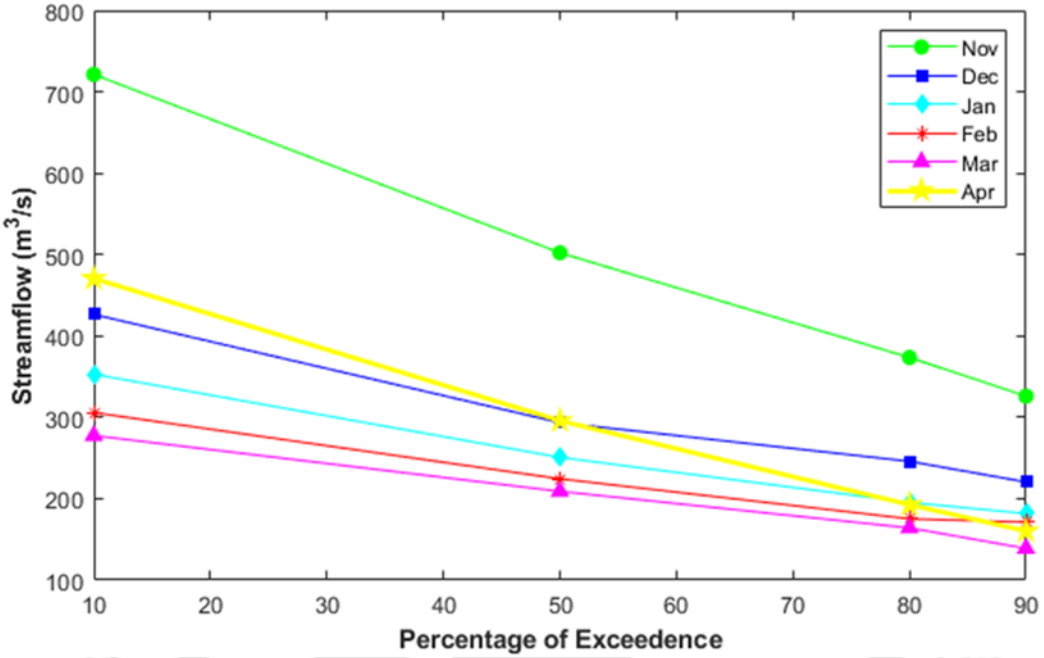

Fig. B1 Available River water upstream of Jamuna river at different risk probabilities

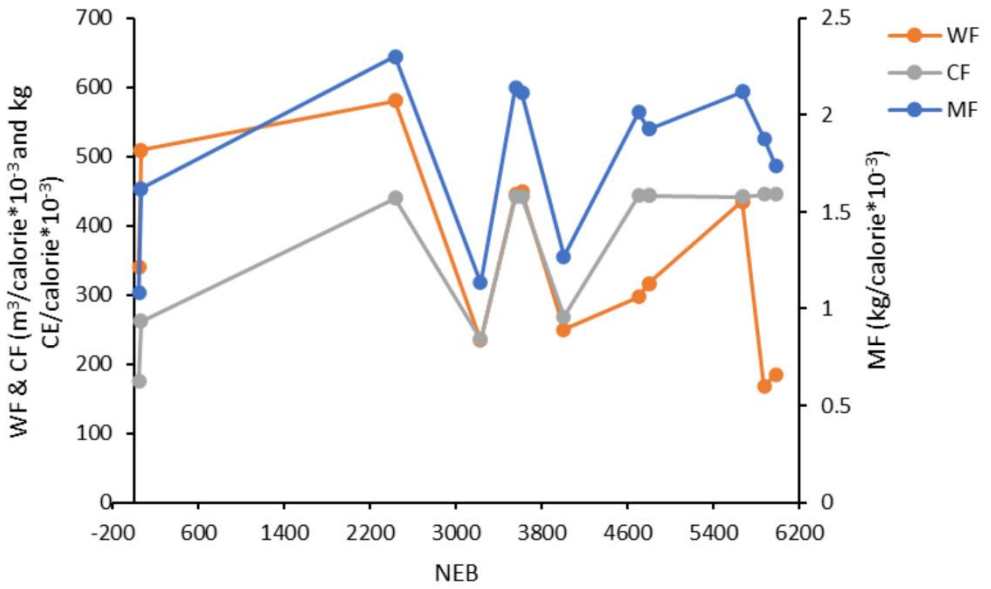

Fig. B2 Impact of water, carbon, and fertilizer availability on NEB.

* NEB means net economic benefit, WF means Water footprint, CF means carbon footprint and MF means Material footprint.

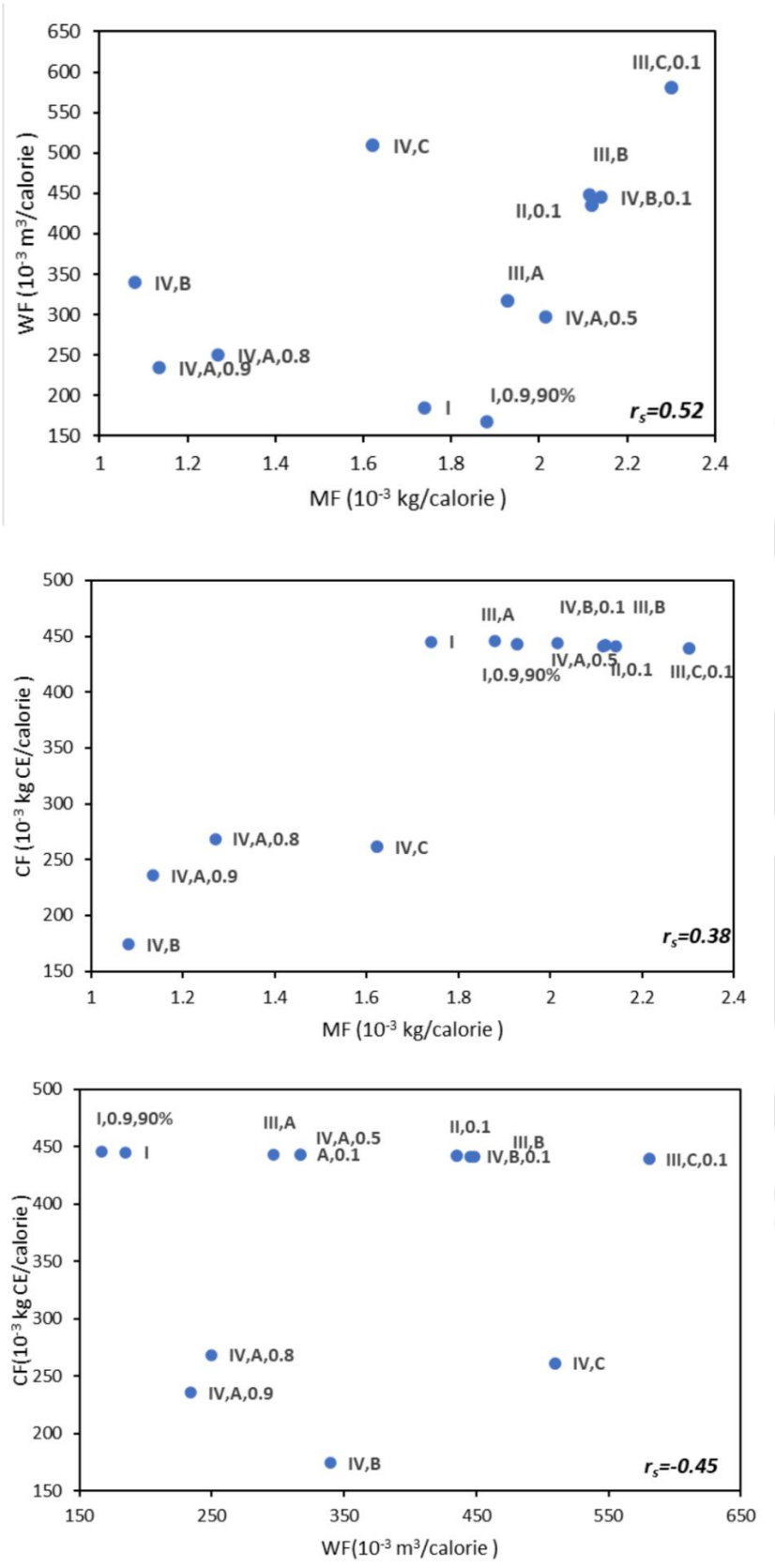

Fig. B3 Pairwise Comparison between environment footprints

Appendix C

Table C1 Performance evaluation of list of predictors selected for MLR bias corrected temperature model

Predictor combination	**R^2**	**Adj R^2**
Tasmax	0.659	0.658
Tasmax+ tas	0.899	0.898
Tasmax +tas+sci	0.899	0.897
Tasmax +tas+sci+rsdcs	0.914	0.912
Tasmax +tas +sci+rsdcs +psl	0.915	0.912
Tasmax +tas +sci+rsdcs +psl +prc	0.927	0.924
Tasmax +tas +sci+rsdcs+psl + prc+hurs	0.928	0.925
Tasmax +tas +sci+rsdcs+psl +prc +hurs+ci	0.931	0.927
Tasmax +tas +sci+rsdcs +psl +prc +hurs+ci +tasmin	0.932	0.927

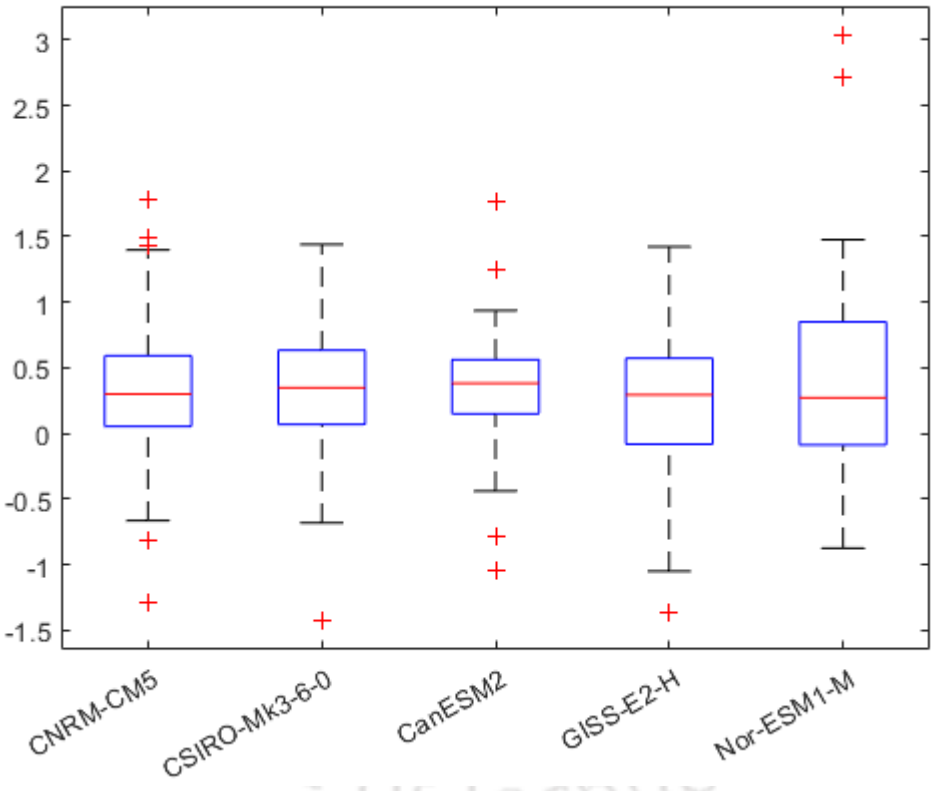

Fig C1 Error values for 5 GCM simulated streamflow values

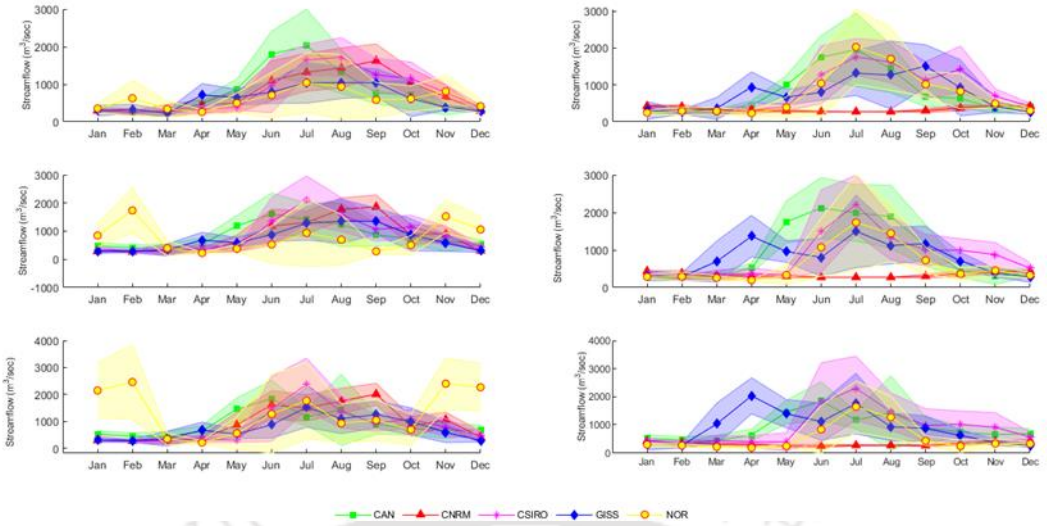

Fig. C2 Simulated monthly streamflow for three time periods 2020s, 2050s and 2080s for GCM climate models for RCP 4.5(leftside) and RCP 8.5(rightside). The area shaded shows the standard deviation for each climate model

Table C2 Coefficient of correlation (corr) and percent bias (pbias) for the runoff quantiles in the calibration and the validation period for the GCMs

Quantile flows	**Calibration**					**Validation**				
	CanESM2	CNRM-CM5	CSIRO-MK3-6-0	GISS-E2-H	NorESM1-M	CanESM2	CNRM-CM5	CSIRO-MK3-6-0	GISS-E2-H	NorESM1-M
Q_{10}corr	0.41	0.51	0	0.72	0.37	0.27	0.17	0.76	0.64	0.64
Q_{10}bias	-3.93	1.62	1.46	-19.25	6.80	46.24	49.57	65.21	53.40	174.94
Q_{95}cor	0.62	0.77	0.63	0.17	0.13	0.08	0.04	0.11	0.53	0.29
Q_{95}bias	3.31	-4.26	6.39	-6.94	3.28	43.55	-10.66	8.17	-15.26	8.18

Appendix D

Fig. D1 Water and soil sample collection

Fig. D2 Rice field of different villages

Fig. D3 Water diverted during monsoon season and excess rain stored in canals

Fig. D4 Fallow lands during rabi season and dry concrete and unlined canals due to no farming activities

References

AAU & DOA (Assam Agricultural University and Department of Agriculture, Assam), 2021. Package of practices for rabi crops of Assam.

Abeysingha N, Islam A, Singh M (2020) Assessment of climate change impact on flow regimes over the Gomti River basin under IPCC AR5 climate change scenarios. Journal of Water and Climate Change 11 (1):303-326

Ahirwar, S., & Shukla, J. (2018). Assessment of groundwater vulnerability in upper Betwa river watershed using GIS based DRASTIC model. Journal of the Geological Society of India, 91(3), 334-340.

Ahmed S, Basumatary A, Das K, Medhi B, Srivastava A (2014) Effect of integrated nutrient management on yield, nutrient uptake and soil fertility in autumn rice on Inceptisol of Assam. Annals of Plant and Soil Research 16 (3):192-197

Ahmed JA, Sarma AK (2007) Artificial neural network model for synthetic streamflow generation. Water resources management 21 (6):1015-1029

Aizen EM, Aizen VB, Melack JM, Nakamura T, Ohta T (2001) Precipitation and atmospheric circulation patterns at mid-latitudes of Asia. International Journal of Climatology: A Journal of the Royal Meteorological Society 21 (5):535-556

Allen RG, Pereira LS, Raes D, Smith M (1998) Crop evapotranspiration-Guidelines for computing crop water requirements-FAO Irrigation and drainage paper 56. Fao, Rome 300 (9):D05109

Anand, V., & Oinam, B. (2019). Future climate change impact on hydrological regime of river basin using SWAT model. Global Journal of Environmental Science and Management, 5(4), 471-484.

Anas M, Liao F, Verma KK, Sarwar MA, Mahmood A, Chen Z-L, Li Q, Zeng X-P, Liu Y, Li Y-R (2020) Fate of nitrogen in agriculture and environment: agronomic, eco-physiological and molecular approaches to improve nitrogen use efficiency. Biological Research 53 (1):1-20

Anderson EP, Jackson S, Tharme RE, Douglas M, Flotemersch JE, Zwarteveen M, Lokgariwar C, Montoya M, Wali A, Tipa GT (2019) Understanding rivers and their social relations: A

critical step to advance environmental water management. Wiley Interdisciplinary Reviews: Water 6 (6):e1381

Arowolo AO, Bhowmik AK, Qi W, Deng X (2017) Comparison of spatial interpolation techniques to generate high-resolution climate surfaces for Nigeria. International Journal of Climatology 37:179-192

Aticho A, Elias E, Diels J (2011) Comparative analysis of soil nutrient balance at farm level: a case study in Jimma Zone, Ethiopia. International Journal of Soil Science 6 (4):259

Aziz O, Hussain S, Rizwan M, Riaz M, Bashir S, Lin L, Mehmood S, Imran M, Yaseen R, Lu G (2018) Increasing water productivity, nitrogen economy, and grain yield of rice by water saving irrigation and fertilizer-N management. Environmental Science and Pollution Research 25 (17):16601-16615

Bandyopadhyay, A., Bhadra, A., Chiphang, N., & Senzeba, K. (2015). Assessment of Snowmelt Runoff in the Eastern Himalayan Region under Climate Change Scenarios. J. Ind. Geophys. Union (July 2015), 19(3), 312-321.

Bassanino M, Sacco D, Zavattaro L, Grignani C (2011) Nutrient balance as a sustainability indicator of different agro-environments in Italy. Ecological Indicators 11 (2):715-723

Basumatary M, Gossaingaon A, Chand P, Bhatinda P (2020) Detection of anomalies and approximate change point in temperature, Assam, India. Transactions 42 (1):129

Batool N, Shah SA, Dar SN, Skinder S (2019) Rainfall variability and dynamics of cropping pattern in Kashmir Himalayas: a case study of climate change and agriculture. SN Applied Sciences 1 (6):1-9

Bayat B, Nasseri M, Delmelle E (2021) Uncertainty-based rainfall network design using a fuzzy spatial interpolation method. Applied Soft Computing 106:107296

Bayazıt M, Oğuz B (1998) Probability and statistics for engineers. Birsen Yayınevi,

Bechmann M (2014) Long-term monitoring of nitrogen in surface and subsurface runoff from small agricultural dominated catchments in Norway. Agriculture, ecosystems & environment 198:13-24

Bennett EM, Carpenter SR, Caraco NF (2001) Human impact on erodable phosphorus and eutrophication: a global perspective: increasing accumulation of phosphorus in soil threatens rivers, lakes, and coastal oceans with eutrophication. BioScience 51 (3):227-234

Berghuijs W, Woods R, Hrachowitz M (2014) A precipitation shift from snow towards rain leads to a decrease in streamflow. Nature climate change 4 (7):583-586

Bijay S, Bronson K (2001) Nitrogen-15 balance and use efficiency as affected by rice residue management in a rice-wheat system in northwest India. Nutrient Cycling in Agroecosystem 59:227-237

Bindraban P, Stoorvogel J, Jansen D, Vlaming J, Groot J (2000) Land quality indicators for sustainable land management: proposed method for yield gap and soil nutrient balance. Agriculture, Ecosystems & Environment 81 (2):103-112

Blaney HF (1952) Determining water requirements in irrigated areas from climatological and irrigation data.

Blumsack SL (1971) On the effects of topography on planetary atmospheric circulation. Journal of Atmospheric Sciences 28 (7):1134-1143

Borah H, Deka S (2020) Morphometric analysis for prioritization of Sub-Watersheds of Jamuna River Watershed, Assam, India using remote sensing and GIS technique. International Journal Control Autom 13 (2):18-26

Borthakur S, Borthakur M, Singh Mk (2016) Food Security Status of Assam: A Districts Level Analysis. Journal of AgriSearch 3 (2):110-114

Brahmanand P, Behera B, Srivastava SK, Singandhupe R, Mishra A (2021) Cultivated land utilization index vis-a-vis cropping intensity for crop diversification and water resource management in Odisha, India. CURRENT SCIENCE 120 (7):1217

Brar BS, Singh K, Dheri GS, Balwinder K (2013) Carbon sequestration and soil carbon pools in a rice–wheat cropping system: Effect of long-term use of inorganic fertilizers and organic manure. Soil and Tillage Research 128:30-36. doi:https://doi.org/10.1016/j.still.2012.10.001

Bray RH, Kurtz LT (1945) Determination of Total, Organic, and Available Forms of Phosphorus in Soils. Soil Science 59:39. doi:10.1097/00010694-194501000-00006

Brookeld VC (1948) An approach towards a rational classification of climate. Geogr Rev 38:5594White

Burchfield EK, de la Poterie AT (2018) Determinants of crop diversification in rice-dominated Sri Lankan agricultural systems. Journal of rural studies 61:206-215

Caldera U, Breyer C (2020) Strengthening the global water supply through a decarbonised global desalination sector and improved irrigation systems. Energy 200:117507

Carmo M, García-Ruiz R, Ferreira MI, Domingos T (2017) The NPK soil nutrient balance of Portuguese cropland in the 1950s: The transition from organic to chemical fertilization. Scientific Reports 7 (1):1-14

Cassman KG, Peng S, Olk D, Ladha J, Reichardt W, Dobermann A, Singh U (1998) Opportunities for increased nitrogen-use efficiency from improved resource management in irrigated rice systems. Field crops research 56 (1-2):7-39

Cesari de Maria S, Bischetti G, Chiaradia E, Facchi A, Miniotti E, Rienzner M, Romani M, Tenni D, Gandolfi C (2017) The role of water management and environmental factors on field irrigation requirements and water productivity of rice. Irrigation science 35:11-26

Chappell NA, Sherlock M, Bidin K, Macdonald R, Najman Y, Davies G (2007) Runoff processes in Southeast Asia: role of soil, regolith, and rock type. Forest environments in the Mekong River basin:3-23

Chawla I, Mujumdar P (2018) Partitioning uncertainty in streamflow projections under nonstationary model conditions. Advances in water resources 112:266-282

Chen X, Wang L, Niu Z, Zhang M, Li J (2020) The effects of projected climate change and extreme climate on maize and rice in the Yangtze River Basin, China. Agricultural and Forest Meteorology 282:107867

Cheng W, Padre AT, Sato C, Shiono H, Hattori S, Kajihara A, Aoyama M, Tawaraya K, Kumagai K (2016) Changes in the soil C and N contents, C decomposition and N mineralization potentials in a rice paddy after long-term application of inorganic fertilizers and organic matter. Soil Science and Plant Nutrition 62 (2):212-219

Cho J-Y, Han K-W, Choi J-K (2000) Balance of nitrogen and phosphorus in a paddy field of central Korea. Soil Science and Plant Nutrition 46 (2):343-354. doi:10.1080/00380768.2000.10408789

Cho J-Y, Han K-W, Choi J-K (2000) Balance of nitrogen and phosphorus in a paddy field of central Korea. Soil Science and Plant Nutrition 46 (2):343-354

Dall'Orsoletta F, Matthews B (2021) Material Footprint and Its Role in Agenda 2030. Decent Work and Economic Growth:683-695

Damseaux, A., Fettweis, X., Lambert, M., & Cornet, Y. (2020). Representation of the rain-shadow effect in Patagonia using an orographic-derived regional climate model. International Journal of Climatology, 40(3), 1769-1783.

Dang MV (2005) Soil–plant nutrient balance of tea crops in the northern mountainous region, Vietnam. Agriculture, ecosystems & environment 105 (1-2):413-418

Dang MV (2005) Soil–plant nutrient balance of tea crops in the northern mountainous region, Vietnam. Agriculture, ecosystems & environment 105 (1-2):413-418

Das PJ (2004) Rainfall regime of northeast India a hydrometeorological study with special emphasis on the Brahmaputra basin.

Das D, Dwivedi B, Datta S, Datta S, Meena M, Agarwal B, Shahi D, Singh M, Chakraborty D, Jaggi S (2019) Potassium supplying capacity of a red soil from eastern India after forty-two years of continuous cropping and fertilization. Geoderma 341:76-92

Das UD, Singh BP, Roy TD (2020) Temporal variation of temperature in Guwahati, Assam: an application of seasonal ARIMA model. J Stat Appl Prob 9 (1):169-180

Dash S, Sharma N, Pattnayak K, Gao X, Shi Y (2012) Temperature and precipitation changes in the north-east India and their future projections. Global and Planetary Change 98:31-44

Datta P, Bose S (2020) Assessing the changes in climate extremes over Karbi Anglong district of Assam, North-East India. Spatial Information Research 28 (5):547-558

Dawson TP, Perryman AH, Osborne TM (2016) Modelling impacts of climate change on global food security. Climatic Change 134 (3):429-440

De Bauw P, Mai TH, Schnepf A, Merckx R, Smolders E, Vanderborght J (2020) A functional–structural model of upland rice root systems reveals the importance of laterals and growing root tips for phosphate uptake from wet and dry soils. Annals of botany 126 (4):789-806

De Jager Ad, Kariuku I, Matiri F, Odendo M, Wanyama J (1998) Monitoring nutrient flows and economic performance in African farming systems (NUTMON): IV. Linking nutrient balances

and economic performance in three districts in Kenya. Agriculture, ecosystems & environment 71 (1-3):81-92

Deka R, Mahanta C, Nath K, Dutta M (2016) Spatio-temporal variability of rainfall regime in the Brahmaputra valley of North East India. Theoretical and applied climatology 124 (3-4):793-806

DES D (2018) Directorate of Economics and Statistics. Department of Agriculture, Cooperation and Farmers welfare, Government of India

Dhamodaran S, Lakshmi M (2021) Comparative analysis of spatial interpolation with climatic changes using inverse distance method. Journal of Ambient Intelligence and Humanized Computing 12:6725-6734

Dolan F, Lamontagne J, Link R, Hejazi M, Reed P, Edmonds J (2021) Evaluating the economic impact of water scarcity in a changing world. Nature communications 12 (1):1915

Döll P, Schmied HM (2012) How is the impact of climate change on river flow regimes related to the impact on mean annual runoff? A global-scale analysis. Environmental Research Letters 7 (1):014037

Dong NM, Brandt KK, Sørensen J, Hung NN, Hach CV, Tan PS, Dalsgaard T (2012) Effects of alternating wetting and drying versus continuous flooding on fertilizer nitrogen fate in rice fields in the Mekong Delta, Vietnam. Soil Biology and Biochemistry 47:166-174. doi:https://doi.org/10.1016/j.soilbio.2011.12.028

Doorenbos J (1975) Guidelines for predicting crop water requirements. Food and Agriculture organization Rome, Irrig Drainage paper 24

Dutta P, Hinge G, Marak JDK, Sarma AK (2021) Future climate and its impact on streamflow: a case study of the Brahmaputra river basin. Modeling Earth Systems and Environment 7 (4):2475-2490

Ekhtiari N, Agarwal A, Marwan N, Donner RV (2019) Disentangling the multi-scale effects of sea-surface temperatures on global precipitation: A coupled networks approach. Chaos: An Interdisciplinary Journal of Nonlinear Science 29 (6):063116

Enriquez Y, Yadav S, Evangelista GK, Villanueva D, Burac MA, Pede V (2021) Disentangling challenges to scaling alternate wetting and drying technology for rice cultivation: Distilling

lessons from 20 years of experience in the Philippines. Frontiers in Sustainable Food Systems 5:675818

Evenson RE, Gollin D (2003) Assessing the impact of the Green Revolution, 1960 to 2000. science 300 (5620):758-762

FAO (2003) Assessment of nutrient balance. In: Natural Resources Management and Environment Department.

FAO (2020) The State of Food and Agriculture 2020. Overcoming Water Challenges in Agriculture. FAO Rome, Italy,

FAO, S. (2016). FAOSTAT database. Food and Agriculture Organization of the United Nations. In.

Feng L, Bouman BAM, Tuong TP, Cabangon RJ, Li Y, Lu G, Feng Y (2007) Exploring options to grow rice using less water in northern China using a modelling approach: I. Field experiments and model evaluation. Agricultural Water Management 88 (1):1-13. doi:https://doi.org/10.1016/j.agwat.2006.10.006

Galán-Martín Á, Pozo C, Guillén-Gosálbez G, Vallejo AA, Esteller LJ (2015) Multi-stage linear programming model for optimizing cropping plan decisions under the new Common Agricultural Policy. Land use policy 48:515-524

Galelli S, Castelletti A (2013) Tree-based iterative input variable selection for hydrological modeling. Water Resources Research 49 (7):4295-4310

Galloway JN, Townsend AR, Erisman JW, Bekunda M, Cai Z, Freney JR, Martinelli LA, Seitzinger SP, Sutton MA (2008) Transformation of the nitrogen cycle: recent trends, questions, and potential solutions. Science 320 (5878):889-892

Gaur S, Bandyopadhyay A, Singh R (2021) Modelling potential impact of climate change and uncertainty on streamflow projections: a case study. Journal of Water and Climate Change 12 (2):384-400

Geisseler D, Linquist BA, Lazicki PA (2017) Effect of fertilization on soil microorganisms in paddy rice systems–A meta-analysis. Soil Biology and Biochemistry 115:452-460

Giller KE, Delaune T, Silva JV, van Wijk M, Hammond J, Descheemaeker K, van de Ven G, Schut AG, Taulya G, Chikowo R (2021) Small farms and development in sub-Saharan Africa: Farming for food, for income or for lack of better options? Food Security 13 (6):1431-1454

Goyal MK, Sarma AK (2017) Analysis of the change in temperature trends in Subansiri River basin for RCP scenarios using CMIP5 datasets. Theoretical and Applied Climatology 129 (3):1175-1187

Gul F, Ahmed I, Ashfaq M, Jan D, Fahad S, Li X, Wang D, Fahad M, Fayyaz M, Shah SA (2020) Use of crop growth model to simulate the impact of climate change on yield of various wheat cultivars under different agro-environmental conditions in Khyber Pakhtunkhwa, Pakistan. Arabian Journal of Geosciences 13:1-14

Gulati A, Wardhan H, Sharma P (2022) Tomato, Onion and Potato (TOP) value chains. Agricultural value chains in India:33

Gumma MK, Thenkabail PS, Teluguntla P, Rao MN, Mohammed IA, Whitbread AM (2016) Mapping rice-fallow cropland areas for short-season grain legumes intensification in South Asia using MODIS 250 m time-series data. International Journal of Digital Earth 9 (10):981-1003

Gupta PK (2004) Soil, Plant, Water and Fertilizer Analysis Agrobios, India

Gupta S, Goyal MK, Sarma AK (2021) Assessment of Hydroclimatological Changes in Eastern Himalayan River Catchment of Northeast India. Journal of Hydrologic Engineering 26 (10):05021027

Gutser, R., Ebertseder, T., Weber, A., Schraml, M., Schmidhalter, U. 2005. Short-term and residual availability of nitrogen after long-term application of organic fertilizers on arable land. J. of Plant Nut. and Soil Sci. 168, 439-446.

Hao L, Su X, Singh VP (2018) Cropping pattern optimization considering uncertainty of water availability and water saving potential. International Journal of Agricultural and Biological Engineering 11 (1):178-186

Harikishan G, Padmakumari B, Maheskumar R, Pandithurai G, Min Q (2016) Aerosol indirect effects from ground-based retrievals over the rain-shadow region in Indian subcontinent. Journal of Geophysical Research: Atmospheres 121 (5):2369-2382

Harmsen K (2000b) A modified Mitscherlich equation for rainfed crop production in semi-arid areas: 1. Theory. NJAS: Wageningen Journal of Life Sciences 48 (3):237-250

Harrell JB (2014) An evaluation of soil sampling methods in support of precision agriculture in northeastern North Carolina. University of Southern California,

Hassan M, Hassan I (2020) Improving ANN-based streamflow estimation models for the Upper Indus Basin using satellite-derived snow cover area. Acta Geophysica 68 (6):1791-1801

Hawkins E, Sutton R (2011) The potential to narrow uncertainty in projections of regional precipitation change. Climate dynamics 37:407-418

Hedley M, Kirk G, Santos M (1994) Phosphorus efficiency and the forms of soil phosphorus utilized by upland rice cultivars. Plant and Soil 158 (1):53-62

Hillier J, Hawes C, Squire G, Hilton A, Wale S, Smith P (2009) The carbon footprints of food crop production. International Journal of Agricultural Sustainability 7 (2):107-118

Hoekstra AY, Chapagain AK, Aldaya MM, Mekonnen MM (2011) The water footprint assessment manual: Setting the global standard. Routledge

IPCC (2014) Climate change 2014: synthesis report. Contribution of Working Groups I, II and III to the fifth assessment report of the Intergovernmental Panel on Climate Change. Ipcc

Jabloun Md, Sahli A (2008) Evaluation of FAO-56 methodology for estimating reference evapotranspiration using limited climatic data: Application to Tunisia. Agricultural water management 95 (6):707-715

Jägermeyr J, Pastor A, Biemans H, Gerten D (2017) Reconciling irrigated food production with environmental flows for Sustainable Development Goals implementation. Nature communications 8 (1):1-9

Jain S, Kumar V, Saharia M (2013) Analysis of rainfall and temperature trends in northeast India. International Journal of Climatology 33 (4):968-978

JCADD (1961) Project Report.

Jensen ME, Haise HR (1963) Estimating evapotranspiration from solar radiation. Journal of the Irrigation and Drainage Division 89 (4):15-41

Jimeno-Sáez P, Senent-Aparicio J, Pérez-Sánchez J, Pulido-Velazquez D (2018) A comparison of SWAT and ANN models for daily runoff simulation in different climatic zones of peninsular Spain. Water 10 (2):192

Jayas DS (2012) Storing grains for food security and sustainability. Agricultural Research 1:21-24

Kaini S, Nepal S, Pradhananga S, Gardner T, Sharma AK (2020) Impacts of climate change on the flow of the transboundary Koshi River, with implications for local irrigation. International Journal of Water Resources Development:1-26

Kandegama WWW, Rathnayake RMPJ, Baig MB, Behnassi M (2022) Impacts of Climate Change on Horticultural Crop Production in Sri Lanka and the Potential of Climate-Smart Agriculture in Enhancing Food Security and Resilience. In: Food Security and Climate-Smart Food Systems: Building Resilience for the Global South. Springer, pp 67-97

Karimi T, Stöckle CO, Higgins SS, Nelson RL (2021) Impact of climate change on greenhouse gas emissions and water balance in a dryland-cropping region with variable precipitation. Journal of Environmental Management 287:112301

Kavzoglu T, Mather P (2002) The role of feature selection in artificial neural network applications. International Journal of Remote Sensing 23 (15):2919-2937

Kim Y, Ohn I, Lee J-K, Kim Y-O (2019) Generalizing uncertainty decomposition theory in climate change impact assessments. Journal of Hydrology X 3:100024

Kisi O, Mirboluki A, Naganna SR, Malik A, Kuriqi A, Mehraein M (2022) Comparative evaluation of deep learning and machine learning in modelling pan evaporation using limited inputs. Hydrological Sciences Journal.

Kothawale D, Kumar KK, Srinivasan G (2012) Spatial asymmetry of temperature trends over India and possible role of aerosols. Theoretical and applied climatology 110 (1):263-280

Kothawale D, Munot A, Kumar KK (2010) Surface air temperature variability over India during 1901–2007, and its association with ENSO. Climate Research 42 (2):89-104

Kotu BH, Abass AB, Hoeschle-Zeledon I, Mbwambo H, Bekunda M (2019) Exploring the profitability of improved storage technologies and their potential impacts on food security and income of smallholder farm households in Tanzania. Journal of Stored Products Research 82:98-109

Kumar V, Singh HR, Srivastava V, Sharma R, Pant N, Tomar P (2018) Nitrogen release pattern of different organic sources under varying levels of NPK fertilizers and their effect on yield and nutrient uptake in hybrid rice-wheat cropping system. Journal of Pharmacognosy and Phytochemistry:618-623

Kumari M, Singh O, Meena DC (2017) Optimising Cropping Pattern in Eastern Uttar Pradesh Using Sen's Multi Objective Programming Approach §. Agricultural Economics Research Review 30 (2):285-291

Ladha J, Tirol-Padre A, Reddy C, Cassman K, Verma S, Powlson D, Van Kessel C, Richter DdB, Chakraborty D, Pathak H (2016) Global nitrogen budgets in cereals: A 50-year assessment for maize, rice and wheat production systems. Scientific reports 6 (1):1-9

Leander R, Buishand TA (2007) Resampling of regional climate model output for the simulation of extreme river flows. Journal of hydrology 332 (3-4):487-496

Lee JK, Kim YO, Kim Y (2017) A new uncertainty analysis in the climate change impact assessment. International journal of climatology 37 (10):3837-3846

Lehner F, Deser C, Maher N, Marotzke J, Fischer EM, Brunner L, Knutti R, Hawkins E (2020) Partitioning climate projection uncertainty with multiple large ensembles and CMIP5/6. Earth System Dynamics 11 (2):491-508

Levy H, Horowitz LW, Schwarzkopf MD, Ming Y, Golaz JC, Naik V, Ramaswamy V (2013) The roles of aerosol direct and indirect effects in past and future climate change. Journal of Geophysical Research: Atmospheres 118 (10):4521-4532

Li C, Kandel M, Anghileri D, Oloo F, Kambombe O, Chibarabada TP, Ngongondo C, Sheffield J, Dash J (2021a) Recent changes in cropland area and productivity indicate unsustainable cropland expansion in Malawi. Environmental Research Letters 16 (8):084052

Li H-C, Hsiao Y-H, Chang C-W, Chen Y-M, Lin L-Y (2021) Agriculture Adaptation Options for Flood Impacts under Climate Change—A Simulation Analysis in the Dajia River Basin. Sustainability 13 (13):7311

Li M, Fu Q, Singh VP, Liu D, Li T, Zhou Y (2020) Managing agricultural water and land resources with tradeoff between economic, environmental, and social considerations: A multi-objective non-linear optimization model under uncertainty. Agricultural systems 178:102685

Li Y, Liu J, Huang G (2014) A hybrid fuzzy-stochastic programming method for water trading within an agricultural system. Agricultural Systems 123:71-83

Li Z, Fang G, Chen Y, Duan W, Mukanov Y (2020) Agricultural water demands in Central Asia under 1.5° C and 2.0° C global warming. Agricultural Water Management 231:106020

Liu X, Xu Y, Sun S, Zhao X, Wu P, Wang Y (2022) What is the potential to improve food security by restructuring crops in Northwest China? Journal of Cleaner Production 378:134620

Liu J, Yuan X, Zeng J, Jiao Y, Li Y, Zhong L, Yao L (2022) Ensemble streamflow forecasting over a cascade reservoir catchment with integrated hydrometeorological modeling and machine learning. Hydrology and Earth System Sciences 26 (2):265-278

Liu T, Chen Y, Li B, Hu Y, Qiu H, Liang Z (2019) Long-term streamflow forecasting for the Cascade Reservoir System of Han River using SWAT with CFS output. Hydrology Research 50 (2):655-671

Liu X, Xu C, Zhong X, Li Y, Yuan X, Cao J (2017) Comparison of 16 models for reference crop evapotranspiration against weighing lysimeter measurement. Agricultural water management 184:145-155

Liu XJ, Wang JC, Lu SH, Zhang F, Zeng X, Ai Y, Peng S, Christie P (2003) Effects of non-flooded mulching cultivation on crop yield, nutrient uptake and nutrient balance in rice–wheat cropping systems. Field Crops Research 83 (3):297-311

Lotfirad, M., Adib, A., Salehpoor, J., Ashrafzadeh, A., & Kisi, O. (2021). Simulation of the impact of climate change on runoff and drought in an arid and semiarid basin (the Hablehroud, Iran). Applied Water Science, 11(10), 1-24.

Ma H, Mao P, Imran S, Raza T, Gao R, Lin Y (2021) Rice Planting Increases Biological Nitrogen Fixation in Acidic Soil and the Influence of Light and Flood Layer Thickness. Journal of Soil Science and Plant Nutrition 21 (1):341-348

Maharjan, M., Aryal, A., Talchabhadel, R., & Thapa, B. R. (2021). Impact of Climate Change on the Streamflow Modulated by Changes in Precipitation and Temperature in the North Latitude Watershed of Nepal. Hydrology, 8(3), 117.

Meng J, Yao Q, Yu Z (2014) Particulate phosphorus speciation and phosphate adsorption characteristics associated with sediment grain size. Ecological engineering 70:140-145

Meshram SG, Meshram C, Santos CAG, Benzougagh B, Khedher KM (2021) Streamflow prediction based on artificial intelligence techniques. Iranian Journal of Science and Technology, Transactions of Civil Engineering:1-11

Minhas P, Yadav R (2015) Long-term impact of wastewater irrigation and nutrient rates II. Nutrient balance, nitrate leaching and soil properties under peri-urban cropping systems. Agricultural Water Management 156:110-117

Mishra J, Aayog N (2019) Revitalising Rainfed Agriculture in India. Challenges and Opportunities in Rainfed Agriculture under Changing Climate Scenario:30

Mo X-G, Hu S, Lin Z-H, Liu S-X, Xia J (2017) Impacts of climate change on agricultural water resources and adaptation on the North China Plain. Advances in Climate Change Research 8 (2):93-98

Mo X-G, Hu S, Lin Z-H, Liu S-X, Xia J (2017) Impacts of climate change on agricultural water resources and adaptation on the North China Plain. Advances in Climate Change Research 8 (2):93-98

Moriasi DN, Arnold JG, Van Liew MW, Bingner RL, Harmel RD, Veith TL (2007) Model evaluation guidelines for systematic quantification of accuracy in watershed simulations. Transactions of the ASABE 50 (3):885-900

Moss RH, Babiker M, Brinkman S, Calvo E, Carter T, Edmonds JA, Elgizouli I, Emori S, Lin E, Hibbard K (2008) Towards new scenarios for analysis of emissions, climate change, impacts, and response strategies.

Motavalli P, Miles R (2002) Soil phosphorus fractions after 111 years of animal manure and fertilizer applications. Biology and fertility of soils 36 (1):35-42

Moya P, Hong L, Dawe D, Chongde C (2004) The impact of on-farm water saving irrigation techniques on rice productivity and profitability in Zhanghe Irrigation System, Hubei, China. Paddy and Water Environment 2:207-215

Mudbhatkal, A., Raikar, R., Venkatesh, B., & Mahesha, A. (2017). Impacts of climate change on varied river-flow regimes of southern India. Journal of Hydrologic Engineering, 22(9), 05017017.

Myhre, G., Samset, B. H., Hodnebrog, Ø., Andrews, T., Boucher, O., Faluvegi, G., . . . Kharin, V. (2018). Sensible heat has significantly affected the global hydrological cycle over the historical period. Nature Communications, 9(1), 1-9.

Nayak AK, Shahid M, Nayak AD, Dhal B, Moharana KC, Mondal B, Tripathi R, Mohapatra SD, Bhattacharyya P, Jambhulkar NN (2019) Assessment of ecosystem services of rice farms in eastern India. Ecological Processes 8 (1):1-16

Negewo TF, Sarma AK (2021) Estimation of water yield under baseline and future climate change scenarios in Genale watershed, Genale Dawa River basin, Ethiopia, using SWAT model. Journal of Hydrologic Engineering 26 (3):05020051

Nikolaou G, Neocleous D, Christou A, Kitta E, Katsoulas N (2020) Implementing sustainable irrigation in water-scarce regions under the impact of climate change. Agronomy 10 (8):1120

Nishiyama S, Okazaki M, Baba M, Quevedo MA (2016) Quantification of Cs, K, and Rb in rice (Oryza sativa) cultivated under paddy and upland conditions. Microchemical Journal 127:22-29

Nourani V, Elkiran G, Abdullahi J (2019) Multi-station artificial intelligence based ensemble modeling of reference evapotranspiration using pan evaporation measurements. Journal of Hydrology 577:123958

Nouri M, Homaee M, Bannayan M (2017) Quantitative trend, sensitivity and contribution analyses of reference evapotranspiration in some arid environments under climate change. Water Resources Management 31 (7):2207-2224

Ongley, E. (1996). Sediment measurements. Water Quality Monitoring - A Practical Guide to the Design and Implementation of Freshwater Quality Studies and Monitoring Programmes.

Oryani B, Koo Y, Rezania S, Shafiee A (2021) Investigating the asymmetric impact of energy consumption on reshaping future energy policy and economic growth in Iran using extended Cobb-Douglas production function. Energy 216:119187

Oue H, Laban S (2020) Water use of rice and mung bean cultivations in a downstream area of an irrigation system in South Sulawesi in the 2nd dry season. Paddy and Water Environment 18 (1):87-98

Ouma G, Jeruto P (2010) Sustainable horticultural crop production through intercropping: The case of fruits and vegetable crops: A review. Agriculture and Biology Journal of North America 1 (5):1098-1105

Pan G, Li L, Wu L, Zhang X (2004) Storage and sequestration potential of topsoil organic carbon in China's paddy soils. Global Change Biology 10 (1):79-92

Pandey D, Agrawal M (2014) Carbon footprint estimation in the agriculture sector. In: Assessment of Carbon Footprint in Different Industrial Sectors, Volume 1. Springer, pp 25-47

Pandey PK, Dabral PP, Pandey V (2016) Evaluation of reference evapotranspiration methods for the northeastern region of India. International Soil and Water Conservation Research 4 (1):52-63

Parisouj, P., Mohebzadeh, H., & Lee, T. (2020). Employing machine learning algorithms for streamflow prediction: a case study of four river basins with different climatic zones in the United States. Water resources management, 34(13), 4113-4131.

Parthasarathi T, Vanitha K, Lakshamanakumar P, Kalaiyarasi D (2012) Aerobic rice-mitigating water stress for the future climate change. International Journal of Agronomy Plant Production 3 (7):241-254

Patil M, Lal D, Karwariya S, Bhattacharya RK, Behera NR (2018) Comparative study of different GCM models for stream flow prediction. Current Journal of Applied Science and Technology 26 (5):1-12

Patra A, Sharma V, Purakayastha T, Barman M, Kumar S, Chakraborty D, Chobhe KA, Nath D (2018) Long-term effect of integrated nutrient management on yield and nutrients uptake by rice (Oryza sativa) in acid soil. Indian Journal of Agricultural Sciences 88 (4):579-583

Pellicciotti F, Buergi C, Immerzeel WW, Konz M, Shrestha AB (2012) Challenges and uncertainties in hydrological modeling of remote Hindu Kush–Karakoram–Himalayan (HKH) basins: suggestions for calibration strategies. Mountain Research and

Phong L, Stoorvogel J, Van Mensvoort M, Udo H (2011) Modeling the soil nutrient balance of integrated agriculture-aquaculture systems in the Mekong Delta, Vietnam. Nutrient Cycling in Agroecosystems 90:33-49

Prasad, B., Chakravorty, S., 2015. Effects of climate change on vegetable cultivation-a review. Nature Environ. and Pollut. Technol. 14, 923.

Priestley CHB, Taylor RJ (1972) On the assessment of surface heat flux and evaporation using large-scale parameters. Monthly weather review 100 (2):81-92

Prodhan, A., Islam, M., Islam, M., Haque, M., Islam, M., 2018. Effect of soil and environment on winter vegetables production. MOJ Food Process. and Technol. 6, 384-389.

Qaswar M, Jing H, Ahmed W, Dongchu L, Shujun L, Lu Z, Cai A, Lisheng L, Yongmei X, Jusheng G (2020) Yield sustainability, soil organic carbon sequestration and nutrients balance under long-term combined application of manure and inorganic fertilizers in acidic paddy soil. Soil and Tillage Research 198:104569

Rahman MM, Hagare D, Maheshwari B (2016) Use of recycled water for irrigation of open spaces: benefits and risks. In: Balanced urban development: options and strategies for liveable cities. Springer, Cham, pp 261-288

Raneesh K, Thampi S (2013) Bias correction for RCM predictions of precipitation and temperature in the Chaliyar River Basin. J Climatol Weather Forecasting 1 (2)

Rao D, Gill H (2000) Residual effects of Sesbania sesban forestry on yield and nitrogen uptake by rice and wheat in a reclaimed alkali soil in Haryana. Long term soil fertility experiments in rice-wheat cropping systems Paper series 6:139-148

Ren C, Li Z, Zhang H (2019) Integrated multi-objective stochastic fuzzy programming and AHP method for agricultural water and land optimization allocation under multiple uncertainties. Journal of cleaner production 210:12-24

Robertson D, Pokhrel P, Wang Q (2013) Improving statistical forecasts of seasonal streamflows using hydrological model output. Hydrology and Earth System Sciences 17 (2):579-593

Saenchai C, Lordkaew S, Rouached H, Rerkasem B (2016) Distribution of iron and zinc in plant and grain of different rice genotypes grown under aerobic and wetland conditions. Journal of Cereal Science 71:108-115

Saha P, Ishaque M, Saleque M, Miah M, Panaullah G, Bhuiyan N (2007) Long-term integrated nutrient management for rice-based cropping pattern: effect on growth, yield, nutrient uptake, nutrient balance sheet, and soil fertility. Communications in Soil Science and Plant Analysis 38 (5-6):579-610

Saharia AM, Sarma AK (2018) Future climate change impact evaluation on hydrologic processes in the Bharalu and Basistha basins using SWAT model. Natural Hazards 92 (3):1463-1488

Saiz E, Sgouridis F, Drijfhout FP, Peichl M, Nilsson MB, Ullah S (2021) Chronic atmospheric reactive nitrogen deposition suppresses biological nitrogen fixation in peatlands. Environmental Science & Technology 55 (2):1310-1318

Sakin E (2012) Relationships between of carbon, nitrogen stocks and texture of the harran plain soils in southeastern Turkey. Bulgarian Journal of Agricultural Science 18 (4):626-634

Sanjay J, Revadekar JV, Ramarao MVS, Borgaonkar H, Sengupta S, Kothawale DR, Patel J, Mahesh R, Ingle S, AchutaRao K, Srivastava AK, Ratnam JV (2020) Temperature Changes in India. In: Krishnan R, Sanjay J, Gnanaseelan C, Mujumdar M, Kulkarni A, Chakraborty S (eds) Assessment of Climate Change over the Indian Region: A Report of the Ministry of Earth Sciences (MoES), Government of India. Springer Singapore, Singapore, pp 21-45. doi:10.1007/978-981-15-4327-2_2

Sarkar, A. (2015). Impact of climate change on the runoff regime of an Eastern Himalayan river basin. Global NEST Journal, 17(2), 323-333.

Sarker A, Swain N, Nath R, Darai R, Ali MO (2021) Sustainable intensification and diversification of cropping and food systems through lentil and grass peas in South Asia. In: Scaling-up Solutions for Farmers. Springer, pp 265-277

Seitzinger S, Mayorga E, Bouwman A, Kroeze C, Beusen A, Billen G, Van Drecht G, Dumont E, Fekete B, Garnier J (2010) Global river nutrient export: A scenario analysis of past and future trends. Global Biogeochemical Cycles 24 (4)

Sethi R, Mandal K, Behera A, Sarangi A, Aggarwal R, Ambast S (2019) Rainfall probability analysis for conservation of water resources for sustainable irrigation planning. Environment Conservation Journal 20 (1&2):87-99

Sofoulaki E, Tzanakakis V, Giannopoulos G, Kapellakis I, Kabourakis E, Chatzistathis T, Monokrousos N (2023) Different Contribution of Olive Groves and Citrus Orchards to Soil Organic Carbon Sequestration: A Field Study in Four Sites in Crete, Greece. Sustainability 2023, 15, 1477

Sah D, Devakumar A (2018) The carbon footprint of agricultural crop cultivation in India. Carbon Management 9 (3):213-225

Shah S, Mishra V Climate change impacts on streamflow in India. In: Climate Change and Water Resources in India, Edition: 24th Conference of the Parties (COP24) to the United Nations Framework Convention on Climate Change (UNFCCC), 2018. pp 39-52

Sharma K (2011) Rain-fed agriculture could meet the challenges of food security in India. Curr Sci 100 (11):1615-1616

Sharma N, Zakaullah M, Tiwari H, Kumar D (2015) Runoff and sediment yield modeling using ANN and support vector machines: a case study from Nepal watershed. Modeling Earth Systems and Environment 1:1-8

Shrestha AB, Agrawal NK, Alfthan B, Bajracharya SR, Maréchal J, Oort Bv (2015) The Himalayan Climate and Water Atlas: impact of climate change on water resources in five of Asia's major river basins. The Himalayan Climate and Water Atlas: impact of climate change on water resources in five of Asia's major river basins

Singh LK, Jha MK, Chowdary V (2021) Evaluation of water demand and supply under varying meteorological conditions in Eastern India and mitigation strategies for sustainable agricultural production. Environment, Development and Sustainability 23 (2):1264-1291

Singh LK, Sannigrahi S, Bhupenchandra I, Das A, Ghosh S, Dutta S, Swain R, Jha RK, Lal M (2021) Assessment of Agricultural Relevance on Groundwater Indicator in a Command Area of Eastern India. Journal of the Indian Society of Remote Sensing 49 (12):3043-3057

Singh M, Saini RK, Singh S, Sharma SP (2019) Potential of integrating biochar and deficit irrigation strategies for sustaining vegetable production in water-limited regions: A review. HortScience 54 (11):1872-1878

Singh V, Sharma N, Ojha CSP (2004) The Brahmaputra basin water resources, vol 47. Springer Science & Business Media

Sivanappan R (1994) Prospects of micro-irrigation in India. Irrigation and drainage systems 8 (1):49-58

Smith CJ, Chalk PM (2018) The residual value of fertiliser N in crop sequences: An appraisal of 60 years of research using 15N tracer. Field Crops Research 217:66-74

Smith DM, Scaife AA, Eade R, Athanasiadis P, Bellucci A, Bethke I, Bilbao R, Borchert L, Caron L-P, Counillon F (2020) North Atlantic climate far more predictable than models imply. Nature 583 (7818):796-800

Soraisam B, Karumuri A, Pai D (2018) Uncertainties in observations and climate projections for the North East India. Global and Planetary Change 160:96-108

Su X, Li J, Singh VP (2014) Optimal allocation of agricultural water resources based on virtual water subdivision in Shiyang River Basin. Water resources management 28:2243-2257

Sulaiman A, Candradijaya A, Syakir M (2019) Technological advancement and the economic benefit of Indonesian rain-fed farming development. Advances in Agriculture 2019

Sultana SN, mani Hazarika U, Misra UK (2017) Improvement of water use efficiency and remote sensing applications for surface soil moisture monitoring. ADBU Journal of Engineering Technology 6 (2)

Sun Y, Huang S, Yu X, Zhang W (2015) Differences in fertilization impacts on organic carbon content and stability in a paddy and an upland soil in subtropical China. Plant and soil 397 (1-2):189-200

Suwal N, Huang X, Kuriqi A, Chen Y, Pandey KP, Bhattarai KP (2020) Optimisation of cascade reservoir operation considering environmental flows for different environmental management classes. Renewable Energy 158:453-464

Syers J, Johnston A, Curtin D (2008) Efficiency of soil and fertilizer phosphorus use. FAO Fertilizer and plant nutrition bulletin 18 (108)

Talukdar N, Bhattacharyya D, Hazarika S (2004) Soils and agriculture. In: The Brahmaputra Basin Water Resources. Springer, pp 35-71

Tan X, Shao D, Liu H, Yang F, Xiao C, Yang H (2013) Effects of alternate wetting and drying irrigation on percolation and nitrogen leaching in paddy fields. Paddy and Water Environment 11:381-395

Tan X, Shao D, Liu H, Yang F, Xiao C, Yang H (2013) Effects of alternate wetting and drying irrigation on percolation and nitrogen leaching in paddy fields. Paddy and Water Environment 11:381-395

Tang S, Cheng W, Hu R, Guigue J, Hattori S, Tawaraya K, Tokida T, Fukuoka M, Yoshimoto M, Sakai H (2021a) Five-year soil warming changes soil C and N dynamics in a single rice paddy field in Japan. Science of The Total Environment 756:143845

Tanguilig V, Yambao E, O'toole J, De Datta S (1987) Water stress effects on leaf elongation, leaf water potential, transpiration, and nutrient uptake of rice, maize, and soybean. Plant and Soil 103 (2):155-168

Taylor KE (2001) Summarizing multiple aspects of model performance in a single diagram. Journal of Geophysical Research: Atmospheres 106 (D7):7183-7192

Terry, J. P., & Wotling, G. (2011). Rain-shadow hydrology: Influences on river flows and flood magnitudes across the central massif divide of La Grande Terre Island, New Caledonia. Journal of Hydrology, 404(1-2), 77-86.

Thampi SG, Raneesh KY, Surya T (2010) Influence of scale on SWAT model calibration for streamflow in a river basin in the humid tropics. Water Resources Management 24 (15):4567-4578

Thomas R, Sheard R, Moyer J (1967) Comparison of conventional and automated procedures for nitrogen, phosphorus, and potassium analysis of plant material using a single digestion 1. Agronomy Journal 59 (3):240-243

Thornthwaite C, Mather JR (1951) The role of evapotranspiration in climate. Archiv für Meteorologie, Geophysik und Bioklimatologie, Serie B 3 (1):16-39

Timsina J, Panaullah G, Saleque M, Ishaque M, Pathan A, Quayyum M, Connor D, Saha P, Humphreys E, Meisner C (2006) Nutrient uptake and apparent balances for rice-wheat sequences. I. Nitrogen. Journal of Plant Nutrition 29 (1):137-155

Tobler WR (1970) A computer movie simulating urban growth in the Detroit region. Economic geography 46 (sup1):234-240

UN (2016) Transforming our world: The 2030 agenda for sustainable development.

UNDP P (2006) Human Development Report 2006. Beyond scarcity: Power, poverty and the global water crisis. New York: UNDP.

Van Vuuren DP, Edmonds J, Kainuma M, Riahi K, Thomson A, Hibbard K, Hurtt GC, Kram T, Krey V, Lamarque J-F (2011) The representative concentration pathways: an overview. Climatic change 109 (1):5-31

Vandana, K., Islam, A., Sarthi, P. P., Sikka, A. K., & Kapil, H. (2019). Assessment of potential impact of climate change on streamflow: a case study of the Brahmani River basin, India. Journal of Water and Climate Change, 10(3), 624-641.

Varghese M, Jose J, Anu A, Konwar M, Murugavel P, Kalarikkal N, Deshpande M, Prabha TV (2021) Vertical profile of aerosol characteristics including activation over a rain-shadow region in India. Atmospheric Environment 262:118653

Velasco-Muñoz JF, Aznar-Sánchez JA, Batlles-delaFuente A, Fidelibus MD (2019) Rainwater harvesting for agricultural irrigation: An analysis of global research. Water 11 (7):1320

Verma P, Sagar R (2020) Effect of nitrogen (N) deposition on soil-N processes: a holistic approach. Scientific Reports 10 (1):1-16

Vico G, Tamburino L, Rigby JR (2020) Designing on-farm irrigation ponds for high and stable yield for different climates and risk-coping attitudes. Journal of Hydrology 584:124634

Walkley A, Black IA (1934) An examination of the Degtjareff method for determining soil organic matter, and a proposed modification of the chromic acid titration method. Soil science 37 (1):29-38

Wang P, Liu Y, Li L, Cheng K, Zheng J, Zhang X, Zheng J, Joseph S, Pan G (2015) Long-term rice cultivation stabilizes soil organic carbon and promotes soil microbial activity in a salt marsh derived soil chronosequence. Scientific reports 5 (1):1-13

Wang W, Yang Z, Zhang A, Yang S (2021) Water retention and fertilizer slow release integrated superabsorbent synthesized from millet straw and applied in agriculture. Industrial Crops and Products 160:113126

Wei, L., Ji, D., Miao, C., Muri, H., & Moore, J. C. (2018). Global streamflow and flood response to stratospheric aerosol geoengineering. Atmospheric chemistry and physics, 18(21), 16033-16050.

Wilby RL, Dawson CW (2013) The statistical downscaling model: insights from one decade of application. International Journal of Climatology 33 (7):1707-1719

Won JG, Choi JS, Lee SP, Son SH, Chung SO (2005) Water saving by shallow intermittent irrigation and growth of rice. Plant Production Science 8 (4):487-492

Wu L, Misselbrook TH, Feng L, Wu L (2020) Assessment of Nitrogen Uptake and Biological Nitrogen Fixation Responses of Soybean to Nitrogen Fertiliser with SPACSYS. Sustainability 12 (15):5921

Xiao G, Zhao Z, Liang L, Meng F, Wu W, Guo Y (2019) Improving nitrogen and water use efficiency in a wheat-maize rotation system in the North China Plain using optimized farming practices. Agricultural Water Management 212:172-180

Xie Y, Xia D, Ji L, Huang G (2018) An inexact stochastic-fuzzy optimization model for agricultural water allocation and land resources utilization management under considering effective rainfall. Ecological indicators 92:301-311

Xu J, Yang S, Peng S, Wei Q, Gao X (2013) Solubility and leaching risks of organic carbon in paddy soils as affected by irrigation managements. The Scientific World Journal 2013

Yan X, Zhou H, Zhu Q, Wang X, Zhang Y, Yu X, Peng X (2013) Carbon sequestration efficiency in paddy soil and upland soil under long-term fertilization in southern China. Soil and Tillage Research 130:42-51

Yip S, Ferro CA, Stephenson DB, Hawkins E (2011) A simple, coherent framework for partitioning uncertainty in climate predictions. Journal of climate 24 (17):4634-4643

Yuan T, Fengmin L, Puhai L (2003) Economic analysis of rainwater harvesting and irrigation methods, with an example from China. Agricultural water management 60 (3):217-226

Zarghami M, Abdi A, Babaeian I, Hassanzadeh Y, Kanani R (2011) Impacts of climate change on runoffs in East Azerbaijan, Iran. Global and Planetary Change 78 (3-4):137-146

Zhang Q, Dong W, Wen C, Li T (2020) Study on factors affecting corn yield based on the Cobb-Douglas production function. Agricultural Water Management 228:105869

Zhang W, Xu M, Wang X, Huang Q, Nie J, Li Z, Li S, Hwang SW, Lee KB (2012) Effects of organic amendments on soil carbon sequestration in paddy fields of subtropical China. Journal of soils and sediments 12 (4):457-470

ZHANG Y-j, HUA J-j, LI Y-c, CHEN Y-y, YANG J-c (2012) Effects of phosphorus on grain quality of upland and paddy rice under different cultivation. Rice Science 19 (2):135-142

Zhou S, Williams AP, Berg AM, Cook BI, Zhang Y, Hagemann S, Lorenz R, Seneviratne SI, Gentine P (2019) Land–atmosphere feedbacks exacerbate concurrent soil drought and atmospheric aridity. Proceedings of the National Academy of Sciences 116 (38):18848-18853

Zhu B, Jiang M, Wang K, Chevallier J, Wang P, Wei Y-M (2018) On the road to China's 2020 carbon intensity target from the perspective of "double control". Energy Policy 119:377-387

Zhu E, Deng J, Wang H, Wang K, Huang L, Zhu G, Belete M, Shahtahmassebi A (2019) Identify the optimization strategy of nitrogen fertilization level based on trade-off analysis between rice production and greenhouse gas emission. Journal of Cleaner Production 239:118060

List of Publications

Conference Publications

1. **Debnath, M.**, Mahanta, C., & Sarma, A. K. (2016, December). Fertilizer inputs and corresponding changes in plant nutrient availability in a rice cultivated soil of Assam, India. In Precision farming and resource management. 2nd international conference on emerging technologies in agricultural and food engineering. IIT Kharagpur, Excel India Publishers, New Delhi (Vol. 351).

2. **Debnath, M,** Kalyani S. & Sarma, A. K. (2023, August). *Machine learning taknik ka upoyog karte huwe rainshadow ksetra mein jalwayu paribartan pravawit streamflow projections.* 7th Rashtriya Jal Sanghosthi. NIH Roorkee, Uttarakhand.

3. **Debnath, M.,** Sarma, A. K. & Mahanta, C. Sensitivity analysis and carbon footprint determination of IFEC Model for improving water use efficiency and minimization of GHG emissions in irrigated areas of India. 5th Global Food Security Conference. (Submitted)

Book Chapter

1. **Debnath, M**., Mahanta, C., & Sarma, A. K. (2020). Nutrient Fluxes from Agriculture: Reducing Environmental Impact Through Optimum Application. In Environmental Processes and Management (pp. 37-51). Springer, Cham.

2. **Debnath, M.**, Sarma, A. K., & Mahanta, C. (2021). Development of ANN Model for Simulation of the Runoff as Affected by Climatic Factors on the Jamuna River, Assam, India. In Water and Energy Management in India (pp. 127-139). Springer, Cham.

Journal Publications

1. **Debnath, M.**, Mahanta, C., Sarma, A. K., Das, A & Upadhayay, A. Participatory design to investigate the effects of farmers' fertilization practices under water-saving conditions toward efficient nutrient uptake in rainfed rice. *South African Journal of Botany, Elsevier* (Under Revision).

2. **Debnath, M.**, Sarma, A. K., & Mahanta, C. Design of sustainable optimized crop planning in the winter fallow season incorporating residual soil nutrients in India: Food security and environmental impact. Heliyon, Elsevier (Under Revision)

3. **Debnath, M.** & Sarma, A. K. Integrated modeling of climate change response to agricultural water demand for intensive cropping in rice-fallow cropland areas: A case study of South Asia. *Mitigation and Adaptation Strategies for Global Change, Springer* (Under Review)
4. **Debnath, M.**, Sarma, A. K., & Mahanta, C. A hybrid neural network model for streamflow projection under climate change in a rain-shadowed river basin of South Asia (Submitted)